Received: 27 February 2024 | Accepted: 27 February 2024

DOI: 10.1097/HEP.0000000000000843

Practice Guideline

AASLD Practice Guideline on imaging-based noninvasive liver disease assessment of hepatic fibrosis and steatosis

Richard K. Sterling[1]
Andres Duarte-Rojo[2]
Keyur Patel[3]
Sumeet K. Asrani[4]
Mouaz Alsawas[5]
Jonathan A. Dranoff[6,7]
Maria Isabel Fiel[8]
M. Hassan Murad[5]
Daniel H. Leung[9]
Deborah Levine[10]
Tamar H. Taddei[6,7]
Bachir Taouli[11]
Don C. Rockey[12]

[1]Section of Hepatology, Virginia Commonwealth University, Richmond, Virginia, USA
[2]Division of Gastroenterology and Hepatology, Northwestern Medicine and Feinberg School of Medicine, Northwestern University, Chicago, Illinois, USA
[3]Division of Gastroenterology and Hepatology, University Health Network, University of Toronto, Toronto, Ontario, Canada
[4]Baylor University Medical Center, Dallas, Texas, USA
[5]Mayo Clinic Evidence-Based Practice Center, Mayo Clinic, Rochester, Minnesota, USA
[6]Section of Digestive Diseases, Yale School of Medicine, New Haven, Connecticut, USA
[7]VA Connecticut Healthcare System, West Haven, Connecticut, USA
[8]Department of Pathology, Molecular and Cell-Based Medicine, Icahn School of Medicine at Mount Sinai, New York, New York, USA
[9]Department of Pediatrics, Baylor College of Medicine and Division of Gastroenterology,

PURPOSE AND SCOPE

Chronic liver disease (CLD) is associated with approximately two million annual deaths worldwide and is an enormous health burden.[1,2] The majority of liver-related outcomes, including liver failure, portal hypertension (PHTN) with its complications, and HCC, occur almost exclusively in those with advanced CLD. Therefore, early identification of patients with any fibrosis and, in particular, moderate-to-advanced fibrosis is essential. Although liver histology has long been the reference standard for assessing fibrosis and steatosis, it is costly, is invasive, and carries a small, but important, risk of complications.[3,4] Over the past few decades, multiple noninvasive blood biomarkers and imaging modalities or tests, here termed "NonInvasive Liver Disease Assessment(s)" (NILDA), have been developed to determine the presence and severity of liver fibrosis (F) and steatosis (S).

The American Association for the Study of Liver Diseases (AASLD) Practice Guidelines Committee commissioned a diverse group of experts across multiple disciplines in the field of adult and pediatric liver disease to develop guidelines and guidance statements along with a systematic review covering imaging-based NILDA to answer specific clinically focused questions ("patient, intervention, comparison, and outcome," henceforth PICO) for the most common CLD etiologies (Table 1). Blood-based NILDA and NILDA for the detection of PHTN are discussed elsewhere.[5,6] These guidelines are intended primarily for adult and pediatric healthcare providers who see patients with CLD to provide guidance (see algorithm summarized at the end of this document). NILDA for autoimmune hepatitis (AIH) is discussed elsewhere.[7]

METHODOLOGY

Overall approach

The guideline writing group consisted of a multidisciplinary panel of experts in both adult and pediatric hepatology, pathology, and radiology, including methodology experts. Two complementary approaches were taken to answer the PICO questions. The first approach

Abbreviations: AIH, autoimmune hepatitis; ALD, alcohol-associated liver disease; ALT, alanine aminotransferase; APRI, AST-to-platelet ratio index; ARFI, acoustic radiation force impulse; AST, aspartate aminotransferase; AUC, area under receiver operating characteristic curve; BA, biliary atresia; BARD, body mass index, AST/ALT ratio, and presence of type 2 diabetes mellitus; BMI, body mass index; CAP, controlled attenuation parameter; CF, cystic fibrosis; CFLD, cystic fibrosis liver disease; CLD, chronic liver disease; DAA, direct-acting antiviral; DOR, diagnostic odds ratio; ELF, Enhanced liver fibrosis; F, fibrosis (used in staging fibrosis with stages F1 to F4); FIB-4, Fibrosis-4 Index; GGT, gamma-glutamyl transferase; HBeAg, hepatitis B envelope or "early" antigen; LR, likelihood ratio; LSM, liver stiffness measurement; M, median; MASLD, metabolic dysfunction–associated steatotic liver disease; MRE, magnetic resonance elastography; MRS, magnetic resonance spectroscopy; NAS, NAFLD activity score; NFS, NAFLD fibrosis score; NILDA, noninvasive liver disease assessments; NPV, negative predictive value; PBC, primary biliary cholangitis; PDFF, proton density fat fraction; PGAA, test combining prothrombin time, GGT, apolipoprotein A1, and α-2-macroglobulin; PHTN, portal hypertension; PICO, patient, intervention, comparison and outcome; PPV, positive predictive value; PSC, primary sclerosing cholangitis; ROI, region of interest; S, steatosis (used in staging steatosis with stages of 0-3); SAFE, sequential algorithm for fibrosis evaluation; SCD, skin-to-(liver) capsule distance; SVR, sustained virologic response; SWE, shear wave elastography; TE, transient elastography; US, ultrasound; XL, extra large.

Supplemental Digital Content is available for this article. Direct URL citations are provided in the HTML and PDF versions of this article on the journal's website, www.hepjournal.com.

Hepatology and Nutrition, Texas Children's Hospital, Houston, Texas, USA
[10]Department of Radiology, Beth Israel Lahey Health, Harvard Medical School, Boston, Massachusetts, USA
[11]Department of Diagnostic, Molecular and Interventional Radiology, Icahn School of Medicine at Mount Sinai, New York, New York, USA
[12]Digestive Disease Research Center, Medical University of South Carolina, Charleston, South Carolina, USA

Correspondence
Richard K. Sterling, Section of Hepatology, Virginia Commonwealth University, 1200 E Broad Street, West Hospital, Rm 1478, Richmond, VA.
Email: Richard.sterling@vcuhealth.org

depended on a commissioned systematic review conducted independently by the Mayo Clinic Evidence-Based Practice Center that led to disease-specific graded recommendations (Supplemental Figure 1, http://links.lww.com/HEP/I346) following the guideline framework using the Grading of Recommendations, Assessment, Development, and Evaluations (GRADE) system approach (Table 2). These recommendations are followed by a section that describes the quality of evidence, when applicable, and other considerations. Strength of recommendations was based on the quality of the evidence, balance of benefits and harms, the burden of testing (access and financial), and feasibility of the recommended action. The "strength of recommendation" determination assumed that performing tests with excellent (>80%) or outstanding (>90%) diagnostic accuracy is associated with improved patient outcomes. The recommendations were graded as either strong (apply to most patients with minimal variation and can be adapted as policy in most situations) or conditional (apply to a majority of patients, but variation in care is acceptable).

In order to address several other important clinical questions that could not be answered by a systematic review due to sparse and/or indirect evidence, the second approach involved a thorough narrative review by the writing group to develop ungraded guideline statements. These statements considered additional sources and the clinical experience of the authors with regard to noninvasive assessments of hepatic fibrosis and steatosis. Technical remarks and supporting evidence for graded and ungraded statements are included with recommendations to help reconcile the level of the recommendation with the quality of the evidence and to facilitate implementation.

TABLE 1 Patient, intervention, comparison, and outcome (PICO) questions in NILDA

Imaging-based with or without blood-based for fibrosis or steatosis in adults	
PICO 1	In adult patients with CLD, including hepatocellular (HCV, HCV/HIV, HBV, HCV/HBV, HBV/HIV, NAFLD, ALD) or cholestatic (PSC, PBC) disorders, are imaging-based NILDA accurate in staging hepatic fibrosis (F0-1 vs. F2-4, F0-2 vs. F3-4, F0-3 vs. F4) using histopathology as the reference?
PICO 2	In adult patients with CLD, including hepatocellular (HCV, HCV/HIV, HBV, HCV/HBV, HIV/HBV, NAFLD, ALD) or cholestatic (PSC, PBC) disorders, is one imaging-based NILDA more accurate than another in staging fibrosis (F0-1 vs. F2-4, F0-2 vs. F3-4, F0-3 vs. F4) using histopathology as the reference?
PICO 3	In adult patients with CLD, including hepatocellular (HCV, HCV/HIV, HBV, HCV/HBV, HIV/HBV, NAFLD, ALD) or cholestatic (PSC, PBC) disorders, are imaging-based NILDA more accurate than blood-based NILDA?
PICO 4	In adult patients with CLD, including hepatocellular (HCV, HCV/HIV, HBV, HCV/HBV, HBV/HIV, NAFLD, ALD) or cholestatic (PSC, PBC) disorders, is the combination of an imaging-based NILDA with a blood-based NILDA more accurate than a single test for staging fibrosis (F0-1 vs. F2-4, F0-2 vs. F3-4, F0-3 vs. F4) using histopathology as the reference?
PICO 5	In adult patients with CLD, including hepatocellular (HCV, HCV/HIV, HBV, HCV/HBV, HIV/HBV, NAFLD, ALD) or cholestatic (PSC, PBC) disorders, do longitudinal imaging-based NILDA accurately predict progression or regression of fibrosis in its natural history or response to therapy relative to longitudinal hepatic histological evaluation as the reference?
PICO 6	In adult patients with NAFLD, are imaging tests such as ultrasound, CT, or transient elastography (TE) with CAP accurate in grading hepatic steatosis (using histology, magnetic resonance [MR] spectroscopy, or MR-proton-density-fat-fraction [PDFF] as the reference)?
Imaging-based testing in children	
PICO 7	In children with CLD (HCV, HCV/HIV, HBV, HCV/HBV, HBV/HIV, BA, Alagille, α1AT, CFLD), are imaging-based tests accurate in staging hepatic fibrosis and steatosis?

Abbreviations: CFLD, cystic fibrosis liver disease; F, fibrosis stage; MR, magnetic resonance; PICO, Patient, Intervention, Comparison, and Outcome; α1AT, α1 antitrypsin disease.

Consensus process

For all guideline statements, we pursued a modified Delphi approach to define the final set of recommendations[11] using previously described methodology and also adapted by the AASLD practice metrics committee.[12] Statements with <75% agreement were rediscussed with (i) review of the scores, (ii) discussion to identify the reasons for variation, (iii) revision of suboptimally worded statements for accuracy by consensus, (iv) deletion of statements that

TABLE 2 Grading of recommendations, assessment, development, and evaluations (GRADE) system approach[a]

1. Rating the quality of evidence

Study design	Initial rating of quality of evidence	Rate down when:	Rate up when:
RCT	High	Risk of bias	Large effect size (e.g., RR = 0.5)
Observational	Moderate	Inconsistency	Very large effect (e.g., RR = 0.2)
	Low	Imprecision	Dose response gradient
	Very low	Indirectness	All plausible confounding would increase the association
		Publication bias	

2. Determinants of strength of a recommendation
   - Quality of evidence
   - Balance of benefits and harms
   - Patient values and preferences
   - Resources and costs

3. Implications of the strength of a recommendation

Strong
- Population: Most people in this situation would want the recommended course of action and only a small proportion would not.
- Health care workers: Most people should receive the recommended course of action.
- Policy makers: The recommendation can be adopted as policy in most situations.

Conditional
- Population: The majority of people in this situation would want the recommended course of action, but many would not.
- Health care workers: Be prepared to help patients make a decision that is consistent with their values using decision aids and shared decision making.
- Policy makers: There is a need for substantial debate and involvement of stakeholders.

[a]Modified from Schünemann et al.[9–10]
Abbreviations: RCT, randomized controlled trial; RR, relative risk.

were deemed problematic or irrelevant by consensus, and (v) identification of additional statements deemed necessary for inclusion in the list of statements. All final guideline statements were unanimously agreed upon by all writing group members.

HISTOPATHOLOGICAL PRINCIPLES UNDERLYING NILDA

Fibrosis scores are generally disease-specific and technically cannot be unified across different CLD. To achieve a cohesive approach for the purposes of NILDA, this AASLD Guideline writing group incorporated the various fibrosis staging systems into a single one and classified them into at least significant fibrosis (equivalent to ≥ fibrosis stage 2, or F2-4), at least advanced fibrosis (F3-4), and cirrhosis (F4). For simplicity, the Guidelines statements use the generic "F" stages throughout the text. Various histologic scoring systems to stage fibrosis and grade inflammation and steatosis have been used as standard reference measures in studies validating NILDA biomarkers (Table 3A, B). For an in-depth discussion of the role and limitations of histopathology to stage fibrosis and steatosis in CLD, please refer to the blood-based NILDA guideline.[6] The reader is asked to critically consider the limitations in liver histology staging described herein because they could, in principle, make NILDA tools appear less accurate than they really are.[22–26] This methodological phenomenon further elevates the relevance of longitudinal validation of NILDA against clinical outcomes.[25]

ASSESSMENT OF DIAGNOSTIC PERFORMANCE OF NONINVASIVE MARKERS

We used several statistical tests and indices in our assessment of the performance of imaging-based NILDA (Table 4). Although studies report test characteristics such as sensitivity and specificity at a selected cutoff, these are dependent on disease prevalence.[27] The diagnostic odds ratio (DOR) is the ratio of the odds of disease in those that test positive to the odds of the disease in those that test negative and provides a reliable estimate of a test's accuracy that is relatively independent from the prevalence of the condition being tested. Area under the receiver operating characteristic curve (AUROC) analysis is another effective way to summarize the overall diagnostic accuracy of the test. The AUROC has a range from 0 to 1, where a value of 0 indicates a perfectly inaccurate test and a value of 1 reflects a perfectly accurate test. In general, an AUROC of 0.5-0.69 suggests no to poor discrimination, 0.7-0.79 is acceptable, 0.8-0.89 is excellent, and 0.9 or more is outstanding.[28]

IMAGING TECHNIQUES

Imaging techniques have been utilized for many years in the evaluation of CLD (Table 5). In clinical practice, standard two-dimensional grayscale ultrasound (US), CT, and MRI are frequently used to identify features of cirrhosis; however, they are not sufficiently sensitive for compensated cirrhosis or precirrhotic stages.[29] Key

TABLE 3A Staging of fibrosis across multiple liver diseases and corresponding classification scores

	Fibrosis stage				
	0	F1	F2	F3	F4
			Significant fibrosis		
				Advanced fibrosis	
					Cirrhosis
Scheuer/Batts-Ludwig (Viral and autoimmune hepatitis)[13,14]	No fibrosis	Enlarged, fibrotic portal tracts	Periportal or portal-portal septa but intact architecture	Fibrosis with architectural distortion but no obvious cirrhosis	Probable or definite cirrhosis
Knodell (Viral and autoimmune hepatitis)[15]	No fibrosis	Fibrous portal expansion	N/A	Bridging fibrosis	Cirrhosis
Ishak (Various etiologies)[16]	0: No fibrosis	1: Fibrous expansion of some portal areas, with or without short fibrous septa	2: Fibrous expansion of most portal areas, with or without short fibrous septa 3: Fibrous expansion of most portal areas with occasional portal to portal bridging	4: Fibrous expansion of portal areas with marked bridging 5: Marked bridging (P-P and/or P-C) with occasional nodules (incomplete cirrhosis)	6: Cirrhosis (probable or definite)
METAVIR (Various etiologies)[17]	No fibrosis	Stellate enlargement of portal tract but without septa formation	Enlargement of portal tract with rare septa formation	Numerous septa without cirrhosis	Cirrhosis
Ludwig (PBC and PSC)[18]	N/A	N/A	N/A	Bridging fibrosis	Cirrhosis
Alcohol-associated liver disease (alcohol hepatitis histological score)[19]	No fibrosis or portal fibrosis	Expansive periportal fibrosis	Bridging fibrosis	Cirrhosis	
Brunt-Kleiner (NAFLD)[20,21]	No fibrosis	1A: delicate perisinusoidal 1B: dense perisinusoidal 1C: portal-only fibrosis	Perisinusoidal and portal/periportal fibrosis	Bridging fibrosis	Cirrhosis

Abbreviations: N/A, not applicable; P-C, port-central; P-*P*, portal-portal.

TABLE 3B Assessment and grading of steatosis based on the percent of hepatocytes affected

Degree of steatosis			
0 (Normal or minimal)	1 (Mild)	2 (Moderate)	3 (Severe)
< 5%	5%-33%	34%-66%	> 66%

Note: Based on Brunt et al.[20] and Kleiner et al.[21]

imaging features that allow for diagnosis of cirrhosis or PHTN include a coarse or heterogenous nodular liver, dilated portal vein (> 12 mm) or presence of collaterals, recanalization of the umbilical vein, ascites, and splenomegaly (most frequently defined as ≥ 13 cm but varies depending on patient sex, size, and morphology of the spleen).

US-based elastography

Transient elastography (TE, or vibration-controlled TE) uses M-mode US to track the speed of propagation of a mild amplitude and low-frequency (50 Hz) elastic wave produced by a mechanical vibrator included in the probe. The liver shear wave speed is expressed as the elastic modulus or liver stiffness measurement (LSM) within a range of 2.5-75 kPa. The faster the shear wave propagates through the liver, the higher the LSM, indirectly indicating a greater degree of fibrosis. The total area of tissue that is evaluated with this technique is approximately 3 cm^3, corresponding to a liver volume at least 100 times larger than a standard liver biopsy specimen. At least 10 valid measurements with an interquartile range (IQR) < 30% of the median value is required for reliable results.[30] Two probes have been developed for adults (M and XL probe), along with one for pediatric use (S probe, which has two settings, S1 and S2, based on thoracic circumference of < 45 cm and 45-75 cm, respectively).[31–33] The M probe is designed to assess patients with a skin-to-(liver) capsule distance (SCD) < 25 mm, and it quantifies stiffness at a distance of 25-65 mm from the skin, whereas the XL probe quantifies stiffness at depths of 35-75 mm from the skin. The XL probe in patients with obesity is successful in LSM in over 95% of patients with body mass index (BMI) ≥ 40 kg/m^2. A more recent study, however, suggested obtaining LSM with the XL probe in all patients with a BMI ≥ 32 kg/m^2, given the high frequency (78%) of SCD ≥ 25 mm in this group.[32] Of note, the XL probe yields lower LSM values than the M probe when tested on the same patient, although no adjustment in the cutoff values has been recommended given that TE yields higher LSM values in patients with obesity for whom the XL probe is normally used, thus potentially counterbalancing any between-probe differences.[31,34,35] TE is unreliable in the presence of ascites and is confounded by other factors (Table 6A and 6B).

Acoustic radiation force impulse (ARFI) techniques assess liver stiffness based on tissue displacement from acoustic compression pulses.[58] The regions of interest (ROIs) are selected with real-time grayscale US imaging and are not limited to the right intercostal area. ARFI encompasses two related techniques: point shear wave elastography (pSWE), which assesses ROIs measuring 10 × 5 mm^2, and two-dimensional shear wave elastography (2D-SWE), which interrogates more than one ROI in rapid succession to decrease sampling error. The 2D-SWE assesses a larger field of analysis than TE-LSM and pSWE because the size of the ROI can be modified by the operator. The recommended depth to locate the ROIs is 4-8 cm from transducer surface for both pSWE and 2D-SWE, and results are expressed in m/s with a range of 0.5-4.4[59] or kPa with ranges as high as 300, depending on the manufacturer.[58]

Conceptually, pSWE and 2D-SWE are similar to TE, with reliable performance standards including an acquisition success rate ≥ 60% (ratio of valid/total acquisitions) and an IQR of 30% or less of the median value. The major difference is the method for generating the elastic modulus (i.e., stiffness estimation), as TE uses vibration to generate a propagation shear wave, whereas ARFI relies on the shear waves generated during tissue absorption of an acoustic pulse. As a result, ARFI results are less affected by ascites or obesity because the shear waves are generated inside the liver.[36,60] The ROIs for the 2D-SWE and pSWE are much larger than that from TE, and ROIs can be moved to avoid interrogating regions with large vessels or masses. A limitation of shear wave elastography (SWE) is the need for technical expertise, including proper selection of ROI within the liver parenchyma (i.e., right lobe, at proper depth, in an area devoid of vascular/biliary structures and without exerting mechanical tissue compression). pSWE/2D-SWE are affected by many similar factors as TE (Table 6A). Finally, liver stiffness cutoff values for pSWE and 2D-SWE are unique to each vendor-specific machine and must be interpreted accordingly. Although TE may not provide as much anatomic information as pSWE and 2D-SWE, it offers a standardized platform to allow for more uniform thresholds for varying levels of fibrosis.

Magnetic resonance (MR)-based elastography

Magnetic resonance elastography (MRE) uses propagating mechanical shear waves generated with an acoustic passive plastic driver placed over the right

TABLE 4 Diagnostic performance indices used in NILDA

Diagnostic index	Calculation	Comments
Sensitivity	TP/(TP+FN)	Not dependent on population. Correctly detect patients who are ill who have the condition. High sensitivity helps rule out the disease (few false negatives).
Specificity	TN/(TN+FP)	Not dependent on population. A high specificity means a test is useful for ruling in disease. High specificity helps ruling in disease (few false positives).
Accuracy	(TP+TN)/(*P*+N)	
PPV	TP/(TP+FP)	The probability that a person with a positive test indeed has the disease or condition of interest. Used to "rule in" disease. Affected by the prevalence of the disease in the population.
NPV	TN/(TN+FN)	The probability that a person with a negative test does NOT have the disease or condition of interest. Important for screening studies to not miss disease. Affected by the prevalence of the disease in the population.
Positive LR	$\frac{TP/(TP+FN)}{FP/(FP+TN)}$	Depends on patient population. Positive LR above 10 suggests strong test
Negative LR	$\frac{FN/(TP+FN)}{TN/(FP+TN)}$	Depends on patient population. Negative LR below 0.1 suggests strong diagnostic evidence
DOR	Positive LR/negative LR	The ratio of odds of positivity of those with disease relative to odds of positivity in those without disease
Area under the receiver operating characteristic curve (AUC)	Graph values of test performance from 0 (a perfectly inaccurate test) to 1 (a perfect test). Plots the diagnostic ability of a binary classifier system as its discrimination threshold is varied.	Summarizes the overall diagnostic accuracy of a test. In general, an AUC of 0.5 suggests no discrimination (i.e., ability to diagnose patients with and without the disease or condition based on the test), 0.7 to 0.8 is considered acceptable, 0.8 to 0.9 is considered excellent, and more than 0.9 is considered outstanding

Abbreviations: AUC, area under the receiver operating characteristic curve; FN, false negative; FP, false positive; N, all negative tests; *P*, all positive tests; TN, true negative; TP, true positive.

upper quadrant. Similar to US-based techniques, the speed of propagation of the shear wave determines tissue stiffness. An advantage of MRE is that it interrogates almost the entire liver and, thus, allows for more complete assessment than the US-based elastography methods. Total acquisition time using a standard 2D Gradient Recalled Echo (2D GRE) sequence is approximately 40-60 seconds, adding minimal time to a standard abdominal MRI exam.[61] Other sequences such as 2D echo planar imaging (EPI) are up to 4 times faster.[62] ROIs with an adequate wave amplitude are selected to quantify the elastic modulus, expressed in a range of 0-20 kPa.[63] Newer methods provide automatic LSM without user interaction. Ascites and, rarely, obesity can limit MRE performance by interfering with shear wave propagation, but more importantly, hepatic iron overload generates an inadequate signal-to-noise ratio (i.e., liver R2* $>$76 s-1 at 1.5T), which can result in MRE failure when using 2D GRE, particularly at 3T.[40,64] New EPI sequences are more immune to susceptibility artifacts from iron deposition.[62] Although there are no large comparative studies assessing failure to obtain LSM across imaging-based NILDA, the rate of failed MRE testing is generally lower than that of US-based techniques.[37,65,66] Similar to US-based elastography, MRE has several factors that can confound results or limit their use (Table 6A).

PICO 1: In adult patients with CLD, including hepatocellular (HCV, HCV/HIV, HBV, HCV/HBV, HBV/HIV, NAFLD, alcohol-associated liver disease [ALD]) or cholestatic (primary sclerosing cholangitis [PSC], primary biliary cholangitis [PBC]) disorders, are imaging-based NILDA accurate in staging hepatic fibrosis (F0-1 vs. F2-4, F0-2 vs. F3-4, F0-3 vs. F4) using histopathology as the reference?

TABLE 5 Operational characteristics of imaging-based techniques for assessment of fibrosis

Method	Availability	Cost	Evidence	ROI size	ROI placement	Failure rate	Reasons for failure	Units	Brand/vendor
TE	Widespread in hepatology offices	Low	Well validated	Small	Restricted - no guidance	< 5%-15%	High BMI (M probe) ascites	Young's modulus (kPa)	Fibroscan, Echosens, Paris
ARFI methods	Moderate	Low	Moderate validation in single etiology CLD with histology as reference standard	Small (pSWE) Medium (2D-SWE)	Flexible up to 8-cm depth with US guidance	< 5%-15%	High BMI	SWE –Young's modulus (kPa) pSWE –Wave speed (m/s)	pSWE: Virtual Touch Quantification [a type of ARFI] by Siemens Healthineers, Erlangen, Germany; and Elast-PQ [EPIQ7 ultrasound], Philips Healthcare, Bothell, WA 2D-SWE: Virtual Touch Imaging Quantification by Siemens Healthineers, Erlangen, Germany; SWE by Aixplorer, Supersonic Imagine, Hologic, Inc., France; ElastQ, Philips Healthcare, Netherlands; Acoustic Structure Quantification by Canon; 2D-SWE LOGIQ E9 ShearWave Elastography, GE Healthcare, WI; Hitachi Medical Systems, Japan; Esaote SpA, Genoa, Italy; and Samsung Medison Co., Seoul, Korea
MRE	Limited	High	Limited validation in single etiology CLD with histology as reference standard	Large	Whole organ coverage (within confidence maps)	< 5%	Liver iron deposition, Large ascites, Very high BMI, 3T (for 2D GRE)	Shear modulus (kPa)	Resoundant (available on GE Healthcare, Siemens Healthineers, Philips)

Abbreviations: GRE, gradient recalled echo; MRE, magnetic resonance elastography; TE, transient elastography; US, ultrasound.

TABLE 6A Clinical factors affecting performance of blood- and imaging-based noninvasive assessment of hepatic fibrosis

Clinical condition	Tools affected	Comments
Obesity[32,35–39]	LSM	Although an XL probe can remediate TE-LSM failure in most cases with SCD ≥ 25 mm, extreme obesity (BMI ≥ 40 kg/m^2) can result in TE-LSM failure. Depending on body frame, extreme obesity can also affect transmission of mechanical wave, leading to MRE failure, but this is far less common than TE failures. SWE acoustic signal transmission can also be affected by obesity, resulting in failure.
Narrow intercostal space	TE	If not corrected by repositioning, leads to failure or falsely elevated estimation
Ascites[36]	LSM TE affected more that SWE, with MR being the least affected	Affects transmission of vibration and mechanical signals, leading to failure Although SWE and MR are relatively insensitive to small amounts of ascites, large amounts can lead to failure.
Splenectomy	APRI FIB-4 Fibroindex FibroMeter NFS	Because these tools use platelets as a biomarker of PHTN, attenuated thrombocytopenia from splenectomy gives a falsely lower estimation. Splenomegaly as an imaging sign of PHTN cannot be assessed.
Thrombocytopenia (not related to PHTN)	APRI FIB-4 Fibroindex FibroMeter NFS	Because these tools use platelets as a biomarker of PHTN, thrombocytopenia from other conditions gives a falsely higher estimation.
Iron overload[40]	MRE	Affects T2 signaling leading to failure
Steatosis[41–43]	TE	Although its clinical impact is unclear, moderate to severe steatosis causes TE-LSM to overestimate fibrosis.
Active alcohol use[44]	FibroTest Hepascore	Increases GGT, leading to falsely elevated estimation
Hepatic venous outflow tract obstruction, sinusoidal obstruction syndrome, hepatic congestion of cardiac/pulmonary vascular origin[45]	LSM	Retrograde vascular congestion results in increased stiffness of hepatic parenchyma and falsely elevated estimation of fibrosis
Obstructive cholestasis[46]	LSM	Large bile duct obstruction results in increased stiffness of hepatic parenchyma and falsely elevated estimation of fibrosis
Hepatic infiltration[47]	LSM	Amyloid or tumoral infiltration results in increased stiffness of hepatic parenchyma and falsely elevated estimation of fibrosis
Elevated ALT and/or AST (inflammatory hepatitis)[33,44,48]	APRI FIB-4 Fibroindex FibroMeter NAFLD fibrosis score LSM	Elevated aminotransferases occurring in relation to acute or acute-on-chronic hepatitis lead to a falsely elevated estimation of fibrosis.
Chronic kidney disease[49–51]	Fibroindex APRI FIB-4 FibroMeter TE-LSM	Elevated urea levels can result in falsely lower estimation. Patients undergoing hemodialysis tend to have lower ALT and AST levels, resulting in falsely lower estimation. Hemofiltration can result in lower stiffness in patients with baseline fluid overload.
Malnutrition	NAFLD fibrosis score	Albumin reduction that is disproportionate to liver dysfunction results in falsely elevated estimation.

TABLE 6A. (*continued*)

Clinical condition	Tools affected	Comments
Inflammatory condition	FibroTest Fibroindex Hepascore FibroMeter	Can result in increased α2-macroglobulin levels and falsely elevated Fibrotest, increased γ-globulin, and falsely elevated Fibroindex
Hemolysis	Fibrotest	Decreases haptoglobin levels and increases total bilirubin, leading to falsely elevated estimation
Gilbert syndrome and other cholestatic diseases	FibroTest Hepascore	Can result in increased total bilirubin and falsely elevated estimation
Postprandial[52]	LSM NFS	Liver stiffness increases up to 26% have been described for TE-LSM 2 hours after a meal. Other methods of assessing LSM are also affected by recent meals. A rise in postprandial glucose (>110 mg/dL) falsely elevates NAFLD fibrosis score.
Gastrectomy[53]	Fibrospect Hepascore ELF	Increases hyaluronic acid, resulting in falsely elevated estimation
Extra-hepatic fibrosing conditions[54]	FibroMeter Fibrospect ELF	Conditions such as interstitial lung disease can increase collagen turnover markers, resulting in elevated estimation
Acute sickle cell crisis[55]	Fibrotest TE	Related to hemolysis (as above) Acute vaso-occlusive crisis increases liver stiffness.
Critically ill[56]	LSM	Deceased liver donors in the ICU show elevated liver stiffness, potentially related to fluid overload and elevated aminotransferases.

Abbreviations: LSM, liver stiffness measurement (applying to all methods, TE, SWE, and MRE); MRE, magnetic resonance elastography; NFS, NAFLD fibrosis score; TE, transient elastography.

Guideline Statements:

1. In adults with chronic HCV, chronic HBV, and NAFLD, AASLD recommends using imaging-based NILDA tests to detect significant fibrosis (F2-4), advanced fibrosis (F3-4), and cirrhosis (F4). (strong recommendation, moderate quality of evidence)
2. In adults with ALD or chronic cholestatic liver disease, AASLD suggests using imaging-based NILDA tests to detect advanced fibrosis (F3-4) and cirrhosis (F4). (conditional recommendation, low quality of evidence)

TECHNICAL REMARKS

- There is considerable experience with the use of TE-LSM in HCV and HBV, with substantial reliability for discriminating between significant fibrosis (F2-4), advanced fibrosis (F3-4), and cirrhosis (F4). The effect of parenchymal inflammation and viremia must be considered when interpreting results.
- The majority of data on TE-LSM are derived from viremic subjects (positive for HCV RNA or HBV DNA); therefore, their use in treated subjects (negative HCV RNA or HBV DNA) is poorly defined.
- In NAFLD, TE-LSM has acceptable sensitivity and specificity for detection of fibrosis but is limited by technical issues in certain patients (e.g., those with obesity). Although less data exist for MRE-LSM, it is a reliable method to detect significant fibrosis (F2-4) and cirrhosis (F4) and particularly useful for the discrimination of advanced fibrosis (F3-4) in NAFLD.

We acknowledge that there has been a recent multisociety endorsement of a nomenclature change from NAFLD to metabolic dysfunction–associated steatotic liver disease (MASLD). Although this is an important change that will impact of future of the study of this entity, all data utilized to develop these guideline statements were based on prior literature that utilized the previous NAFLD definition. Therefore, NAFLD is the term used throughout this document when referring to the existing literature. Current evidence indicates >98% overlap

TABLE 6B Clinical factors affecting performance of imaging-based noninvasive assessment of steatosis

Clinical condition	Tools affected	Comments
Obesity[57]	TE-CAP	Readings need to be corrected deducting or adding 4.4 dB/m per BMI above or below 25 kg/m^2 (within the 20-30 range).
Diabetes mellitus[57]	TE-CAP	Readings need to be corrected by deducting 10 dB/m in patients with diabetes mellitus.
NAFLD[257]	TE-CAP	Readings need to be corrected by deducting 10 dB/m in patients with known NAFLD.

Abbreviation: TE-CAP, transient elastography measured CAP.

between patients who meet criteria for diagnosis of NAFLD/NASH and the new criteria for MASLD/metabolic dysfunction–associated steatohepatitis (MASH) in large cohort studies, indicating that the analyses and recommendations provided in these Guidelines for patients with NAFLD/NASH are likely to pertain to patients characterized by the new nomenclature of MASLD and MASH.

- For patients with ALD and cholestatic liver disease, the evidence for use of imaging-based NILDA to assess fibrosis is not as extensive as for HCV, HBV, and NAFLD. Furthermore, the effect of acute-on-chronic flares and extrahepatic biliary obstruction must be considered when interpreting results.
- Clinicians should be aware of pitfalls and limitations when ordering and interpreting imaging-based NILDA for staging fibrosis (Table 6A).

EVIDENCE AND RATIONALE

In the systematic review developed to address this PICO question,[67] imaging-based methods showed acceptable to outstanding diagnostic accuracy, with most sensitivities and specificities in the range of 70%-100%, and with narrow confidence intervals (i.e., more precise) and higher reliability than blood-based NILDA[68] to detect advanced fibrosis or cirrhosis (Figure 1). All imaging NILDA methods evaluated had predominantly moderate to high strength of evidence and low-to-moderate risk of bias, although there were more publications for TE-LSM than pSWE-LSM and fewer for 2D-SWE-LSM and MRE-LSM. Some MRE-LSM studies could not be included in analyses because they included heterogenous populations.[69] However, in a meta-analysis of studies in mixed disease populations, MRE-LSM had summary AUROCs of 0.88, 0.93, and 0.92 for the identification of F2-4, F3-4, or F4, respectively.[65] Importantly, cutoff values for each stage varied across liver diseases and between studies. Below follows a discussion of the use of imaging NILDA in specific liver diseases.

HCV

For the detection of significant fibrosis in patients with chronic HCV (with viremia), all US-based methods had acceptable to outstanding accuracy, with pSWE-LSM showing wider confidence intervals for specificity. For the detection of advanced fibrosis and cirrhosis, all US-based methods had excellent to outstanding accuracy with sensitivities and specificities in the high 80%-90%.[67] These findings agree are consistent with other meta-analyses assessing the accuracy of TE-LSM and 2D-SWE-LSM in chronic HCV, which also found AUROC in the excellent to outstanding range.[60,70] Based on two studies of patients with HCV, MRE-LSM showed acceptable to outstanding sensitivity and specificity for all fibrosis staging categories in the range of 76%-100%.[71,72]

HBV

All US-based methods had acceptable to excellent accuracy for detection of significant fibrosis to advanced fibrosis and cirrhosis in untreated HBV. TE-LSM and pSWE-LSM showed a wider variability in sensitivity (TE and pSWE) and specificity (pSWE), particularly for significant fibrosis. Of note, a single study assessing MRE-LSM had the highest sensitivities and specificities, 95%-100%, respectively.[67] Another meta-analysis comparing MRE-LSM (n = 1470) and TE-LSM (n = 3641) found similar results to ours for both techniques.[73] Importantly, we could not perform a separate analysis for patients with either high or low alanine aminotransferase (ALT) determinations to select an optimal cutoff value in the setting of inflammation, an important variable that can increase LSM and can falsely elevate the fibrosis estimate.[48] This is an important consideration, as higher TE cutoff values have been recommended for patients with elevated ALT, and TE has been deemed inaccurate to estimate fibrosis when ALT is 5-10 times the upper limit of normal.[74]

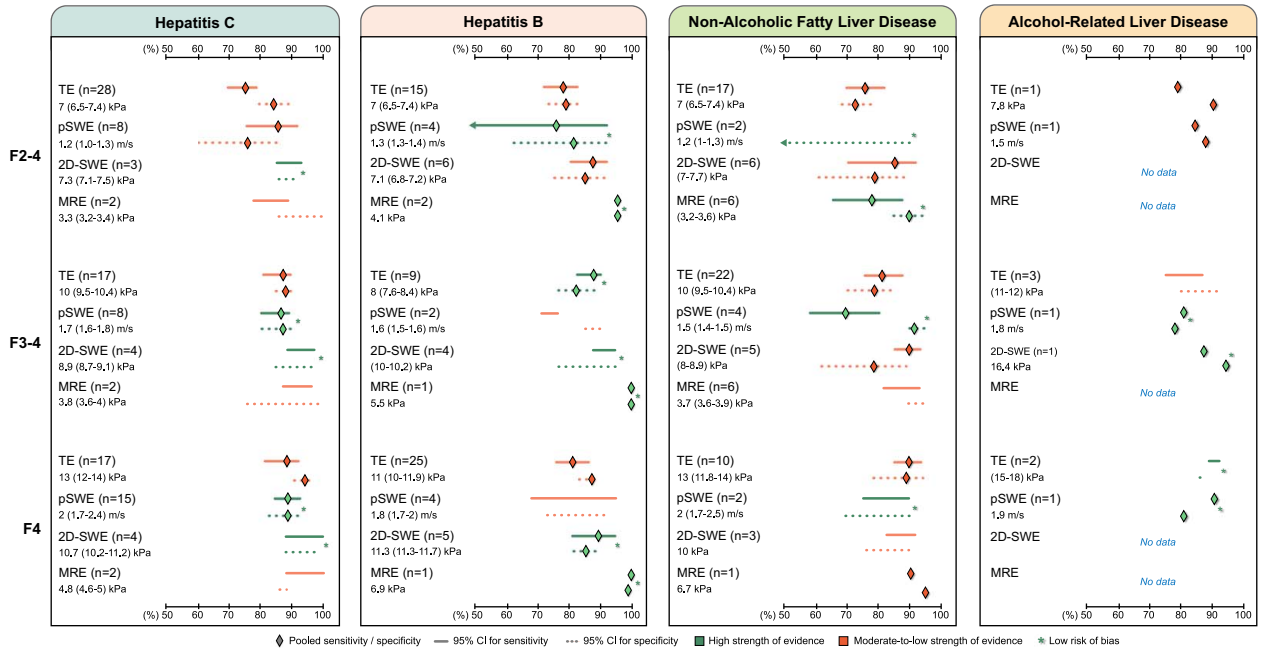

FIGURE 1 Systematic review of imaging-based NILDA thresholds for detection of fibrosis. Systematic review pooled sensitivities and specificities for each imaging-based noninvasive liver disease assessment modality, according to disease (HCV, HBV, NAFLD, ALD) and fibrosis staging (clinically significant fibrosis [F2-4], advanced fibrosis [F2-3], cirrhosis [F4]). The diamond-shaped dot on a continuous line shows the pooled sensitivity with its 95% confidence interval, whereas the diamond-shaped dot on a dotted line shows the pooled specificity with its 95% confidence interval. An arrow at the end of a line means that the 95% confidence interval for sensitivity or specificity continued below the 50% sensitivity/specificity limit. The green color represents high strength of evidence, whereas the blue color represents moderate to low strength of evidence. An asterisk next to each line stands for low risk of bias, otherwise, high to moderate risk of bias must be assumed. The best mean (range) cutoff value identified by the systematic review at each stage of fibrosis can be found immediately below each method, along with the number of studies summarized between parentheses. Abbreviations: MRE, magnetic resonance elastography; TE, transient elastography.

NAFLD

The discriminative capacity for significant fibrosis among the US-based methods was acceptable to excellent, with the widest variability for US-based methods observed for pSWE-LSM. However, TE-LSM and 2D-SWE-LSM showed broader confidence intervals than in other CLD, which reached the poor discriminative performance range.[67] Other meta-analyses have found equivalent accuracy for pSWE-LSM (AUROC = 0.86), 2D-SWE-LSM (AUROC = 0.85), and TE-LSM (AUROC = 0.85) to detect significant fibrosis.[60,75] For advanced fibrosis and cirrhosis, US-based methods also performed in the acceptable to excellent range, although with some improvement in accuracy when compared to significant fibrosis, particularly for TE-LSM.[67] Various meta-analyses have found AUROC, sensitivities, and specificities in the 0.80-1.0 range for all US-based methods when estimating either advanced fibrosis or cirrhosis.[60,76,77] Using dual cutoff values, a methodology not included in our formal analysis, a recent study examining 1765 patients included in clinical trials proposed TE-LSM cutoff values of < 9.9 kPa to rule out (sensitivity 83%, specificity 61%) and ≥ 11.4 kPa to rule in advanced fibrosis (sensitivity 75%, specificity 71%).[78] In clinical practice, TE-LSM < 8 kPa are used to rule out advanced fibrosis whereas TE-LSM > 12 kPa is used to rule it in.[79] In our systematic review, MRE-LSM had sensitivities and specificities in the excellent to outstanding range, which were higher than any other method[67] and similar in performance to that in a recent meta-analysis including 910 patients with NAFLD (AUROC = 0.93, 0.93, and 0.95 for F2-4, F3-4, and F4, respectively).[80]

ALD

A limited number of studies in ALD have assessed TE-LSM, pSWE-LSM, and 2D-SWE-LSM for identification of significant fibrosis, advanced fibrosis, and cirrhosis.[67] They all showed excellent to outstanding performance with test sensitivity increasing at more advanced stages of fibrosis, except for 2D-SWE-LSM, which was evaluated for the detection of advanced fibrosis only (sensitivity of 88% and specificity of 95%). A meta-analysis assessing TE-LSM in 834 patients with ALD found sensitivities and specificities of 92% and

70% for F3-4 and 95% and 71% for cirrhosis, respectively.[81] This study proposed a TE-LSM cutoff value of 12.5 kPa for cirrhosis, which contrasts the cutoff values we identified (from 15-18 kPa) that portend a higher specificity. A recent meta-analysis also favored a higher cutoff value of 18.6 kPa which resulted in an 85% specificity for cirrhosis, which is likely more useful in ruling in this degree of fibrosis.[80]

Similar to viral hepatitis, for both NAFLD and ALD, one must consider aminotransferase levels, as LSM is less reliable when ALT or aspartate aminotransferase (AST) are >100 U/mL,[33,82] particularly in the setting of alcohol-associated hepatitis.[83] A meta-analysis confirmed that AST and elevated bilirubin are directly associated with LSM in ALD.[44] Although inflammation, active alcohol use, and bilirubinostasis/cholestasis are best described as TE-LSM modifiers, they likely affect fibrosis estimates with most imaging-based NILDA.

Other CLD

TE-LSM was the only method investigated in patients with HCV/HIV coinfection, showing a similar sensitivity (83% for significant fibrosis and 83-100% for cirrhosis) and specificity (74% for significant fibrosis and 84-93% for cirrhosis) when compared to HCV monoinfection.[67] The data were also limited for cholestatic diseases. In PBC, we identified at least one study for each of the studied techniques. US-based techniques showed sensitivities of 67%-100% which improved along with higher stages of fibrosis while associated with varying specificities in the 77%-100% range.[67] Using a dual cutoff approach (LSM ≤ 6.5 and >11 kPa) in 167 patients with PBC, the AUROC was 0.89 for F3-4 with a negative predictive value (NPV) of 94% and a positive predictive value (PPV) of 89%, independent of the liver chemistries or BMI.[84] The high specificity cutoff value in this study was similar to that identified in our systematic review.[85] Interestingly, the accuracy of MRE-LSM was numerically inferior to that from US-based LSM, particularly with respect to sensitivity (range of 51-70%).[67] Our systematic review identified two PSC studies fulfilling inclusion/exclusion criteria (with acceptable to outstanding performance) across all fibrosis stages.[67] In clinical practice, TE-LSM thresholds of 9.6 and 14.4 kPa are used to detect F3 and F4, respectively.[86]

Data in post-transplant patients are limited and studies mainly addressed populations with mixed causes of liver disease prior to transplant. Using TE-LSM, a threshold of 10.5 kPa identified recipients who developed F3-4 with an AUROC of 0.94 at a fixed sensitivity of 90% and an NPV of 99%.[87] Another study with 2D-SWE found a median LSM of 12 kPa (range of 10-13) to detect F3-4 stage at lower sensitivity and NPV (76% and 94%); however, recipients with an LSM ≥ 11 kPa had lower survival irrespective of their true histopathological fibrosis stage.[88] Two meta-analyses focused on post-transplant studies showed excellent to outstanding accuracy for the diagnosis of F2-4 or F3-4 with TE-LSM or ARFI methods while outperforming blood-based NILDA such as AST-to-platelet ratio index (APRI) and Fibrosis-4 Index (FIB-4).[89,90] A pooled analysis of 141 transplant recipients also showed excellent to outstanding accuracy for the identification of F3-4 and F4 with MRE at thresholds of 4.1 and 5.9 kPa, respectively.[91] Although rejection[92] and other allograft complications[93] can affect liver stiffness, the high sensitivity and NPV of LSM makes imaging-based NILDA a valuable monitoring tool to guide the need for biopsies in the assessment of recurrent disease and allograft health.[85,94] This is particularly important for patients transplanted for conditions with a high risk of recurrence and progressive disease (e.g., NASH 38% recurrence rate) or alloreactivity, such as immune-mediated liver diseases.[95]

PICO 2: In adult patients with CLD, including hepatocellular (HCV, HCV/HIV, HBV, HCV/HBV, HIV/HBV, NAFLD, ALD) or cholestatic (PSC, PBC) disorders, is one imaging-based NILDA more accurate than another in staging fibrosis (F0-1 vs. F2-4, F0-2 vs. F3-4, F0-3 vs. F4) using histopathology as the reference?

Guideline Statement:

3. In adults with CLD, AASLD recommends utilizing either US-based elastography methods or MRE to stage fibrosis. Depending on local availability and expertise, it is reasonable to perform MRE as an investigation when concomitant cross-sectional imaging is needed or for patients in whom the accuracy of US-based elastography might be compromised (ungraded statement).

TECHNICAL REMARKS

- US-based elastography methods are comparable overall because of their similar performance.
- In patients with chronic HBV and HCV, different US-based elastography methods have acceptable diagnostic accuracy for detecting significant (F2-4) or advanced fibrosis (F3-4) and

good to excellent diagnostic accuracy for detecting cirrhosis (F4).

- In patients with NAFLD (not necessarily MASLD), different US-based elastography methods have comparable, acceptable diagnostic accuracy for detecting significant (F2-4) or advanced fibrosis (F3-4), and excellent diagnostic accuracy for detecting cirrhosis (F4).
- There are insufficient data comparing different imaging-based NILDA in cholestatic liver diseases.
- There are a limited number of studies comparing US elastography and MRE. Although many studies of MRE-LSM were not included in our systematic review because they had heterogenous patient populations or lacked histology as a reference standard, the overall sensitivity and specificity of MRE-LSM for advanced fibrosis (F3-4) and cirrhosis (F4) was typically above 90%. More head-to-head comparisons between MRE and US-based elastography are needed to determine improved accuracy of the former.
- There are differences in shear wave speeds provided by ARFI-LSM techniques due to the large number of vendors with different implementations, which makes the comparison between studies difficult. In contrast, MRE uses standardized acquisition and processing, which makes the LSM values obtained with clinical MRE platforms generally comparable.
- Interpretation study results comparing imaging-based NILDA should consider multiple potential effect modifiers and confounding factors such as whether the study was performed in a screening versus diagnostic environment, population included (i.e., whether at high or low risk for fibrosis), the sample size, and whether cutoffs for various fibrosis stages were used a priori or were based on the sampled population.

EVIDENCE AND RATIONALE

TE compared to pSWE and 2D-SWE

pSWE-LSM and 2D-SWE-LSM methods have been introduced more recently than TE-LSM and are thus less well studied in the literature. In patients with HBV[96–98] and HCV,[39,99,100] data demonstrate excellent diagnostic performance for liver fibrosis staging. Studies comparing TE-LSM to pSWE-LSM[101] and 2D-SWE-LSM[102,103] have found these methods to provide similar,[66,96–99,101,104–106] superior,[98,102,103] or inferior[100,107] diagnostic performance to TE-LSM (Table 7). However, when comparing the imaging tests head-to-head with liver histology in studies using validated cutoff values, there do not appear to be significant differences among the imaging elastography techniques in cohorts of patients with HCV, HBV, and NAFLD.[67]

MRE compared to US elastography methods

Given the limited availability and recent clinical use of MRE-LSM, less published data comparing MRE-LSM and TE-LSM/ARFI-LSM methods are available. Pooled analysis from 3 NAFLD studies[109–111] showed higher diagnostic accuracy for MRE-LSM compared to TE-LSM for each stage of fibrosis,[112] and a clear trend was observed in another two studies for F3-4.[106,113] A meta-analysis in NAFLD populations showed that MRE-LSM and SWE-LSM had the highest AUROCs for significant fibrosis and advanced fibrosis compared to TE.[77] Similar diagnostic accuracy between MRE-LSM and 2D-SWE-LSM for F2-4 and F3-4 was reported in another study.[106] Other studies have found MRE-LSM to be superior[114–116] or equivalent[117] to TE-LSM

TABLE 7 Summary results from systematic review of imaging-based biomarkers for fibrosis stage

Disease	Fibrosis stage	TE cutoff	pSWE/2D-SWE cutoff[a]	References	POR (95% CI)
HCV	F0-1 vs. F2-4	6.5-6.7 kPa	1.2 m/s (pSWE)	[107,108]	2.67 (0.40-17.66)
	F0-2 vs. F3-4	9.6 kPa	1.6 m/s (pSWE)	[100]	2.20 (0.28-17.04)
	F0-3 vs. F4	12.2-13.1 kPa	1.8-2 m/s (pSWE)	[100,107]	2.18 (0.56-8.49)
HBV	F0-1 vs. F2-4	6.9-7.3 kPa	7.1 kPa (2D-SWE)	[102,104]	0.40 (0.16-1.01)
	F0-3 vs. F4	10.6-11.2 kPa	11.3 kPa (2D-SWE)	[104]	0.71 (0.10-5.24)
			1.75 m/s (pSWE)	[105]	0.71 (0.20-2.47)
NAFLD	F0-3 vs. F4	16.1 kPa	2 m/s (pSWE)	[37]	2.36 (0.86-6.48)

[a]m/s for pSWE (which can be converted to kPa for comparisons), kPa for 2D-SWE.
Abbreviation: TE, transient elastography.

in mixed etiology cohorts. MRE-LSM was found to be equivalent to 2D-SWE-LSM in a mixed etiology cohort,[118] whereas a study in NAFLD found that MRE-LSM outperformed pSWE-LSM, especially in patients with obesity.[119]

PICO 3: In adult patients with CLD, including hepatocellular (HCV, HCV/HIV, HBV, HCV/HBV, HIV/HBV, NAFLD, ALD) or cholestatic (PSC, PBC) disorders, are imaging-based NILDA more accurate than blood-based NILDA?

Guideline Statement:

4. In adults with CLD, AASLD suggests imaging-based NILDA be incorporated into the initial fibrosis staging process because it is more accurate than blood-based NILDA. (conditional recommendation, low quality of evidence)

TECHNICAL REMARKS

- More than half of studies performing imaging-based to blood-based NILDA head-to-head comparisons that meet entry criteria showed improved accuracy for imaging-based tests, whereas no comparison favored blood-based tests (Table 8).
- Use of multiple threshold values for each analyzed stage of fibrosis in the case of blood-based NILDA made it challenging to provide precise diagnostic estimates.
- Choice of tests among imaging-based and blood-based NILDA is based on local expertise, test availability, test cost, and patient's preference.

EVIDENCE AND RATIONALE

Head-to-head comparative studies between blood-based and imaging-based NILDA methods in the same patients using histology as the reference are mostly available in HCV, HBV, and NAFLD (Table 9); the reader is referred to the associated systematic review for considerations regarding quality of evidence.[67] Of note, studies could have different DORs depending on the selected blood-based NILDA thresholds.[108]

HCV

A meta-analysis including 8 studies comparing TE-LSM versus APRI showed no difference between the two modalities for detection of significant fibrosis (F2-4) and found that TE-LSM had significantly better performance than APRI for detection of cirrhosis (F4).[70] In our systematic review,[67] we found most studies demonstrating improved accuracy of US-based elastography over simple blood tests, particularly for detection of F3-4 and F4. However, there were some inconsistencies between calculated DOR and original AUROC. For example, for the detection of cirrhosis, results were mixed with some studies showing TE-LSM superiority over APRI, FIB-4, and FibroTest,[108,129,132,142] whereas other studies showed no difference in accuracy[108,130,133,138,140,141] (Table 9).

HCV/HIV

No difference in diagnostic performance between TE-LSM and blood tests (FIB-4 and FibroTest) was observed for detection of significant fibrosis based on two studies.[143,144] TE had better performance than APRI for one of two tested cutoff values (i.e., 0.5).

HBV

Diagnostic performance of enhanced liver fibrosis (ELF), FibroTest, and TE-LSM were similar for prediction of significant fibrosis, whereas TE-LSM and FibroTest had higher AUROCs than ELF for predicting advanced fibrosis, and TE-LSM predicted cirrhosis more accurately than ELF and FibroTest in treatment-naïve patients with HBV.[163] In another study of treatment-naïve patients with HBV, TE-LSM outperformed ELF for detection of advanced fibrosis/cirrhosis.[164] In our systematic review,[67] four showed improved accuracy of US-based elastography over APRI and FIB-4 for detection of advanced fibrosis and cirrhosis, based on DOR.[148–151] Of note, 2 studies demonstrated higher AUROC for TE-LSM compared to blood tests for F2-F4[147] and for cirrhosis.[151]

HBV/HIV

In one study not included in our systematic review, TE-LSM outperformed APRI and FIB-4 for detection of advanced fibrosis in HBV/HIV coinfected adults on combined antiretroviral therapy.[165]

NAFLD

A meta-analysis comparing blood-based, US elastography, or MRE in NAFLD (64 articles, 13,046 subjects) showed that MRE-LSM and SWE-LSM had the highest diagnostic accuracy for diagnosing any fibrosis and cirrhosis.[77] The AUROC values using

TABLE 8 Components of blood-based biomarker algorithms for fibrosis[a]

References	Study cohort	Clinical variables	Indirect markers	Direct markers	Model algorithm
APRI,[120]	HCV	—	AST, platelets	—	[(AST level/ULN)/platelet count (10^9/L)]×100
Fibrosis-4 Index (FIB-4),[121]	HIV-HCV	Age	AST, ALT, platelets	—	Age (y)×AST (U/L) Platelet count (10^9/L)×$\sqrt{}$ALT (U/L)
NAFLD Fibrosis Score (NFS),[122]	NAFLD	Age, BMI, IFG/diabetes	AST, ALT, platelets, albumin	—	−1.675+(0.037×age)+(0.094×BMI)+1.13×IFG/diabetes (yes = 1, no = 0) +0.99×(AST/ALT ratio) − (0.013×platelets) − (0.66×albumin)
Easy Liver Fibrosis Test (eLIFT),[123]	Mixed	Age, Sex	GGT, AST, platelets, prothrombin index	—	Component weighted scores (0-4)
FibroTest,[124]	HCV	—	α2M, GGT, total bilirubin, haptoglobin, ApoA-I[1]	—	Proprietary
ELF,[125]	Mixed	Age	—	HA, PIIINP, TIMP-1	Proprietary
FibroSpect II,[126]	HCV	—	α2M	HA, TIMP-1	Proprietary
HepaScore,[127]	HCV	Age, Sex	Total bilirubin, α2M, GGT	HA	Proprietary
FibroMeter,[128]	Mixed	Age	Platelets, prothrombin index, urea, AST, α2M	HA	Proprietary

[a]Original study cohorts are referenced.

Abbreviations: APoA-1, apolipoprotein A-1; eLIFT, easy liver fibrosis; FIB-4, Fibrosis-4 index; HA, hyaluronic acid; IFG, impaired fasting glucose; INR, international normalized ratio (also known as prothrombin time); NFS, NAFLD fibrosis score; PIIINP, amino-terminal propeptide of type III procollagen; TIMP-1, tissue inhibitor matrix metalloproteinase 1; U, units; ULN, upper limit of normal; α2M, α2-macroglobulin.

TABLE 9 Performance of blood-based markers compared with imaging methods for diagnosis of liver fibrosis

Disease	Fibrosis stage	Imaging test[a] (cutoff)	Blood test (cutoff)	POR (95% CI)	References
HCV	F0-1 vs F2-4	TE 7 (6.5 to 7.4) kPa	APRI 0.5 (0.37 to 0.67)	2.31 (0.39-13.54)	[108,129–131]
			APRI 1.5	2.05 (0.49-8.58)	[132]
			APRI 1 (0.75 to 1.1)	1.41 (0.51-3.94)	[133,134]
			FIB-4 1.05	**8.48 (4.88-14.76)**	[129]
			FIB-4 1.45 (1.29 to 1.47)	2.85 (0.84-9.61)	[108,133]
			FIB-4 2.1	0.05 (0.001-26.71)	[130]
		pSWE 1.22 m/s	FIB-4 1.45 (1.26 to 1.53)	0.59 (0.21-1.65)	[108,133]
			APRI 0.67	0.70 (0.20-2.42)	[108]
			APRI 0.75	0.28 (0.02-3.53)	[133]
	F0-2 vs F3-4	TE 10 (9.5 to 10.4) kPa	**APRI 0.62**	**11.62 (1.58-85.47)**	[135,136]
			APRI 1.13	1.92 (0.56-6.62)	[134]
			FIB-4 1.45	**2.58 (1.50-4.43)**	[123]
			FIB-4 1.87	4.77 (0.48-47.85)	[135]
			FIB-4 3.25	**51.44 (22.53-117.48)**	[137]
		pSWE 1.7 (1.61 to 1.84) m/s	FIB-4 3.25 (3.21 to 3.97)	1.47 (0.15-14.33)	[138,139]
			APRI 0.62	**11.58 (2.37-56.53)**	[140]
	F0-3 vs F4	pSWE 2 (1.73 to 2.48) m/s	APRI 0.5 (0.25 to 0.75)	0.71 (0.12-4.16)	[140]
			APRI 1.5 (1.27 to 1.73)	2.34 (0.04-140.56)	[133,138]
			FIB-4 4	0.05 (0.001-29.81)	[133]
		TE 11 (10 to 11.9) kPa	APRI 2	0.83 (0.002-441)	[141]
		TE 13 (12 to 14) kPa	**APRI 1 (0.76 to 1.2)**	**31.99 (4.54-225.58)**	[129]
			APRI 1.5 (1.27 to 1.73)	2.65 (0.32-22.12)	[130,133]
			APRI 2 (2 to 4.3)	**10.33 (3.76-28.37)**	[108,132]
			FIB-4 1.45 (0.8 to 2)	**7.09 (1.94-25.82)**	[129,135]
			FIB-4 2.31	**24.48 (1.87-320.86)**	[130]
			FIB-4 4	0.11 (0.001-76.52)	[133]
			FibroSure/FibroTest 0.75 (0.7 to 0.81)	**2.98 (1.04-8.55)**	[142]

TABLE 9. (*continued*)

Disease	Fibrosis stage	Imaging test[a] (cutoff)	Blood test (cutoff)	POR (95% CI)	References
HCV/HIV	F0-1 vs F2-4	TE 7 (6.5 to7.4) kPa	**APRI 0.5**	**4.57 (1.81-11.56)**	[143,144]
			APRI 1.1	1.30 (0.34-5.07)	[144]
			APRI 1.5 (1.3 to 1.54)	2.38 (0.86-6.60)	[143,144]
			FIB-4 1.45 (1.21 to 1.65)	3.00 (0.83-10.82)	[144]
			FibroSure/FibroTest 0.48 (0.4 to 0.5)	0.85 (0.31-2.39)	[143,144]
HBV	F0-1 vs F2-4	pSWE 1.2 (0.95 to 1.26) m/s	APRI 0.36	0.99 (0.140-7.09)	[145]
			APRI 1	1.46 (0.17-12.66)	[145]
			FIB-4 0.63	3.43 (0.39-29.63)	[145]
			FIB-4 2.2	0.80 (0.10-6.56)	[145]
		TE 7 (6.5 to7.4) kPa	APRI 0.5 (0.17 to 0.67)	5.01 (0.98-25.58)	[146]
			FIB-4 3.25 (2.71 to 4.9)	0.86 (0.10-7.82)	[147]
	F0-2 vs F3-4	TE 8 (7.6 to 8.4) kPa	**FIB-4 1.45**	**16.73 (3.76-74.47)**	[148]
			FIB-4 3.25	7.59 (0.90-63.71)	[148]
	F0-3 vs F4	pSWE 1.8 (1.74 to 1.98) m/s	**APRI 0.5**	**19.95 (1.54-258.17)**	[149]
			FIB-4 2.83	**34.03 (3.41-339.16)**	[149]
		TE 11 (10 to 11.9) kPa	**APRI 0.5**	**3.03 (1.17-7.85)**	[150]
			APRI 0.8	**9.25 (4.99-17.13)**	[151]
			APRI 2	0.65 (0.001-344.43)	[141,152]
			FIB-4 1.45 (0.8 to 1.94)	**3.09 (1.65-5.79)**	[150,151]
NAFLD	F0-1 vs F2-4	TE 7 (6.5 to 7.3) kPa	APRI 0.5	0.94 (0.27-3.30)	[153]
	F0-2 vs F3-4	pSWE 1.55 (1.4 to 1.59) m/s	APRI 0.5 (0.43 to 0.71)	2.28 (0.81-6.42)	[154]
		TE 10 (9.5 to 10.4) kPa	APRI 0.5	1.46 (0.64-3.37)	[155]
			APRI 1	4.35 (0.39-48.46)	[156]
			APRI 1.5	1.75 (0.26-11.91)	[155,157]
			FIB-4 1.3 (0.85 to 1.3)	**1.57 (1.02-2.43)**	[155,158]
			FIB-4 2.67 (2.09 to 2.67)	1.27 (0.69-2.34)	[155,156,158]
			FIB-4 3.25	3.32 (0.24-45.54)	[159]
				9.01 (0.95-85.67)	[160]

TABLE 9. (*continued*)

Disease	Fibrosis stage	Imaging test[a] (cutoff)	Blood test (cutoff)	POR (95% CI)	References
		MRE 3.7 (3.6 to 3.8) kPa	APRI 1		
			FIB-4 1.3	6.16 (0.75-50.39)	[160]
			FIB-4 2.67	5.98 (0.55-65.38)	[160]
ALD	F0-2 vs F3-4	2D-SWE 16.1 kPa	**APRI 1**	**25.35 (7.68-83.62)**	[161]
			FIB-4 3.25	**10.35 (3.13-34.23)**	[161]
		TE 15 kPa	**APRI 1**	**16.79 (5.56-50.76)**	[161]
			FIB-4 3.25	**6.86 (2.26-20.78)**	[161]
	F0-3 vs F4	TE 15 kPa	**FibroSure/FibroTest 0.75**	**5.00 (1.54-16.25)**	[162]

Note: Studies with significant differences are bolded.
[a]Significant differences in AUC.
Abbreviation: TE, transient elastography.

BARD score, APRI, FIB-4, NFS, TE-LSM M probe/XL probe, SWE-LSM, and MRE-LSM for diagnosing advanced fibrosis were 0.76, 0.77, 0.84, 0.84, 0.88, 0.85, 0.95, and 0.96, respectively; SWE-LSM and MRE-LSM were significantly higher than all blood-based NILDA.[77] Improved performance for F3-4 was also found for MRE when compared to FIB-4 and NFS[113] and for TE-LSM when compared to FIB-4, NFS, BARD, and APRI.[166] However, evidence is not consistent on improved accuracy of imaging-based over blood-based NILDA for NAFLD. A large study comparing NFS, FIB-4, ELF, and TE-LSM (AUROC 0.74 for NFS, 0.78 for FIB-4, and 0.80 for ELF and TE) for the detection of F3-4[78] and another study comparing proprietary blood markers and TE-LSM found no difference; TE-LSM did outperform FIB-4 and NFS.[167] Similarly, a third study found TE-LSM and FibroMeterV2G (second generation FibroMeter) to be the two best-performing tests (F3-4 AUROCs of 0.83 and 0.82, respectively).[167] Of note, the pooled analysis of 2 studies showed superior performance for TE-LSM over FIB-4 for detection of F3-4 in our systematic review,[155,158] but no differences were identified in the 6 remaining studies.[153,154,156,157,159,160]

ALD

In a prospective study comparing ELF, FibroTest, and TE-LSM, the latter had the best accuracy for F3-4 with an AUROC of 0.97,[161] although another study found equivalent performance among TE-LSM, FibroTest, and PGAA (an index combining prothrombin time, gamma-glutamyl transferase [GGT], apolipoprotein A1, and α-2-macroglobulin).[162] In our systematic review,[67] US-based elastography demonstrated higher performance for F3-4 and F4 when compared to APRI, FIB-4, and FibroTest[168,169] (Table 9).

Other CLD

NILDA for AIH is covered elsewhere.[7] A systematic review of 16 studies in AIH hepatitis showed that TE-LSM had better performance for detection of F3-4 compared to APRI and FIB-4.[170] In a small PSC prospective study, TE-LSM performance was comparable to that of hyaluronic acid but superior to APRI, FIB-4, and Mayo risk score for F2-4 and F3-4.[169] In 103 patients with PBC, TE-LSM performed better than blood-based NILDA (APRI, FIB-4, hyaluronic acid, AST/ALT ratio, and Mayo risk score) for diagnosis of F2-4, F3-4, and cirrhosis.[170] These results contrasted with a mixed etiology cohort revealing comparable diagnostic performance for TE-LSM, FibroTest, and ELF.[171]

PICO 4: In adult patients with CLD, including hepatocellular (HCV, HCV/HIV, HBV, HCV/HBV, HBV/HIV, NAFLD, ALD) or cholestatic (PSC, PBC) disorders, is the combination of an imaging-based NILDA with a blood-based NILDA more accurate than a single test for staging fibrosis (F0-1 vs. F2-4, F0-2 vs. F3-4, F0-3 vs. F4) using histopathology as the reference?

Guideline Statement:

5. In adults with CLD undergoing initial fibrosis staging, AASLD suggests combining blood-based and imaging-based NILDA, particularly for the detection of significant fibrosis (F2-4) and advanced fibrosis (F3-4). (conditional recommendation, low quality of evidence)

TECHNICAL REMARKS

- Most studies have included TE-LSM, and there are limited data on MRE-LSM or other US elastography methods, combined with blood-based markers.
- Tests can be utilized in a concomitant or sequential fashion. Although synchronous combinations of blood-based NILDA and TE-LSM reduce misclassification rates for advanced fibrosis, they result in a "gray zone" classification and thus increase accuracy at the expense of increasing the number of needed liver biopsies.
- Improved accuracy for F2-4, F3-4, and F4 for combined versus single testing, varies according to the tests under consideration and how they are combined in a synchronous or sequential fashion.
- Utilization of blood-based and imaging-based NILDA algorithms have been validated for specific pragmatic applications, such as population-based screening, referral pathways in primary care, or staging in specialty clinics, which the clinician will need to consider prior to combining NILDA tests and drawing clinical conclusions from their results.
- The studies on chronic HCV are from the interferon era, and there were no studies that assessed combined tests relative to liver histology following direct-acting antiviral (DAA) therapy. In patients with chronic HCV (with viremia), the addition of blood-based NILDA to US-based elastography improves diagnostic accuracy for detecting significant fibrosis.
- Combination studies in chronic HBV were from Asian cohorts, and there were no studies using combined tests to assess fibrosis in non-Asian cohorts. In patients with chronic HBV (HBeAg positive and HBeAg negative), the addition of blood-based NILDA to US-based elastography does not improve diagnostic accuracy for detecting significant fibrosis.
- Combination studies in NAFLD (not necessarily MASLD) included TE-LSM in the assessment of advanced fibrosis but not cirrhosis. In patients with NAFLD, the sequential combination of imaging-based elastography and blood-based NILDA may improve diagnostic accuracy for detecting advanced fibrosis.
- There are very few studies in patients with other CLD.

EVIDENCE AND RATIONALE

Combination algorithms of blood-based biomarkers and elastography were initially developed for the management of patients with HCV. The performance of these have been evaluated as either synchronous (paired application of tests) or sequential (second test following an inconclusive initial test) approaches (Table 10A-C). Combined noninvasive approaches, usually in sequence, may have pragmatic indications for use in clinical practice to identify advanced stage, improve population-based screening, and simplify referral pathways from primary to tertiary care.[186,187] However, the choice of which noninvasive test is done first (blood- or imaging-based NILDA) has not been established.

HCV

An early study assessed a synchronous combination of TE-LSM with FibroTest in 183 patients with HCV. Compared to TE-LSM alone, synchronous TE-LSM +FibroTest had a higher AUROC for significant and advanced fibrosis but not for cirrhosis.[172] This combination was subsequently compared to a sequential APRI and FibroTest blood-marker algorithm (sequential algorithm for fibrosis evaluation [SAFE]) in patients with HCV. For significant fibrosis, the accuracy of TE-LSM +FibroTest was lower than SAFE, but it was estimated that fewer liver biopsies would be required to assess discordant cases with the former. For cirrhosis, the accuracy for combined TE-LSM+FibroTest was higher than SAFE, but there was no effect on the need for liver biopsy.[188] Both algorithms were evaluated in independent HCV cohorts; one study confirmed prior observations of lower diagnostic accuracy for significant fibrosis and fewer required biopsies for TE-LSM+FibroTest compared to SAFE. For F4, the TE-LSM+FibroTest combination had a higher diagnostic accuracy than SAFE, but in contrast to prior observations, this approach required a higher rate of liver biopsy.[189] Compared to TE-LSM alone, a synchronous classification with FibroMeter+TE-LSM had increased accuracy

TABLE 10A Combination of elastography and blood-based markers for diagnosis of significant fibrosis (F2-4)

References	No. of biopsies (F2-4 prevalence)	Elastography type and optimal LSM	Single test AUC	*Combined test AUC	Comments
HCV[172]	183 (74%)	TE-LSM 7.1 kPa	TE-LSM = 0.83 FT = 0.85 APRI = 0.78	TE-LSM+APRI = 0.84 TE-LSM+FT = 0.88 TE-LSM+FT +APRI = 0.88	Agreement FT and TE-LSM 77%; biopsy confirmed F2-3 = 84%
HCV[173]	729 (58.4%)	TE-LSM NA	TE-LSM = 0.79 FM = 0.81	TE-LSM+FM = 0.85	Improved AUC for combination compared to FM or TE-LSM alone
HCV[141]	382 (47%)	TE-LSM 5.2 kPa	TE-LSM = 0.82 FM = 0.83 FT = 0.81 APRI = 0.78 ELF = 0.78 HS = 0.82 FIB-4 = 0.78	Not provided	Accuracy increased from 70%-73% (single test) to 78%-82% for TE-LSM combination
HBV[96]	81 (63%)	ARFI 1.295 m/s TE-LSM 8.3 kPa	ARFI = 0.76 TE-LSM = 0.75 Forns = 0.73	Accuracy ARFI+Forns = 90.7% TE-LSM +Forns = 76.1%	Discordance 24%-34% for synchronous tests
HBV[98]	92 (72%)	ARFI 1.27 m/s TE-LSM 6.6 kPa	ARFI = 0.91 TE-LSM = 0.87 APRI = 0.79	ARFI+TE-LSM +APRI = 0.92	No difference for linear combination over elastography alone
HBV[174]	70 (34%)	TE-LSM 7.5 kPa	TE-LSM = 0.87 Blood markers = 0.86	TE-LSM +markers = 0.86	No difference for combination compared with TE-LSM or blood-marker panel (HA, PIIINP, type IV collagen, ALT, AST) alone
HBV[145]	101 (55%)	ARFI 0.97 and 1.36 m/s	ARFI = 0.70 APRI = 0.62 FIB-4 = 0.64	ARFI+APRI+FIB-4—not provided	New thresholds for APRI/FIB-4. Combination at upper/lower cutoffs reduced biopsy for F2-4 in 44%
HIV-HCV[141]	116 (41%)	TE-LSM 7.1 kPa	TE-LSM = 0.87 FT = 0.85 APRI = 0.71	Accuracy TE-LSM+FT = 61.2%	Synchronous algorithm. Lower correct classification (61.2%) compared with TE-LSM (80.2%) and FT (73.3%) alone
HIV-HBV[175]	59 (61%)	TE-LSM 5.9 kPa	TE-LSM = 0.85 FT-Accuracy 81%	Sequential TE-LSM → FT = not provided	Most receiving cART and 68% with normal ALT Sequential TE-LSM and FT biopsy required in 33% discordant cases
NAFLD[176]	215 (32%)	TE-LSM 5.8 kPa	TE-LSM = 0.85 FM = 0.77 APRI = 0.65 FIB-4 = 0.65 NFS = 0.65	FM-TE-LSM = 0.85	Proprietary algorithm combining FM-TE-LSM. High NPV for TE-LSM Sequential application for FM after TE-LSM increased PPV 71% to 84%
PBC[177]	114 (84%)	TE-LSM 5.9 kPa	TE-LSM = 0.89 APRI = 0.66 FIB-4 = 0.59 Forns = 0.73	TE-LSM+APRI = 0.89 TE-LSM+FIB-4 = 0.89 TE-LSM+Forns = 0.89	No increase in diagnostic accuracy for combination compared to TE-LSM alone

TABLE 10A. (*continued*)

References	No. of biopsies (F2-4 prevalence)	Elastography type and optimal LSM	Single test AUC	*Combined test AUC	Comments
Mixed CLD, 2009[178] CHC/CHB = 49% ALD = 27%	390 (74%)	TE-LSM NA	TE-LSM = 0.87 FM = 0.83	TE-LSM+FM = 0.89	Synchronous algorithm; higher AUC for combined test
Mixed CLD[179] CHC/CHB = 40% HIV-HCV = 22%, NAFLD = 13% ALD = 11%	1968 (58%)	TE-LSM/A	TE-LSM = 0.79-0.92 FM = 0.70-0.85	TE-LSM+FM = 0.84-0.90	Higher AUC for combined tests for CHC

Note: All synchronous (paired) assessments unless stated; sequential tests denoted by (→).
Abbreviations: AUC, area under the receiver operating characteristic curve; cART, combined antiretroviral therapy; CHB, chronic hepatitis B; CHC, chronic hepatitis C; FIB-4, Fibrosis-4 index; FM, FibroMeter; FT, FibroTest; HS, HepaScore; NA, not available/not applicable; NFS, NAFLD fibrosis score; TE, transient elastography.

for F2-4 and F3-4 but not F4.[173] Overall accuracy for FibroMeter with TE-LSM was comparable to TE-LSM +FibroTest and able to eliminate biopsy for a diagnosis including six classes of fibrosis.[189] Another study noted that synchronous combinations of blood markers, such as FibroTest, FibroMeter, or HepaScore, and TE-LSM were able to improve accuracy and reduce need for biopsy for significant fibrosis but not cirrhosis.[141] Other studies with mixed liver disease cohorts have indicated an incremental benefit in diagnostic accuracy for significant fibrosis[178] and cirrhosis[179] in patients with HCV using combined TE-LSM and FibroMeter.

HBV

A study in 156 patients with HBV, using different LSM thresholds for normal or elevated ALT, indicated that a sequential TE-LSM and Forns Index algorithm was able to improve confirmatory diagnosis for advanced fibrosis compared to TE-LSM alone.[180] A subsequent study of 85 patients with HBV confirmed that the performance for a sequential TE and ELF algorithm for advanced fibrosis was comparable to TE-LSM alone.[181] Another study of 81 patients compared synchronous Forns Index with ARFI or TE-LSM and noted a higher accuracy for significant fibrosis with ARFI+Forns Index compared to TE-LSM+Forns Index, but comparisons with single tests were not provided.[96] A study in 92 patients with HBV, using an integrated analysis that combined ARFI, TE-LSM, and APRI into a linear algorithm noted no differences in AUROCs for significant fibrosis and cirrhosis as compared to single tests.[98] In another study, a synchronous combination of 5 blood biomarkers (hyaluronic acid, N-terminal propeptide of procollagen type III, type IV collagen, ALT, and AST) and TE-LSM had a similar AUROC compared to TE alone for significant fibrosis.[190] Another study in 101 patients with chronic hepatitis B evaluated the synchronous combination of ARFI+APRI +FIB-4 but did not improve sensitivity and specificity compared to newly derived upper and lower thresholds for individual tests.[145] In a single center study of 222 patients with HBV, the sequential TE-LSM and ELF algorithm was more accurate than synchronous TE-LSM+ELF in detecting advanced fibrosis and cirrhosis but comparisons to single tests were not provided.[174]

For patients coinfected with HBV/HIV on stable antiretroviral therapy, sequential combinations of TE and FibroTest more accurately detected significant and advanced fibrosis than single tests.[175] The addition of APRI or FIB-4 did not improve diagnostic accuracy or reduce misclassification rates for advanced fibrosis compared to TE-LSM alone for these patients who are coinfected.[165] No studies were identified that evaluated combination algorithms to assess changes in fibrosis on histology, either as part

TABLE 10B Combination of elastography and blood-based markers for diagnosis of advanced fibrosis (F3-4)

References	No. of biopsies (F2-4 prevalence)	Elastography type and optimal LSM	Single test AUC	*Combined test AUC	Comments
HCV[172]	183 (45%)	TE-LSM 9.5 kPa	TE-LSM = 0.90 FT = 0.90 APRI = 0.84	TE-LSM+APRI = 0.91 TE-LSM+FT = 0.95 TE-LSM+FT+APRI = 0.95	Agreement FT and TE-LSM 70% Biopsy confirmed F3-4 in 95%
HCV[173]	729 (33%)	N/A	TE-LSM = 0.85 FM = 0.83	TE-LSM+FM = 0.87	Improved AUC for combination compared with FM or TE-LSM alone
HBV[180]	238 (36%)	TE-LSM 9-12 kPa (normal-elevated ALT)	TE-LSM = 0.80-0.88 Forns = 0.70-0.72	TE-LSM+Forns—Not provided	Results provided for training and validation cohorts; new thresholds for Forns (5.2 and 8.4) Reduced proportion of incorrect diagnosis for LSM-Forns (3%-5%) than LSM alone (3%-15%)
HBV[181]	323 (40%)	TE-LSM 9-12 kPa (normal-elevated ALT)	TE-LSM = 0.73-0.83 ELF = 0.68-0.69	TE-LSM+ELF—Not provided	Results provided for training and validation cohorts; new thresholds for ELF 8.4 (exclusion) and 10.8 (confirmatory); similar performance for ELF-LSM and LSM alone
HBV[174]	222 (64%)	TE-LSM 7.5/8-10.5/11 kPa (normal-elevated ALT)	TE-LSM = 0.89 ELF = 0.70	TE-LSM+ELF—Paired or sequential AUC not provided	Sequential TE-LSM-ELF better than concurrent use for avoiding biopsy (69%-72% vs 42%-59%)
HIV-HBV[175]	59 (33%)	TE-LSM 7.6 kPa	TE-LSM = 0.85 FT-Accuracy 81%	TE-LSM+FT—Not provided	Most receiving cART and 68% with normal ALT; sequential TE-LSM and FT Biopsy required in 29% discordant cases
HIV-HBV[165]	63 (21%)	TE-LSM 7.8 kPa	TE-LSM = 0.78 APRI = 0.68 FIB-4 = 0.63	TE-LSM+FT or APRI—Not provided	No discriminatory benefit for TE-LSM+APRI or FIB-4 New optimal thresholds for APRI = 0.42, and FIB-4 = 1.76
NAFLD[182]	321 (22%)	TE-LSM 7.9 and 9.6 kPa	TE-LSM = 0.85-0.86 FIB-4 = 0.70-0.79 NFS = 0.73-0.80	TE-LSM+FIB-4 = 0.85-0.89 TE-LSM+NFS = 0.84-0.88	Included training and validation cohorts TE-LSM+NFS best diagnostic performance, but uncertainty in 41%-48%
NAFLD[176]	215 (20%)	TE-LSM 7.9 kPa	TE-LSM = 0.94 FM = 0.77 APRI = 0.72 FIB-4 = 0.70 NFS = 0.65	FM-TE-LSM = 0.90	Proprietary algorithm combining FM-TE-LSM high NPV for TE0-LSM-sequential application for TE-LSM-FM after TE-LSM increased PPV 61% to 89%
NAFLD[158]	761 (31%)	TE-LSM 7.9 and 9.6 kPa	TE-LSM = 0.86 FIB-4 = 0.79 NFS = 0.77 APRI = 0.72	Accuracy TE-LSM+NFS = 39% TE-LSM+ FIB-4 = 43% Sequential NFS or FIB-4 → TE-LSM = 70%	Paired combination had lower accuracy and 54%-58% uncertainty Better accuracy and lower uncertainty (19%-20%) for sequential tests
NAFLD[78]	3202 (71%)	TE-LSM 9.9 and 11.4 kPa (n = 1765)	TE-LSM = 0.80 ELF = 0.80 FIB-4 = 0.78 NFS = 0.74	Accuracy or AUC not provided for paired or sequential tests	Paired combination of TE-LSM+NFS or FIB-4 had 4%-5% misclassified but increased indeterminates (IND) (64%-65%) Sequential FIB-4 followed by TE-LSM reduced IND to 20% but higher misclassified rate (20%)

TABLE 10B. (*continued*)

References	No. of biopsies (F2-4 prevalence)	Elastography type and optimal LSM	Single test AUC	*Combined test AUC	Comments
NAFLD[183]	938 (41%)	TE-LSM 7.9 and 9.6 kPa	TE-LSM = 0.84 NFS = 0.72 FIB-4 = 0.76 FT = 0.74 HS = 0.76 FM = 0.79	Accuracy for Sequential tests FIB-4 → FM^{TE-LSM} = 88% TE-LSM → FM^{TE-LSM} = 90% NFS → TE-LSM = 80% FIB-4 → TE-LSM = 80%	Training and validation cohorts. FM^{TE-LSM} had higher accuracy and sensitivity as second-line test compared with TE-LSM alone
NAFLD[184]	278 (28%)	TE-LSM 9.9 kPa	TE-LSM = 0.89 APRI = 0.79 FIB-4 = 0.83 NFS = 0.80	FIB-4+TE-LSM = 0.92 NFS+TE-LSM = 0.91 APRI +TE-LSM = 0.90	Regression index of TE-LSM with various blood-based markers improved diagnostic accuracy
NAFLD[185]	224 (36%)	TE-LSM 11.45 kPa	TE-LSM = 0.84 ELF = 0.81 FIB-4 = 0.78	Accuracy Combined ELF+TE-LSM = 79% Sequential ELF+TE-LSM = 75%	Variable cohort-specific new ELF and LSM thresholds for optimal performance. No difference in accuracy for combined vs. sequential use, or compared with single tests
PBC[178]	114 (49%)	TE-LSM 7.6 kPa	TE-LSM = 0.92 APRI = 0.67 FIB-4 = 0.63 Forns = 0.67	TE-LSM+APRI = 0.92 TE-LSM+FIB-4 = 0.92 TE-LSM+Forns = 0.92	No increase in diagnostic accuracy for combination compared with TE-LSM alone
ALD[162]	193 (40%)	TE-LSM 12 kPa	TE-LSM = 0.90 FT = 0.85 APRI = 0.59 FIB-4 = 0.63 Forns = 0.64	TE-LSM+FT = 0.91	No increase in diagnostic accuracy for combination compared with TE-LSM alone
ALD[161]	289 (23%)	TE-LSM 15.5 kPa 2D-SWE 16.4 kPa	TE-LSM = 0.89 2D-SWE = 0.93 ELF = 0.92 FT = 0.88 APRI = 0.80 FIB-4 = 0.85 Forns = 0.86	TE-LSM+ELF = 0.96—Other combinations not provided	No difference in accuracy for TE-LSM in combination with blood-based markers (including ELF) compared with TE-LSM alone
Mixed CLD[179] CHC/CHB = 40% HIV-HCV = 22% ALD = 13% NAFLD = 11%	1968 (34%)	TE-LSM (N/A)	TE-LSM = 0.83-0.89 FM = 0.67-0.86	TE-LSM+FM = 0.85-0.92	Higher AUC for combined tests for CHC

Note: All synchronous (paired) assessments unless stated; sequential tests denoted by (→)

Abbreviations: AUC, area under the receiver operating characteristic curve; cART, combined antiretroviral therapy; CHB, chronic hepatitis B; CHC, chronic hepatitis C; FIB-4, Fibrosis-4 index; FM, Fibrometer; FT, Fibrotest; HS, Hepascore; NA, not available/not applicable; NFS, NAFLD fibrosis score; TE, transient elastography.

TABLE 10C Combination of elastography and blood-based markers for diagnosis of advanced fibrosis (F3-4)

References	No. of biopsies (F2-4 prevalence)	Elastography type and optimal LSM	Single test AUC	*Combined test AUC	Comments
HCV[172]	183 (25%)	TE-LSM 12.5 kPa	TE-LSM = 0.95 FT = 0.87 APRI = 0.83	TE-LSM+APRI = 0.95 TE-LSM+FT = 0.95 TE-LSM+FT+APRI = 0.95	Agreement FT and TE-LSM = 79% Biopsy confirmed F4 = 94%
HCV[173]	729 (15%)	TE-LSM (NA)	TE-LSM = 0.90 FM = 0.86	TE-LSM+FM = 0.92	No difference in AUC for combination vs LSM alone
HCV[141]	382 (15%)	TE-LSM 12.9 kPa	TE-LSM = 0.93 FM = 0.90 FT = 0.87 APRI = 0.87 ELF = 0.87 HS = 0.89 FIB-4 = 0.84	Not provided	Combination did not improve accuracy (93%) compared to single tests (86-92%)
HBV[98]	92 (31%)	ARFI 1.65 m/s TE-LSM 9.47 kPa	ARFI = 0.96 TE-LSM = 0.96 APRI = 0.85	ARFI+TE-LSM+APRI = 0.98	No difference for linear combination over elastography alone
HBV[174]	222 (53%)	TE-LSM 7.6/8 12/13 kPa, for normal-elevated ALT	TE-LSM = 0.85 ELF = 0.71	TE-LSM+ ELF- -Paired or sequential AUC and accuracy not provided.	Sequential TE-LSM→ELF better than concurrent use for avoiding biopsy (61-65% vs 24-49%)
HIV-HCV[143]	116 (11%)	TE-LSM 12.5 kPa	TE-LSM = 0.92 FT = 0.78 APRI = 0.73	Accuracy TE-LSM+FT = 68.1%	Synchronous algorithm. Lower correct classification (68.1%) compared to TE-LSM (85.3%) and FT (72.4%) alone
PBC[177]	114 (15%)	TE-LSM 11.4 kPa	TE-LSM = 0.99 APRI = 0.84 FIB-4 = 0.74 Forns = 0.86	TE-LSM+APRI = 0.99 TE-LSM+FIB-4 = 0.99 TE-LSM+Forns = 0.99	No increase in diagnostic accuracy for combination
ALD[162]	193 (15%)	TE-LSM 15 kPa	TE-LSM = 0.93 FT = 0.88 APRI = 0.63 FIB-4 = 0.80 Forns = 0.80	TE-LSM+FT = 0.94	No increase in diagnostic accuracy for combination compared to TE-LSM alone
Mixed CLD[178] CHC/CHB = 49% ALD = 27%	390 (31%)	TE-LSM (NA)	TE-LSM = 0.92 FM = 0.83	TE-LSM+FM = 0.92	Synchronous algorithm; no difference for combination vs LSM alone
Mixed CLD[179] CHC/CHB = 40% HIV-HCV = 22% ALD = 13% NAFLD = 11%	1968 (18%)	TE-LSM (NA)	TE-LSM = 0.90-0.95 FM = 0.73-0.92	TE-LSM+FM = 0.88-0.96	Higher AUC for combined tests for CHC

[a]All synchronous (paired) assessments unless stated; sequential tests denoted by (→).

Abbreviations: AUC, area under the receiver operating characteristic curve; cART, combined antiretroviral therapy; CHB, chronic hepatitis B; CHC, chronic hepatitis C; FIB-4, Fibrosis-4 index; FM, FibroMeter; FT, FibroTest; HS, HepaScore; NA, not available/not applicable; NFS, NAFLD Fibrosis Score.

of the natural history of HBV or secondary to antiviral therapy.

NAFLD

A study in 321 patients with NAFLD showed that synchronous TE-LSM+NFS provided the best diagnostic accuracy for fibrosis but increased the diagnostic "gray zone" to 48%, yielding a correct fibrosis classification in just over one-half of patients.[182] Another study noted high NPV for significant and advanced fibrosis using TE-LSM alone; however, PPV improved when using the combined TE-LSM+Fibrometer algorithm as a sequential second-line test in patients with LSM above a designated threshold.[176] A cohort study of 761 patients from 3 centers in Europe and Asia compared various synchronous and sequential combinations of TE-LSM, NFS, and FIB-4 for advanced fibrosis. Paired combinations had lower accuracy and uncertainty for advanced fibrosis in over one-half of patients. Sequential TE-LSM for patients in the indeterminate range for NFS or FIB-4 or using these simple blood-based markers following TE >7.9 kPa was associated with an increased accuracy of 70%. This approach reduced uncertainty to 20% with 9-11% misclassified.[158]

Clinical trials in NAFLD continue to provide important data regarding noninvasive tests for advanced fibrosis. The diagnostic performance of combined TE-LSM with ELF, FIB-4, or NFS for advanced fibrosis was evaluated in a large multicenter phase III trial of 3202 patients with NAFLD (71% of participants had F3-4). Synchronous combinations of TE-LSM+FIB-4 or NFS reduced the misclassification rates to $<5\%$ but increased the indeterminate classification for nearly two-thirds of patients. Sequential FIB-4 and TE-LSM reduced the indeterminate range classification to 20% but increased the proportion misclassified to 20% in this high advanced fibrosis prevalence cohort.[78] Another cohort study of 938 patients from 4 centers in France determined that combining either FIB-4 or NFS with sequential TE-LSM increased the accuracy for advanced fibrosis.[183] Other studies from Asian cohorts found that synchronous or sequential strategies (ELF or FIB-4 followed by TE-LSM) did not improve diagnostic accuracy (0.75-0.79) for advanced fibrosis over single tests (0.74-0.78).[185] Conversely, another study combining TE and blood-based markers into a regression index increased diagnostic accuracy for advanced fibrosis.[184] A model combining TE-LSM, controlled attenuation parameter (CAP; for steatosis), and AST (FAST score) with upper and lower index cutoffs for sensitivity and specificity at ≥ 0.9 has been proposed to identify patents with NASH, elevated NAFLD activity score (NAS ≥ 4), and $\geq$ F2. However, 30-39% of patients were still classified as indeterminate.[191] More recently, a study of 577 subjects with suspected NASH compared combination FIB-4 with TE-LSM and/or 2D-SWE-LSM and observed that combining FIB-4 (using a threshold of 1.3) with either TE-LSM or 2D-SWE-LSM (both thresholds 8 kPa) in a two-step process performed better than either test alone. When all three tests were combined, the performance remained high (accuracy 81%, sensitivity 70%, specificity 89.5%, PPV 82%, NPV 81%) and reduced the need for liver biopsy to 7.3%.[192] Finally, a recent cost-effectiveness analysis assessed FIB-4 followed by either LSM (by either TE or MRE) or initially performing liver biopsy to detect cirrhosis. FIB-4+TE-LSM was the least costly strategy, followed by FIB-4 +MRE-LSM, with FIB-4+liver biopsy being the most expensive.[193] In clinical practice, a sequential approach using TE-LSM or ELF in those with FIB-4 ≥ 1.3 is recommended.[79]

Other CLD

Few studies have evaluated combination elastography and blood-based markers to assess fibrosis in nonviral or non-NAFLD CLD. A study in 114 patients with PBC noted no differences in diagnostic accuracy for significant, advanced fibrosis, or cirrhosis using synchronous combinations of TE-LSM and simple blood-based markers APRI, FIB-4, Forns Index, or FibroIndex compared to TE alone.[177] A study in 193 patients with ALD determined that combined TE+FibroTest had comparable diagnostic accuracy to TE-LSM alone for advanced fibrosis and cirrhosis.[162] A study in 289 patients with ALD found no incremental change in diagnostic accuracy for advanced fibrosis combining TE with ELF or other blood-based tests, including FibroTest, APRI, and FIB-4.[161]

PICO 5: In adult patients with CLD, including hepatocellular (HCV, HCV/HIV, HBV, HCV/HBV, HIV/HBV, NAFLD, ALD) or cholestatic (PSC, PBC) disorders, does longitudinal imaging-based NILDA accurately predict progression or regression of fibrosis in its natural history or response to therapy relative to longitudinal hepatic histological evaluation as the reference?

Guideline Statements:

6. AASLD suggests against the use of imaging-based NILDA as a standalone test to assess regression or progression of liver fibrosis. (ungraded statement)

7. AASLD suggests interpreting a longitudinal decrease or increase in liver stiffness within an individualized clinical context that considers the effect of NILDA modifiers and other supportive evidence of improving or worsening clinical course. (ungraded statement)
8. In patients with treated HBV and HCV, AASLD suggests using the LSM obtained prior to the start of antiviral therapy as the most accurate longitudinal NILDA parameter for the effect of prognostication, given the limited amount of evidence associating LSM with clinical outcomes once viral suppression or eradication is achieved. (ungraded statement)

TECHNICAL REMARKS

- LSM is affected by disease activity parameters other than fibrosis (Table 6A), and there is still insufficient evidence that changes in LSM values accurately identify regression or progression of fibrosis.
- In limited studies with serial imaging-based NILDA and paired liver biopsies, LSM changed in parallel with the increase or decrease in histological fibrosis in patients with HCV, HBV, or NAFLD. Reduced LSM after HCV eradication and HBV suppressive treatment suggests some degree of reversion of fibrosis, whereas the increase in stiffness during long-term follow-up in PBC and PSC suggests fibrosis progression.
- Reductions in LSM immediately following antiviral treatment should not be interpreted as clear evidence of fibrosis regression. Absolute cutoffs for meaningful changes following viral eradication have not been established.
- Although promising data on the utility of imaging-based NILDA to study fibrosis trajectory and clinical course are accumulating, there is need for further research to determine whether they can be used alone to predict histologic change in fibrosis following disease-modifying therapies in all CLDs.

EVIDENCE AND RATIONALE

Multiple studies have assessed changes in liver fibrosis by means of serial biopsy, showing fibrosis regression[194–197] in viral hepatitis, regression/progression in NASH,[198,199] and progression in PBC.[200] Although imaging-based NILDA has opened the possibility of studying fibrosis trajectory without liver histology,[201] there is paucity of evidence to fully endorse this approach. Most published studies did not perform paired liver biopsies along with NILDA or did not have a baseline NILDA for comparison. Rather, conclusions were reached after contrasting observed against expected results (i.e., baseline histology vs. follow-up elastography) or by including indirect evidence of regression of fibrosis (i.e., changes in PHTN manifestations).[202,203] Even though such reports are valuable, they have inherent biases, as imaging-based NILDA is affected by factors other than fibrosis (Table 6A). As such, the Writing Group agreed to emphasize studies with scientific rigor, including concomitant NILDA and liver histology at baseline and follow-up (Table 11).

Rapid LSM changes are common in patients with chronic HBV during a flare[48] or in ALD with alcohol-induced hepatitis.[44,82] In HCV, viral eradication is followed by an abrupt, substantial decrease in LSM (up to 15 kPa following DAA).[219,220] Rather than reflecting fibrosis regression, rapid changes likely reflect reduced inflammation as they parallel ALT/AST decrease[74,82]; similar rapid changes have been described for blood-based NILDA.[221,222] It remains unclear to what degree improved inflammation contributes to decreased stiffness following successful treatment in HCV or HBV.[223–225] Hence, when aiming to stage fibrosis in viral hepatitis, NILDA values obtained prior to the initiation of antiviral therapy are considered reflective of fibrosis. In fact, most of the LSM cutoff values that have been reported to detect cirrhosis or predict clinical outcomes were identified in patients who were viremic, although the field is rapidly evolving. As such, until the inflammatory component—or bile duct obstruction in cholestatic liver disease—can be separated from the changes in stiffness that are exclusively related to improving/worsening fibrosis, the imaging NILDA trajectory should be used to support regression or progression of fibrosis but not as conclusive evidence.

TE-LSM is the most studied imaging-based NILDA evaluated longitudinally at par with liver histology (Table 11). In HCV-HIV, TE-LSM increased in the subset of patients with progressive fibrosis,[144] whereas in an HCV cohort there was a remarkable reduction in serial 6-monthly TE-LSM after up to 5.5 years of sustained virologic response (SVR).[204] In 12 of 15 patients who underwent post-SVR liver biopsies, a decrease in liver fibrosis was confirmed by histopathology. Interestingly, improved LSM correlated better with the collagen proportional area than with routine histologic staging, likely in relation to the location of "persistent post-SVR fibrosis," which is sinusoidal

TABLE 11 Longitudinal studies investigating the role of liver stiffness in the identification of fibrosis regression or progression

Author, year of study; assessed tool (reference)	CLD and staging	Biopsy N (follow-up n)	Change in biopsy fibrosis	NILDA change	NILDA interval	Comments/supporting evidence
Schmid, 2015; TE-LSM[144]	HIV-HCV F0-4 (F4 in 13%)	105	10/42 (24%) progressed by ≥ 1 stage	LSM increased by 3.4 kPa in progressors (vs. −0.15 in nonprogressors)	3 y	LSM detected rapid progression in 2 subjects. Effect of antivirals not assessed (only 8 patients with SVR)
Pan, 2018; TE-LSM[204]	HCV F ≥ 3 DAA-SVR (F4 in 67%)	84 (15)	12/15 (80%) regressed by ≥ 1 stage	LSM staging decreased in 62% (45% by ≥ 2 stages) (59% from F4 and 68% from F3)	Mean of 2 y	Decline in collagen proportionate area from 7.1% to 38% Platelets increased significantly
Wong, 2011; TE-LSM[205]	HBV NUC Rx (F4 in 11%)	71 (71)	11/71 (15%) progressed and 17/71 (24%) regressed by ≥ 1 stage	LSM changed by 0.4 kPa (−4.6 to 1.4) in progressors, by −2.7 kPa (−6.1 to −1.8) in regressors, and −1.7 kPa (−4.0 to 0) in static fibrosis	1 y	LSM changes weakly correlated with changes in histological fibrosis staging (Spearman's $r = 0.25$); potential confounding effect of ALT
Liang, 2018; TE-LSM[206]	HBV NUC Rx (F3-4 in 32%)	534 (164)	98/164 (60%) regressed by ≥ 1 stage	LSM changed by −3.3 kPa in regressors, and by 0.3 kPa in progressors	2 y	Two improvement phases, initial at −2.2 kPa/24 week, paralleling ALT changes, and late at −0.3 kPa/24 week
Dong, 2019; TE-LSM[76]	HBV NUC Rx (F3-4 in 21%)	556 (182)	72/182 regressed by ≥ 1 stage	LSM changed by −4.1 in regressors, and by −2.7 in progressors	1.5 y	The improvement in LSM correlated with improved inflammatory activity ($r = 0.395$, $p < 0.001$) and mildly with fibrosis ($r = 0.156$, $p = 0.03$)
Kong, 2019; TE-LSM[207]	HBV NUC Rx (F4 in 17%)	255 (212)	86/212 (41%) regressed by ≥ 1 stage	LSM decreased by 43% in regressors vs. 32% in non-regressors	1.5 y	Steeper LSM decline among regressors vs. non-regressors (-2.19% per month; $p < 0.001$) during initial 6 mo of treatment
Sun, 2019; TE-LSM[208]	HBV NUC Rx (F4 in 4%)	148 (148)	53/148 (36%) regressed by ≥ 1 stage	Drop in LSM from 9.3 ± 3.8 to 5.4 ± 1.4 kPa ($p < 0.05$)	2 y	LSM change in regressors or progressors was not reported. LSM did not predict regressed fibrosis, whereas high HBV DNA and METAVIR did
Wei, 2019; TE-LSM[209]	HBV NUC Rx ± p-IFN (All F2-F3)	289 (141)	39/141 (39%) regressed by ≥ 1 stage	LSM decreased from 8.7 kPa (6.7-13.7) to 5.8 (4.8-7.5) in regressors and 6.6 (5.4-8.9) in non-regressors	1.5 y	Along with AST, platelets, WBC, cholinesterase, ALT, and sex, LSM predicted fibrosis regression according to an artificial neural network model
Kamarajah, 2018; TE-LSM[210]	NAFLD F0-4 (F4 in 2%)	113 (80)	9/80 (11%) progressed and 19/80 (24%) regressed by ≥ 1 stage	LSM staging increased in 19% and decreased in 29%	1 y	LSM F3-4 without regression and F3-4 progressors had higher risk of adverse outcomes

Garg, 2018; TE-LSM[211]	NAFLD (F3-4 in 15%)	42 (32)	3/32 (9%) progressed and 18/32 (56%) regressed by 1 stage	Drop in LSM from 8.6 (6.2-10.5) to 6 (4.2-8.9) kPa, p = 0.003	1 y	Changed in LSM occurred early (third month) and there were significant drops in ALT, AST and BMI Ten patients did not consent for repeat liver biopsy
Nogami, 2019; TE-LSM[212]	NAFLD F0-4 (F4 in 12%)	34 (14)	2/14 (14%) regressed by ≥ 1 stage	LSM staging decreased in 32% and increased in 18%	10 y	Change in LSM correlated with fibrosis but not with inflammation or steatosis
Jayakumar, 2019; MRE[213]	NAFLD 2-3 (F3 in 63%)	54 (54)	8/54 (15%) progressed and 18/54 (33%) regressed by ≥ 1 stage	The AUROC was 0.57 (0.36-0.79) to detect progression of fibrosis and 0.79 (0.67-0.91) for regression	0.5 y	Poor correlation between MRE and baseline fibrosis stage ($r = 0.33$) or CPA ($r = 0.19$), but fair correlation with 24-week ($r = 0.55$ and $r = 0.54$, respectively)
Ajmera, 2020; MRE[202]	NAFLD F0-4 (F3-4 in 26%)	102 (102)	25% progressed and 28% regressed	18% had an increase in LSM of ≥ 15%	1.4 y	≥ 15% increase in LSM was strongest variable associated with rapid progression to advanced fibrosis (OR = 3.36, $p = 0.03$)
No baseline liver biopsy						
Puente, 2019; TE-LSM[214]	HCV F0-4 DAA-SVR (F4 in 37%)	271 (13)	N/A	LSM staging decreased in 34%	2 y	In 6/13 cases, LSM and biopsy stages coincided. LOXL2 levels lower if LSM < 9 kPa
No follow-up liver biopsy						
Stasi, 2013; TE-LSM[215]	HCV F0-4 IFN-based Rx (F4 in 23%)	74 (21)	N/A	LSM dropped from 10.8 ± 8.5 to 6.8 ± 4.6 ($p = 0.01$) in 30 patients with SVR	3 y	N/A
Enomoto, 2010; TE-LSM[216]	HBV F0-4 NUC Rx (F4 in 30%)	50 (38) NUC in 20	N/A	LSM dropped from 11 (7-15) to 8 (5-12) in NUC-treated	1 y	Fair correlation between LSM and biopsy staging ($r = 0.46$). LSM properly identified 1 regressor and 1 progressor of fibrosis (biopsy-proven)
Rinaldi, 2018; TE-LSM[217]	HBV F0-4 NUC Rx (F3-4 in 63%)	200 (171) NUC in 149	N/A	LSM dropped from 14 to 8 in F3-F4 and from 7 to 5 in F0-2 among NUC-treated	2 y	No changes in LSM among untreated patients
No baseline NILDA						
D'Ambrosio, 2013; TE-LSM[218]	HCV F4 IFN-based Rx SVR	37 (37)	20/37 (61%) regressed by ≥ 1 stage	LSM 9.1 kPa in regressed vs. 12.9 in nonregressed patients	5 y	Cirrhosis regression in 61%. Post-SVR LSM 61% sensitive and 95% specific to diagnose cirrhosis (threshold 12 kPa)

Abbreviations: IFN, interferon; LOXL2, lysyl oxidase like 2; MRE, magnetic resonance elastography; NUC, nucleotide; Rx, treatment; SVR, sustained viral response; TE, transient elastography; WBC, white blood cell count.

and not accounted for in typical staging systems.[204] Evidence in treated HBV shows an initial substantial decline in TE-LSM that is likely due to resolved inflammation, whereas a more gradual and sustained decline occurs after the first year of treatment, likely corresponding to improved fibrosis,[206] although there are conflicting data.[226] In NAFLD, patients without LSM-based regression or with F3-4 progression had the highest risk for adverse outcomes, further substantiating the clinical usefulness of changes in imaging-based NILDA,[210] and there is evidence of changes in LSM better correlating with fibrosis trajectory than with inflammation/steatosis.[212] After bariatric surgery, studies confirmed regression of fibrosis in almost half of patients along with a concomitant drop in TE-LSM.[211]

Given historical evidence of regression of cirrhosis (20-60% of post-SVR HCV and 40-100% of post-treatment HBV), repeat imaging-based NILDA provide indirect evidence of regression of fibrosis even in the absence of concomitant histology.[227–229] In TE-based studies without baseline histology (Table 11), one showed decreased fibrosis staging on the basis of LSM among patients with HCV after 2 years of follow-up.[214] In cases without follow-up histology, a decrease in LSM was observed among patients with HCV or HBV with a positive antiviral response after 1 to 3 years but not among patients with ongoing viremia.[208,215–217] In a cohort of patients with HCV, a decrease of >1 kPa/year was associated with improved survival.[230] In a study reporting long-term follow-up imaging-based NILDA only (i.e., no baseline NILDA) for patients with HCV with known F3-4 staging at baseline, those who experienced fibrosis regression on paired liver biopsies had remarkably lower LSM values, whereas almost all with persistent histological cirrhosis had TE-LSM ≥ 12 kPa.[218]

Serial TE in 150 patients with PBC followed for up to 5 years showed that an increase in LSM over time was a predictor of clinical outcomes.[170] In a study of 130 patients with PSC, there was an average increase of 3.9 ± 2.1 kPa/year between the first and last TE-LSM, and the change in LSM along with total bilirubin were the only variables linked to clinical outcomes.[169] The study also showed that patients exhibiting a positive response to ursodeoxycholic acid had an attenuated LSM rise versus nonresponder.[169] Because the non-invasive assessment was useful in predicting adverse events, including mortality, these data serve as indirect NILDA validation for determining progressive disease in PBC and PSC.

Data on SWE-LSM and MRE-LSM to follow fibrosis are limited. Following DAA-SVR in HCV, median LSM by MRE decreased from 4.2 to 3.3 kPa in 308 patients, and it decreased by 20% or more in almost half of them.[231] Two studies in patients with NASH plus paired biopsy showed conflicting results for MRE-LSM. The first was based on a clinical trial and found acceptable performance for detecting regression but poor discrimination for progressive fibrosis,[213] whereas the second (untreated patients) showed that an increase by $\geq 15\%$ in MRE-LSM reflected progression from early to advanced fibrosis with no association with regression[232] (Table 11). These results highlight the need to consider confounding factors such as CLD pharmacological/lifestyle interventions potentially affecting inflammation/steatosis when interpreting changes in sequential imaging-based NILDA. Newer technologies better correlating with histologic steatohepatitis, such as 3D MRE, would be of help to disentangle regression/progression of fibrosis from its confounders.[233]

PICO 6: In adult patients with NAFLD, are imaging tests such as US, CT, and TE-CAP accurate in grading hepatic steatosis (using histology, magnetic resonance spectroscopy [MRS], or MRI-proton density fat fraction [PDFF] as the reference)?

Guideline Statements:

9. In adults, TE-CAP has good diagnostic accuracy to grade steatosis and can be used in clinical practice. (ungraded statement)
10. In adults, imaging-based NILDA, specifically TE-CAP and MRI-PDFF or MRS, are superior to blood-based NILDA tests and should be used in the assessment of hepatic steatosis where available. (ungraded statement)

TECHNICAL REMARKS

- In adult patients with CLD, MRI-PDFF and MRS have excellent correlation with histology for the detection and grading of steatosis and can be used as a reference standard and for following response to treatment.
- TE-CAP is a point-of-care test that can be used as the first-line screening tool for quantitative steatosis assessment. However, there are overlapping values to differentiate adjacent grades, and TE-CAP does not have sensitivity to assess changes with therapy.
- The optimal cutoff to maximize sensitivity for detecting at least grade 1 ($\geq 5\%$) steatosis is 275 dB/m when using TE-CAP.

- The degree of steatosis decreases and may even disappear as fibrosis progresses, and as such, the lack of steatosis in a patient with advanced fibrosis or cirrhosis does not exclude fatty liver disease as an etiology.
- Conventional grayscale US can be used to screen for steatosis but is limited by operator dependence and lacks sensitivity and specificity for detection of steatosis. Furthermore, conventional US is unreliable for evaluating changes with therapy. However, steatosis quantification incorporated into conventional US machines is becoming more widely available.
- Noncontrast CT does not have sufficient sensitivity to detect mild degrees of steatosis and exposes patients to radiation. Thus, it is not recommended for assessing steatosis.
- MRI-PDFF has excellent diagnostic accuracy, better than that of grayscale US and TE-CAP, and can be used to assess changes with therapy and for clinical endpoints. However, MRI-PDFF may not widely available and is more expensive than TE-based assessment.
- The combination of blood- and imaging-based NILDA in algorithms to improve steatosis screening or diagnostic performance requires further study.

EVIDENCE AND RATIONALE

MRS accurately quantifies lipid fraction relative to water in the liver and is accepted as a reference standard for the assessment of hepatic steatosis.[234,235] Similarly, MRI-PDFF has shown excellent correlation with MRS[236–238] and liver histology[112,239–241] and can be used to assess the entire liver. Thus, these two MR techniques are NILDA but can also act as reference standards in the quantification of hepatic steatosis. These imaging tests have advantages compared to histology in that they are noninvasive, can assess larger amounts of liver while avoiding regions of focal fatty deposition, and avoid issues of intra- and interobserver variability associated with histologic assessment.[242,243] MRI-PDFF can be used to assess clinical outcomes in phase IIa clinical trials.[244] Studies have shown it is superior to CAP.[109,110,112,245] Unlike CAP, it is unaffected by BMI[246] (as long as the patient can fit in the magnet) or fibrosis. Using multipeak modeling with T2 correction, MRI-PDFF had 100% sensitivity, specificity, and AUROC for detecting at least 5.56% steatosis.[237] It has also been used to assess changes with therapy[247–250] and eligibility for living liver donation.[251]

However, MR is relatively expensive and is not universally available. Thus, less expensive and more available assessments are needed. Conventional imaging with US, CT, and MRI can assess for fatty liver with variable accuracy, particularly at low levels of fat, and cannot be used to follow steatosis after treatment. US-based quantification is now available with TE-CAP, and similar assessments are becoming available on newer conventional US machines. Thus, imaging tests to assess the severity of steatosis can be divided into US- or MRI-based techniques[244] (Table 12).

EVIDENCE AND RATIONALE

Grayscale US

This is the most common technique used to assess steatosis because of wide availability and the morphologic assessment that is helpful when patients present with abnormal liver tests. Features on US suggestive of steatosis include liver

TABLE 12 Comparison of imaging techniques for hepatic steatosis[a]

Criteria	Grayscale US	CAP	Noncontrast CT	MRI-PDFF
Objective	Yes	Yes	Yes	Yes
Subjective	Yes	No	No	No
Quantifiable (separation of steatosis grades)	No	No	No	Yes
Interobserver reliability	Moderate	Moderate	High	High
Sensitive to change (with therapy)	No	No	No	Yes
Used in clinical trials	No	No	No	Yes
Cost	Low	Low	High	High

[a]Modified from Siddiqui et al.[247]
Abbreviations: CAP, controlled attenuation parameter; US, ultrasound.

hyperechogenicity as compared to the kidneys, distal attenuation of vessels, and classic areas of focal fatty sparing.[252–254] However, conventional grayscale US has limitations, including operator dependency, lower accuracy in obesity and in those with renal dysfunction, and its qualitative rather than quantitative assessment.[255,256] Furthermore, it cannot accurately detect < 20% and therefore is not useful for those without significant steatosis.[257] A recent meta-analysis of conventional US identified 49 studies that included 4720 participants.[254] The overall sensitivity, specificity, and positive and negative likelihood ratio (LR) to detect at least 20%-30% steatosis compared to liver histology were 84.8% (95% CI, 79.5-88.9), 93.6% (95% CI, 87.2-97.0), 13.3 (95% CI, 6.4-27.6), and 0.16 (95% CI, 0.12-0.22), respectively. The AUROC was 0.93 (95% CI, 91-95), whereas the reproducibility (kappa) ranged from 0.54-0.92 and 0.44-1.00 for intrarater and interrater assessments, respectively. The authors concluded that because of the low cost, safety, and accessibility, conventional US was reliable and accurate for detection of moderate to severe steatosis in the general population. Based on these observations, European guidelines recommend grayscale US as an initial imaging choice to identify steatosis.[258] However, this approach lacks sensitivity to detect lesser amounts of steatosis (< 20%) and is not useful to follow changes in steatosis over time.

Newer quantitative assessments of attenuation and backscatter steatosis have been incorporated into conventional US machines for use in quantifying steatosis[259–264] in a manner similar to that of TE-CAP. These systems allow for selection of larger ROIs than TE-CAP. Vessels and strong artifacts can be automatically filtered out. Although these results are promising and many showed statistically better performance than for TE-CAP, the amount of data for these different systems are limited. Because the quantitative reporting of fat using these machines is relatively new to widespread clinical use, further studies are needed to assess which systems work best and how to implement these systems in a more standardized manner across different conventional US platforms.

CT

With noncontrast CT, hepatic steatosis can be diagnosed if the attenuation of the liver is at least 10 Hounsfield units (HU) lower than that of the spleen, the liver/spleen HU ratio is ≤ 0.8, or the attenuation of the liver is < 40 HU.[252,265–268] However, because of concerns for radiation exposure and inability to detect mild steatosis, CT is not used for a primary indication of assessment of steatosis. Nevertheless, if a noncontrast CT is performed for other indications, it can be used to diagnose moderate to severe steatosis.

CAP measured with TE

This technique measures the attenuation of hepatic fat at the same time as it measures LSM.[269–271] Attenuation occurs as soundwaves lose energy as they travel through tissue.[269,270] Results range from 100 to 400 dB/m. CAP has very good interobserver reproducibility (concordance correlation coefficient 0.82 to 0.84)[272,273] but is influenced by BMI,[272,274–277] LSM,[166,278] and recent food ingestion[252,279,280] but not inflammation.[281] The failure rate is as high as 24% and is associated with increased BMI, age, female sex, and type of probe (M vs. XL).[282–285]

Thresholds for grading steatosis vary and are dependent on the population studied[57,257,286] and the underlying liver disease and its fibrosis severity[166,287]; In addition, there can be overlap between adjacent grades[269,277,288] and discordant results in those with high CAP (> 300 dB/m).[289,290] Although it has been suggested that the reliability of CAP is decreased when the IQR/median range is above 30 dB/m[246] to 40 dB/m,[291,292] excluding patients with IQR/median greater than these thresholds may not impact performance.[275,278] Table 13[211,246,263,270,274–276,278,281,287,290–292,298–302,304–306,308–311,313,314] shows the performance of CAP compared to liver histology or MRI-PDFF/MRS in CLD,[263,300,308–310,314,355] bariatric surgery,[211,306,311] deceased and living liver donors[56,312,313] and post-liver transplantation.[87] When the M and XL probes were compared in the same patient, the performance was similar in some studies using histology,[302,304] whereas the M probe underestimates CAP values when compared to the XL probe.[246]

More recently, a method to optimize cutoffs to improve accuracy is to set both the sensitivity and specificity at 90%, respectively, thus allowing one to balance both these performance metrics. By setting the sensitivity to 90%, the cutoffs had high PPV (96%) and the chance of false negative results (NPV 15%) and missing steatosis was minimized.[278,315] Several studies applying this analysis method identified CAP thresholds of 263-285 dB/m for detecting ≥ 5% steatosis (Table 13). Until a meta-analysis combining these data is performed, the writing group suggests a threshold of 275 dB/m across various CLD etiologies. Interpretation of CAP needs to consider the type of probe used, the fasting state, the level of stiffness, whether high sensitivity or specificity is desired, and the IQR/median range.[166,316] Nevertheless, CAP is superior to blood-based algorithms.[276,305,307] CAP has also been used to

assess changes with therapy. In a study of 65 patients, a change of at least 35 dB/m was highly associated with improvements in steatosis.[317]

PICO 7: In children with CLD (HCV, HIV-HCV, HBV, HCV/HBV, HIV/HBV, biliary atresia (BA), Alagille, alpha-1-antitrypsin (α1AT), cystic fibrosis liver disease, NASH/NAFLD), are imaging-based NILDA accurate in staging hepatic fibrosis and steatosis?

Guidance Statement:

11. In the pediatric population, there is insufficient evidence to recommend a single imaging-based NILDA over another to assess liver fibrosis or steatosis. (ungraded statement)

TECHNICAL REMARKS

- There are limited studies evaluating NILDA imaging tests as surrogates of liver fibrosis or steatosis with histologic confirmation in children with CLDs.
- There is high correlation of several US elastography-based platforms with histologically proven fibrosis in children.
- Different fasting and sedation requirements for each NILDA, as well as cooperation challenges and adherence to fasting protocols in younger children, can confound test results.
- Imaging-based NILDA have different disease-specific fibrosis staging thresholds than the adult population.
- Profound extrahepatic cholestasis that is unique to BA lessens accuracy of LSM to assess fibrosis.
- MRE and TE-based imaging are the most commonly used imaging NILDA to quantify liver steatosis in children with NASH and cystic fibrosis (CF).

EVIDENCE AND RATIONALE

Imaging-based NILDA in children and adolescents remain an understudied field, though there has recently been an increase of pediatric histology-validated studies using primarily US-based elastography[243,318–326] (Table 14). In adults, NAFLD-associated fibrosis is typically centrilobular, and other CLDs are typically portal-based. In children, fibrosis is often triggered by a genetic or persistent environmental insult or by biliary injury; thus, patterns of fibrosis distribution depend on the etiology and response to injury. A cohort analysis of 154 children and young adults (ages 3 wk to 24 y) with a spectrum of CLD[328] concluded that with more advanced fibrosis, inflammation did not appear to contribute to LSM, lending caution to interpreting LSM in children with substantial hepatic inflammation. The role of elastography is confounded in children with edema, extrahepatic cholestasis, and venous congestion, which can increase LSM independent of fibrosis.[329] This study also highlighted that the wide spectrum of liver diseases in children likely have distinct thresholds for fibrosis severity and that elastography has difficulty differentiating between individual stages of fibrosis in children, particularly at early stages (F1 and F2).

Biliary atresia

One of the first studies using TE-LSM in infants with BA ($n = 47$) found a significant positive correlation of LSM obtained with TE and fibrosis stage ($\rho = 0.63$)[318], with excellent to outstanding diagnostic performance: AUROCs were 0.86 and 0.96 for diagnosis of F3 and F4, respectively, with cutoffs of 9.6 kPa for F3 (sensitivity 89.5% and specificity 75%) and 18.1 kPa for F4 (sensitivity 100% and specificity 90.5%). In a different study investigating markers for histologic liver fibrosis after successful hepatoportoenterostomy (defined as total bilirubin less than 20 μM/L) with protocol liver biopsies ($n = 83$) in 39 children with BA, TE-LSM was the most accurate predictor of cirrhosis (F4) (AUROC 0.82; $p < 0.001$) compared with liver biochemistries and APRI.[319]

In a study of 50 consecutive infants with BA and 50 healthy infants who underwent pSWE-LSM examination, in which all infants with BA underwent a liver biopsy within 3 days after imaging, the mean shear wave speed in the BA group was significantly higher than controls (1.89 ± 0.45 versus 1.12 ± 0.06 m/s; $p < 0.001$).[324] A significant correlation was also found between the pSWE-LSM values and fibrosis stages ($r = 0.72$). Notably, the cutoff values for predicting significant fibrosis, advanced fibrosis (F3-4), and cirrhosis (F4) were 1.53 (AUROC 0.823), 1.80 (0.884), and 2.16 (0.917) m/s, respectively.

Similarly, in a study using 2D-SWE-LSM in 24 children with BA (mean age 6.6 y) who underwent hepatoportoenterostomy within 1 week of liver biopsy, LSM was significantly higher in F3-4 versus F0-2 (23.5 kPa, IQR 6.7-10.7 vs. 7.5 kPa, IQR 12-40.3) and demonstrated a strong positive correlation with fibrosis stage ($r = 0.762$) with an AUROC of 0.79, 0.81, and 0.82 to predict F2, F3, and F4, respectively.[321]

TABLE 13 Performance of imaging tests for the diagnosis of hepatic steatosis

References	Test	Steatosis grade (by histology or MRI-PDFF)	Cutoff (dB/m for CAP or % fat by MRI-PDFF)	Sensitivity %	Specificity %	AUROC
Sasso[269]	CAP	≥ 11%[a]	238	91	81	0.91
		≥ 34%[a]	259	89	86	0.95
		≥ 66%[a]	292	100	78	0.89
Friedrich-Rust[293]	CAP	≥ 33%[a]	245	97	67	0.78
		≥ 66%[a]	301	76	68	0.72
Kumar[294]	CAP	≥ 33%[a]	258	78	73	0.79
		≥ 66%[a]	283	71	68	0.77
de Lédinghen[277]	CAP	≥ 33%[a]	310	79	71	0.80
		≥ 66%[a]	311	87	47	0.66
Imajo[109]	CAP MR-PDFF	≥ 5%[a]	236	82	91	0.88
		> 33%[a]	270	78	80	0.73
		> 66%[a]	302	64	74	0.70
		≥ 5%	5.2%	90	93	0.96
		> 33%	11.3%	79	84	0.90
		> 66%	17.1%	74	81	0.79
Park[110]	CAP MR-PDFF	≥ 5%[a]	261	72	86	0.85
		> 33%[b]	305	63	69	0.70
		> 66%[b]	312	64	70	0.73
		≥ 5%	3.71	96	100	0.99
		> 33%	13.03	80	83	0.90
		> 66%	16.37	82	84	0.92
Runge[295]	CAP MR-PDFF	≥ 5%[a]	260	90	60	0.77
		> 33%[a]	296	92	55	0.78
		> 66%[a]	334	78	76	0.78
		≥ 5%	4.14	94	100	0.98
		> 33%	15.72	92	97	0.97
		> 66%	20.88	100	83	0.95
Chan[283]	CAP	≥ 5%[a]	260	91	87	0.94
		> 33%[b]	266	91	87	0.80
		> 66%[b]	267	100	47	0.69
Naveau[296]	CAP	≥ 5%[b]	308	68	69	0.85
		> 33%[b]	335	65	79	0.56
		> 66%[b]	341	74	74	0.36
Karlas[297]	CAP	> 5%[a]	215	93	87	0.93
		> 33%[a]	268	97	81	0.94
		> 66%[a]	300	82	76	0.82
Myers[287]	CAP	> 11%[a]	289	68	88	0.73
		> 33%[a]	288	85	62	0.68
		> 66%[a]	283	94	47	0.52
Sasso[270]	CAP	> 11%[a]	222	76	71	0.80
		> 33%[a]	233	87	74	0.86
		> 66%[a]	290	78	93	0.88
Jung[275]	CAP	≥ 5%[a]	250	69	93	0.86
		> 33%[a]	301	82	88	0.90
		> 66%[a]	325	50	81	0.74

TABLE 13. (*continued*)

References	Test	Steatosis grade (by histology or MRI-PDFF)	Cutoff (dB/m for CAP or % fat by MRI-PDFF)	Sensitivity %	Specificity %	AUROC
Shen[274]	CAP	≥ 5%[a]	253	89	82	0.92
		> 33%[a]	285	93	83	0.92
		> 66%[a]	310	92	79	0.88
Lupsor-Planton[298]	CAP	≥ 5%[a]	260	65	87	0.81
		> 33%[a]	285	70	85	0.82
		> 66%[a]	294	83	82	0.84
Wong[291]	CAP	≥ 5%[a]	222	87	62	0.85
			290	60	90	
Jun[290]	CAP	≥ 5%[a]	247	92	86	0.90
			300	51	100	0.74
Lee[299]	CAP	≥ 5%[a]	247	88	100	0.95
		> 33%[a]	280	85	80	0.85
		> 66%[a]	300	73	61	0.73
Chon[276]	CAP	≥ 5%[a]	250	73	95	0.88
		> 33%[a]	299	82	86	0.89
		> 66%[a]	327	79	84	0.80
Price[300]	CAP	≥ 5%[a]	238	84	75	0.85
Garg[211]	CAP	≥ 5%[b]	323	59	83	0.75
		> 33%[b]	336	74	75	0.74
		> 66%[b]	357	100	78	0.82
Andrade[281]	CAP	> 5%[a]	206	82	76	0.82
		> 33%[a]	232	93	84	0.96
		> 66%[a]	282	95	89	0.97
Mendes[292]	CAP	> 5%[a]	248	92	83	0.86
		> 33%[a]	268	81	99	0.94
		> 66%[a]	280	84	99	0.96
Darweesh[301]	CAP	> 5%[a]	297	81	73	0.77
		> 33%[a]	366	85	96	0.92
Eddowes[278]	CAP	> 5%[a,b]	302	80	83	0.87
		> 33%[a,b]	331	70	76	0.77
		> 66%[a,b]	337	72	63	0.70
de Lédinghen[302]	CAP	> 5%[a,b]	246/242	75/75	75/75	0.82/0.83
		> 33%[a,b]	269/267	80/80	81/81	0.89/0.88
		> 66%[a,b]	285/286	81/84	81/84	0.92/0.93
Siddiqui[303]	CAP	≥ 5%[a]	285[c]	80	77	0.76
		> 33%[b]	263	90	35	0.70
		> 66%[b]	353	29	90	0.58
			311[c]	77	57	
			280	90	35	
			367	20	90	
			306[c]	80	40	
			274	90	20	
			380	3	90	

TABLE 13. (*continued*)

References	Test	Steatosis grade (by histology or MRI-PDFF)	Cutoff (dB/m for CAP or % fat by MRI-PDFF)	Sensitivity %	Specificity %	AUROC
Chan[304]	CAP	≥5%[a,b]	253/279	93/83	71/88	0.84/0.91
		≥33%[a,b]	294/303	85/79	59/65	0.76/0.78
		≥66%[a,b]	294/325	88/76	36/54	0.61/0.65
Caussy[246]	CAP	≥5%	288	75	77	0.80
		≥10%	306	79	82	0.87
Xu[305]	CAP	≥5%[a]	224	69	76	0.78
		≥33%[a]	246	100	78	0.93
		≥66%[a]	284	100	96	0.99
Ooi[306]	CAP	≥33%[a]	285	85	47	0.69
Caussy[307]	CAP	≥5%[a]	294/261/316	75/90/59	78/50/90	0.83
		≥5%[b]	307/281/323	73/90/62	75/65/90	0.858
		≥10%[a]	311//293/326	79/90/58	85/71/90	0.88
		≥10%[b]	322/314/323	83/90/83	65/83/90	0.93
Ferraioli[263]	CAP	≥5%[a]	273[c]	80	83	0.85
Petroff[308]	CAP[b]	≥5%	294/263[c]/354[c]	79/90/52	74/50/90	0.81
		≥33%	310/286[c]/372[c]	79/90/25	59/39/90	0.73
		≥66%	331/297[c]/385	72/90/22	62/34/90	0.71
Beyer[309]	CAP	≥5%	269[c]	89	100	0.95
		≥33%	308[c]	78	41	0.60
		≥66%	337[c]	61	59	0.63
Audière[310]	CAP	≥5%	273[c]			0.89
Garteiser[311]	CAP	≥5%	316[c]	79	84	0.83
		≥33%	316[c]	87	61	0.79
		≥66%	343[c]	77	64	0.73
Yen[312]	CAP	10%-30%	257[c]	100	89	0.96
Zhuang[313]	CAP	≥5%	270[c]	100	83	0.94
Duarte-Rojo[56]	CAP	≥34%	230[c]	100	53	0.79
Siddiqui[87]	CAP	≥5%	270[c]	74	87	0.88
		≥34%	295[c]	100	89	0.94
		≥67%	295[c]	100	84	0.89

[a]M probe.
[b]XL probe.
[c]Youden's index or equivalent optimal threshold.
Abbreviation: CAP, controlled attenuation parameter.

CF-related liver disease (CFLD)

Several studies have examined the use of US-based elastography to detect liver fibrosis in patients with CF, but few have correlated imaging-based NILDA with histological fibrosis. A cross-sectional study to evaluate the accuracy of TE-LSM in 160 consecutive children who presented with CF (9.0 ± 0.4 y old, 53% male) at a tertiary referral pediatric center in Australia found that LSM correlated positively with fibrosis stage in patients with histology-proven CFLD ($r = 0.67$).[322] Fibrosis severity was determined from histologic analysis of dual-pass liver biopsies from children with CFLD as the reference standard. A TE-LSM cutoff value of 8.7 kPa differentiated patients with F3-4 from patients with F1-2 (AUROC, 0.87; 75% sensitivity; 100% specificity). The combination of TE-LSM with pSWE-LSM further improved the differentiation of patients with F3-4 fibrosis versus F1-2 fibrosis (AUROC, 0.92; 83% sensitivity; and 100% specificity; $p < 0.01$).

Hepatic steatosis is a common manifestation of CFLD. Using TE-CAP, the relationship of CAP and

TABLE 14 Selected pediatric imaging NILDA studies

References	Imaging NILDA	Pediatric liver disease	AUROC (sensitivity/specificity %) and correlation when available	Correlation with fibrosis (*r*)	Biopsy measure	Comments
Shin[318]	VCTE	BA (n = 47)	0.86 for F3 (89.5%/75%) 0.96 for F4 (100%/90.5%)	0.63	METAVIR fibrosis	All were pre-Kasai hepatoportoenterostomy Cutoff for F3: 9.6 kPa Cutoff for F4: 18.1 kPa Success rate with the pediatric S probe (100%) vs M probe (77%; $p < 0.001$)
Hukkinen[311]	VCTE	BA (n = 39)	0.82 for F4 (76%/75%)	0.48	METAVIR fibrosis	All were s/p Kasai Cutoff for F4: 23.8 kPa AUROC increased with age
Gao[320]	ARFI	BA (n = 50)	0.82 for F ≥ 2 (91.4%/61.5%) 0.88 for F ≥ 3 (94.7%/74.2%) 0.92 for F = 4 (87.5%/90.5%)	0.72	Batts-Ludwig fibrosis	All were pre-Kasai. Cutoff for F ≥ 2: 1.53 m/s Cutoff for F ≥ 3: 1.80 m/s Cutoff for F = 4: 2.16 m/s
Chen[321]	SSWE	BA (n = 24)	0.79 for F ≥ 2 (80%/73.7%) 0.81 for F ≥ 3 (77.8%/80%) 0.82 for F4 (93.8%/87.5%)	0.76	METAVIR fibrosis	All were s/p Kasai Cutoff for F2: 9.4 kPa Cutoff for F3: 10.8 kPa Cutoff for F4: 24.4 kPa
Lewindon[322]	VCTE	CFLD (n = 22)	0.87 for F3-4 (75%/100%)	0.67	METAVIR fibrosis	Cutoff for F3-4: 8.7 kPa
Garcovich[323]	SWE	NASH (n = 68)	0.92 for ≥ F1 (85%/95%) 0.97 for ≥ F2 (87%/96%)	0.84	Brunt fibrosis	Brunt classification (0-4) Cutoff for F ≥ 1: 5.1 kPa Cutoff for F ≥ 2: 6.7 kPa
Middleton[243]	MRI-PDFF	NAFLD (n = 83)	0.87 for S1 vs S2-3 (74%/90%) 0.79 for s-2 vs S3 (60%/90%)		NASH CRN Steatosis (1-3)	Cutoff for S2-3: 17.5% Cutoff for S3: 23.3%
Schwimmer[324]	MRE	NAFLD (n = 90)	0.77 for ≥ F1[a] (44.4%/90.7%) 0.89 for ≥ F3[a] (33.3%/90.5%)	0.53[b]	NASH CRN Fibrosis (0-4)	Cutoff for ≥ F1: 2.78 kPa+ Cutoff for ≥ F3: 3.33 kPa+
Behairy[325]	VCTE	HCV (n = 50)	0.70 for ≥ F1 0.87 for ≥ F2 0.80 for ≥ F3	0.56	Ishak fibrosis	Cutoffs not available
Awad[327]	VCTE	HCV (n = 30)	1.0 for F4 0.82 for F3	0.77	METAVIR fibrosis	Cutoff for F3: 9.5 kPa Cutoff for F4: 12.5 kPa

[a]Using automated reading.
[b]Mean of 3 centers.
Abbreviations: CFLD, cystic fibrosis liver disease; CRN, clinical research network; HCV, hepatitis C; MRE, magnetic resonance elastography; S, steatosis; TE, transient elastography.

CFLD severity, clinical factors, and LSM was examined in a cross-sectional study of CF. CAP was normal in 86 (67%) of 129 children and young adults with CF and was not associated with increases in liver chemistries except for direct bilirubin.[330] Steatosis (CAP ≥ 230 dB/m) was seen in 27% of subjects without CFLD, 48% in CFLD without PHTN, and 20% in CFLD with PHTN ($p < 0.05$ for comparison between CLFD without PHTN and the other 2 groups, and no significant difference between subjects without CFLD and those with CFLD and PHTN). Although the authors concluded that CAP was higher in patients with liver disease, CAP was not validated with liver histology.

NAFLD IN CHILDREN

Steatosis

Emerging data studying MRI as a surrogate marker of steatosis in children have been encouraging but has not been adequately validated with liver histology. In one study, liver MRI-PDFF estimated by MRI was strongly correlated ($r = 0.725$) with steatosis grade by liver histology.[331] The study included 174 children with a mean age of 14 years. The correlation was stronger in girls ($r = 0.86$) than in boys ($r = 0.70$, $p < 0.01$). Interestingly, the correlation was significantly weaker in children with stages F2-4 ($r = 0.61$) than children with no fibrosis ($r = 0.76$) or stage F1 ($r = 0.78$). The diagnostic accuracy of commonly used threshold values to distinguish between no steatosis and mild steatosis ranged from 0.69 to 0.82. The overall accuracy of predicting the histologic steatosis grade from MRI-PDFF was 56%. No single threshold had sufficient sensitivity and specificity to be considered diagnostic for an individual child. However, a prospective, cross-sectional study of 77 patients with NAFLD and liver histology, of whom 65 were children, demonstrated good correlation of MRI-PDFF with histologic steatosis grade ($\rho = 0.69$, $p < 0.001$).[239] The AUROC was 0.99 for distinguishing patients with steatosis grade 0 from those with ≥ grade 1, 0.83 to distinguish those with ≤ grade 1 from those with ≥ grade 2, and 0.89 to distinguish those with ≤ grade 2 from those with grade 3. In a study of MRI-PDFF in children with NAFLD who stratified steatosis grade before and after treatment with cysteamine bitartrate, 110 (65%) and 83 (49%) enrolled children had MRI and liver histology at baseline and at the end of treatment (52 wk), respectively.[243] MRI-PDFF classified grade S1 versus S2-3 and grades S1-2 versus S3 with AUROCs of 0.87 and 0.79, respectively. MRI-PDFF cutoffs at 90% specificity were 17.5% for grades 2-3 and 23.3% for grade 3 steatosis. At end of treatment, MRI-PDFF change classified steatosis grade improvement and worsening with AUROCs of 0.76 (95% CI, 0.66-0.87) and 0.83 (95% CI, 0.73-0.92), respectively. MRI-PDFF change cutoff values at 90% specificity were −11.0% and +5.5% for improvement and worsening. In this study, MRI-PDFF had high diagnostic accuracy to both classify and predict histological steatosis grade and change in histological steatosis grade in children with NAFLD.

In the only pediatric study of TE-CAP correlation with steatosis in 69 children with a mean age of 16 years (38% female) who had a liver histology within 1.3 months, there were significant differences between CAP values in children with no steatosis versus mild/moderate steatosis ($p < 0.0001$), no steatosis versus marked steatosis ($p < 0.0001$), and mild/moderate versus marked steatosis ($p = 0.004$).[332] Children with no steatosis had mean CAP of 198, whereas children with mild/moderate and marked steatosis had mean CAP values of 265 and 313, respectively. A CAP threshold of 225 dB/m for predicting steatosis demonstrated an AUROC of 0.93 with 87% sensitivity and 83% specificity.

Fibrosis

The diagnostic accuracy of SWE-LSM in identifying different degrees of fibrosis in a cohort of consecutive children and adolescents with NASH has been less well studied. In a cohort of children with histology-proven NASH (37 boys and 31 girls; mean age 12.6 y ± 2.5; age range 8-17 y), SWE-LSM was performed in 68 of 69 patients and showed a strong correlation with liver fibrosis stage ($r = 0.84$).[323] The AUROCs for the association of any (F1-4) and significant fibrosis (F2-4) were 0.92 and 0.97, respectively. The intraclass correlation coefficient for absolute agreement was 0.95 (95% CI, 0.90-0.97). In another prospective study of 67 consecutive adolescents with histology-proven NAFLD, liver stiffness measured by time-harmonic elastography demonstrated an AUROC for the detection of any fibrosis (≥ stage F1), moderate fibrosis (≥ stage F2), and advanced fibrosis (≥ stage F3) of 0.88, 0.99, and 0.88, respectively.[333] Based on Youden's index, the optimal liver stiffness thresholds were 1.52 m/s for ≥ F1, 1.62 m/s for ≥ F2, and 1.64 m/s for ≥ F3.

A study of TE-LSM in 52 consecutively biopsied children with proven NASH (20 female) with a mean age of 13.6 years found that the AUROC for the prediction of F2-4 and F3-4 were 0.992 and 1, respectively.[334] TE-LSM values between 7 and 9 kPa predicted F1-2 but could not discriminate between stages (i.e., F2 or above). TE-LSM values of ≥ 9 kPa were associated with F3-4 with an intraclass correlation coefficient for absolute agreement of 0.961. Similarly, using the NASH Clinical Research Network fibrosis staging, another pediatric cohort of 67 children with histology-proven NAFLD had TE performed and demonstrated an AUROC of 1 using an LSM score of ≥ 8.6 kPa to detect F2-4.[335]

MRE-LSM has also been used in children. In a case series of 35 children and adolescents with a median age of 13 years (49% female) and BMI of 33.9 kg/m^2, this histology-validated study proposed a cutoff of 2.71 kPa based on an AUROC of 0.92 with 88% sensitivity and 85% specificity for detecting significant fibrosis (> F2). In a prospective multicenter study of MRE in 90 children with NAFLD (mean age 13.1 ± 2.4 y), the median LSM was 2.35 kPa.[331] Stiffness values derived by each reading center were strongly correlated with each other ($r = 0.83$). All three analyses were significantly correlated with fibrosis stage (center 1, $\rho = 0.53$; center 2, $\rho = 0.55$; and using an automated analysis, $\rho = 0.52$). Overall cross-validated accuracy for detecting any fibrosis was 72% (95% CI, 62-81). Overall cross-validated accuracy for assessing advanced fibrosis was 89% (95% CI, 81-95) for center 1, 90% (95% CI, 82-95) for center 2, and 87% (95%

CI, 78-93) for an automated analysis, suggesting clinical utility of MRE-LSM.

Other CLD in children

A limited number of imaging studies in children with other CLD have validated findings with liver histology, including HBV and HCV. Importantly, children with a variety of biologically distinct liver conditions have often been clustered into such analyses; one such study included 115 children (CF [n = 42], viral infection [HBV or HCV, n = 22], BA [n = 13], Wilson's disease [n = 9], AIH [n = 7], congenital hepatic fibrosis [n = 4], and other [n = 18]).[336] Of the 33 patients who underwent liver biopsy in this study, median values of LSM, FibroTest, and APRI demonstrated good correlation with METAVIR fibrosis stage, with highest values among children with F4. TE-LSM significantly correlated with METAVIR fibrosis stages ($r = 0.53$) and the AUROC of LSM to detect cirrhosis was 0.88. Unfortunately, only 2 patients with viral hepatitis had biopsies; thus, these data may not be generalizable to other children.

In a study of 90 children (n = 50 HCV, n = 20 AIH, n = 20 Wilson's disease) who underwent TE-LSM, the majority of the HCV group had minimal inflammatory activity (80%) and no/mild fibrosis (72%). LSM values for the same stage of fibrosis varied by disease, highlighting biological differences, but correlated well among children with HCV ($r = 0.885$).[325] Furthermore, the AUROC of LSM to detect F1-4, F2-4, and F3-4 among the pediatric HCV group was 0.70, 0.87, and 0.80, respectively, although no specific cutoffs were provided.

In an Egyptian study of 30 children with chronic HCV who had liver histology, there was a strong positive correlation between TE-LSM and METAVIR fibrosis stages ($r = 0.774$).[326] The highest predictive performance of LSM was for F4 (AUROC 1.0) followed by F3-4 (0.82) using cutoff values of 12.5 and 9.5 kPa, respectively. The NPV to exclude F3-4 and F4 at these cutoffs were high (100%), whereas PPV were only modest (60%-83%).

A recent meta-analysis that included 723 children with various CLD who underwent TE-LSM demonstrated sensitivity of 95% and specificity of 90% for the diagnosis of F2-4.[327] The diagnostic accuracies of TE-LSM were also clinically acceptable to excellent, measuring up to a sensitivity of 86% and specificity of 86% for diagnosing cirrhosis, suggesting that TE-LSM is a reliable imaging NILDA of cirrhosis in children, although less so with earlier stages.

A SIMPLIFIED NILDA ALGORITHM FOR DETECTION OF FIBROSIS AND STEATOSIS

In an effort to facilitate incorporation of NILDA into clinical practice for adults, the AASLD NILDA Writing Group developed an algorithm intended to be used by clinicians in need of a readily available and simple decision support tool (Figure 2A). There were insufficient data for a pediatric algorithm. This adult algorithm was developed with summary NILDA evidence highlighted previously. The fibrosis staging algorithm can start at either blood- or imaging-based NILDA and does not imply the use of sequential testing. However, sequential testing has been found to be more informative than single testing and could be considered.[337,338] The AASLD NILDA Writing Group decided to move away from etiology-specific individualized cutoff values and rather endorse similar cutoff values across liver diseases to favor NILDA implementation.[339–341] Non-disease-specific cutoff values are expected to improve access to early hepatology referral and continued hepatology care as well as the rate of screening for complications. Whenever more granularity is needed (i.e., start of antiviral treatment for a patient with HBV and significant fibrosis), clinicians should refer to the associated NILDA Systematic Reviews[67,68,342] or specific guidance documents.[7,79] The thresholds are poorly defined in those with treated viral hepatitis (HCV RNA or HBV DNA negative).

Step 1: Determine the stage of fibrosis

The left side of the algorithm aims to rule out significant/advanced fibrosis. FIB-4 and NFS showed sensitivities ranging from 60% to 75% and the lowest negative LR at proposed cutoff values across etiologies.[68] Regarding imaging-based testing, a recent study including > 16,000 individuals revealed normal TE-LSM to be below 5 kPa, with the consideration that obesity, steatosis, and diabetes mellitus can increase LSM.[339,343] As such, significant/advanced fibrosis can be confidently ruled out with a TE/SWE-LSM < 5 kPa (or MRE-LSM < 2.5 kPa). However, with TE/SWE-LSM ≥ 5 kPa (or MRE-LSM ≥ 2.5 kPa) in a patient with a low pretest probability for significant or more advanced fibrosis, the clinician is asked to consider NILDA modifiers affecting the accuracy of the test (Table 7A) and consider a liver biopsy or longitudinal surveillance with NILDA.[344]

The middle box at the top represents the "gray zone" for FIB-4 and NSF, and patients with results falling within those ranges should proceed with alternative strategies to determine the stage of fibrosis, including the possibility of a liver biopsy. The recommended cutoff value to identify the presence of significant or more advanced fibrosis using US-based LSM is around 7 to 8 kPa.[67] We decided to use a TE/SWE-LSM < 8 kPa (or MRE-LSM < 3.1 kPa) when FIB-4 is ≥ 1.3 (NAFLD) or ≥ 1.45 (non-NAFLD) as an area of uncertainty, wherein patients will need to undergo further assessment. A TE/SWE-LSM of 8-11 kPa (or MRE-LSM 3.1-3.5 kPa) is compatible with at least significant fibrosis while not being able to rule out advanced fibrosis.[341] Such ranges are consistent with a recent

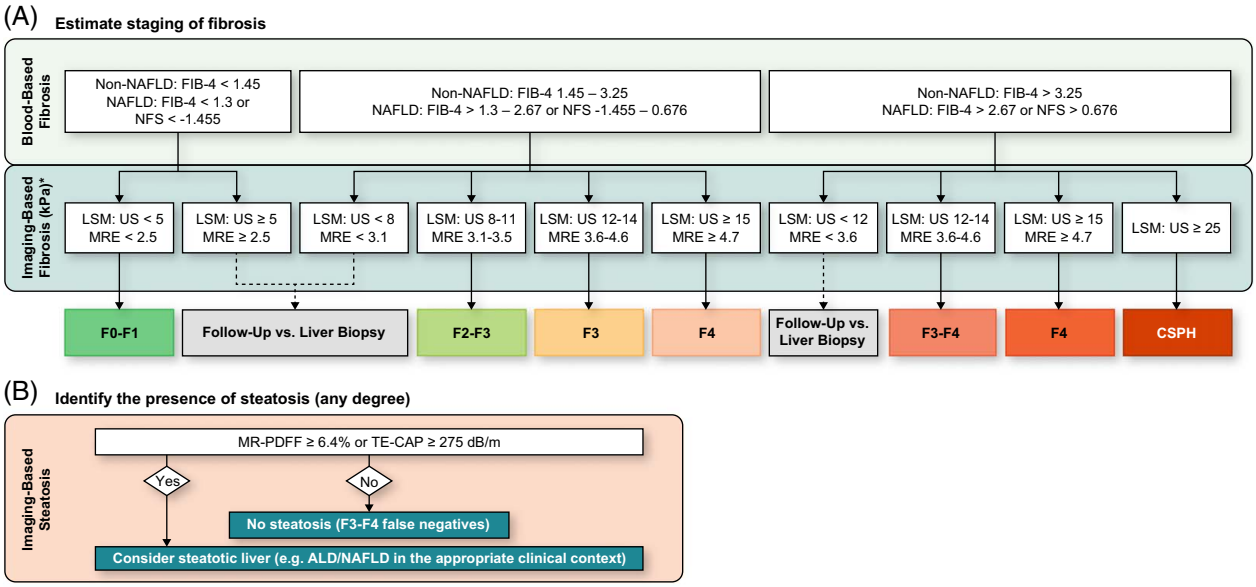

FIGURE 2 Simplified NILDA algorithm for the clinician. AASLD recommends use of simple non-proprietary tests with thresholds for both non-NAFLD and NAFLD because of their wide availability and performance compared to proprietary tests, though these can be used where available. NFS can be considered as equivalent to FIB-4 in patients with NAFLD for assessment of advanced fibrosis. Although imaging-based LSM-NILDA (TE and SWE) are more accurate than blood-based in some situations, they are not as not widely available. Being the most accurate method, MRE is highly attractive, but due to the lack of a robust evidence base, LSM cutoff values suggested herein might need to be revised as new evidence in the field is made available. For viral hepatitis, it is important to note that the majority of data in both imaging and blood-based NILDA have been studied in viremic (HCV RNA or HBV DNA positive) subjects. Therefore, the simplified algorithm is not intended for use in patients who are nonviremic (HCV RNA or HBV DNA negative). The degree of steatosis decreases and may even disappear as fibrosis progresses, and as such, the lack of steatosis in a patient with advanced fibrosis or cirrhosis does not exclude fatty liver disease as an etiology. The diagnosis of NAFLD or ALD mandates supporting clinical information and ruling out other causes of fatty liver disease. Abbreviations: AdvCLD, advanced chronic liver disease; CAP, ultrasound-based continuous attenuation parameter; CSPH, clinically significant portal hypertension; EGD, esophagogastroduodenoscopy; MRE, magnetic resonance elastography; NFS, NAFLD fibrosis score; SWE, shear wave elastography; US, ultrasound. *Some ultrasound methods of fibrosis detection give results in m/s and need to be converted.

large study proposing a TE-LSM ≥ 9.1 kPa as the optimal threshold to detect significant fibrosis in the general population (≥ 9.5 kPa in patients with CLD risk factors).[340] Based on a large study not fulfilling criteria for our systematic review, we incorporated TE/SWE-LSM ≥ 12 kPa and ≥ 15 kPa as thresholds for the identification of advanced fibrosis and cirrhosis with specificities of 92% and 96%[341] (proposed corresponding MRE-LSM thresholds of ≥ 3.6 kPa and ≥ 4.7 kPa, respectively).

Finally, the left-sided box in Figure 2A corresponds to the highly specific cutoff values validated for the recognition of advanced fibrosis (FIB-4 and NFS, specificity of 91% to 97%) or cirrhosis. With a blood-based fibrosis assessment that is predictive of advanced fibrosis/cirrhosis, a TE/SWE-LSM value < 12 kPa (or MRE-LSM < 3.6 kPa) would merit further study. In isolation, a result < 12 kPa likely rules out cirrhosis in patients with NAFLD.[303] Under these circumstances, if a liver biopsy was viewed as undesirable, repeat imaging-based NILDA would help increase the certainty of the fibrosis estimates because it was demonstrated that 6-month apart longitudinal LSM values show increased accuracy over an isolated assessment.[345,346] TE/SWE-LSM values ≥ 12 kPa (or MRE-LSM ≥ 3.6 kPa) and ≥ 15 kPa (or MRE ≥ 4.7 kPa), would be more reliable in their prediction of advanced fibrosis and cirrhosis, respectively, when they occur in the presence of a blood-based NILDA that agrees versus when the latter falls within the indeterminate zone. In fact, both FIB-4 ≥ 3.25 and TE-LSM ≥ 12 kPa are associated with a higher risk for HCC in treated HCV, even in the absence of histologically proven cirrhosis.[347,348] Among 871 patients with CLD, a TE-LSM ≥ 13 kPa was used to identify occult cirrhosis with increased HCC risk.[349] Lastly, although a TE-LSM < 20 kPa along with a platelet count ≥ 150,000 has a very high NPV for the absence of varices at upper endoscopy, it is recommended for patients showing a TE/SWE-LSM ≥ 20 kPa plus a platelet count < 150,000 to undergo screening for esophageal varices as well as for patients with a TE/SWE-LSM ≥ 25 kPa, irrespective of the platelet count.[350] For the identification of clinically significant PHTN, please see our systematic review and discussion.[5,342] A recent study showed PPV exceeding 90% when LSM was ≥ 25 kPa across all etiologies, irrespective of platelet count.[351] Of note, MRE-LSM values above 5 kPa have a high risk for decompensation, need for liver transplantation, or death.[352–354]

Step 2: Determine the presence of steatosis

MRI-PDFF has become the most accurate method and comparable to liver histology (AUROC 96%-99%).[109,110] With the integration of CAP in TE, a bedside steatosis assessment is now routinely available. Multiple cutoff values for the identification of any degree of steatosis (≥5%) have been proposed for TE-CAP (median 274 [range 248-295] dB/m),[57,303,308] and in subjects with a low pretest probability of fatty liver disease, a cutoff of 270 dB/m rules out steatosis (AUROC 0.942) with a 100% NPV.[313] Meta-analyses identified that a TE-CAP threshold of 263 dB/m has a 90% sensitivity to rule out steatosis across different CLD diseases and found a threshold of ≥275 dB/m as 79%-92% specific for ALD and NAFLD.[8,308,355] We selected 275 dB/m as a convenient threshold to screen for steatosis under most clinical circumstances (Figure 2B).

SUMMARY OF RECOMMENDATIONS

Imaging-based NILDA have replaced liver histology in clinical practice in many situations. Because of the rapid evolution of the field and predetermined inclusion and exclusion criteria considered for our systematic reviews, we were not able to include every published study on the topic. In particular, studies with smaller sample size, those that did not have liver histology as the reference standard to assess fibrosis, and many studies with mixed etiologies or overlapping diseases were excluded.

SUMMARY GUIDANCE STATEMENT OF IMAGING-BASED NILDA

- Recognizing that liver histology is an imperfect reference standard, prior to considering a liver biopsy to assess fibrosis staging in patients with CLD, AASLD recommends using blood and imaging-based NILDA as the initial tests to detect significant (F2-4) to advanced fibrosis (F3-4) and cirrhosis (F4). (ungraded statement)

TABLE 15 Areas for future research

Studies on NILDA should include diverse populations.
Comparative studies combining both blood-based and imaging-based tests performed synchronously and sequentially are needed to match clinical practice, with recognition of test utility by insurance and third-party payors.
Prospective data on the diagnostic utility of simple and proprietary blood tests compared to imaging are needed. Ideally, validation studies should include paired comparisons with both imaging-based and blood-based tests from the same individual compared against liver histology (or if assessing fat, with histology or MRI-PDFF as reference).
Further define the role of imaging-based NILDA in treated patients with HCV and HBV.
Define the performance and threshold of imaging-based NILDA in MASLD.
Additional studies are needed to further develop the assessment of hepatic inflammation either via US (i.e., use of shear wave dispersion slope)[356] or with alternative MRI methods (i.e., multiparametric iron-corrected T1 mapping [cT1]).[357]
Regarding steatosis, additional studies comparing sonographic liver attenuation tools are needed, along with their potential combination in screening algorithms with blood-based NILDA. The role of US-based and MRI-PDFF/MRS to monitor changes in steatosis with therapies also merits further study.
The diagnosis of NASH (not just fibrosis in NAFLD) represents a particular challenge for NILD,[358,359] and there is need for further study. Emerging MRE techniques, such as 3D MRER[360] and multifrequency acquisition,[236,361] show promising results in NASH and should be further evaluated.
In light of these emerging data and the fact that NAFLD will soon become the primary indication for liver transplantation in adults, a reliable and validated method for detecting and quantifying steatosis in children to prevent sequelae in adulthood should be a priority.
Utilization of artificial intelligence and machine learning should allow for incorporation of demographics and a wide array of clinical data including genome-wide association studies, microbiome, and metabolomic tests to improve diagnosis and management of CLD.
Research is needed on the generalizability of NILDA, including simplified algorithms across imaging-based modalities and expanded initiatives to further standardize LSM acquisition and quality reporting across manufacturers and across different disease etiologies, if needed.
Study of novel approaches to reduce hardware/software costs necessary for widespread implementation of advanced imaging techniques is needed.
Longitudinal studies of NILDA to assess the natural history of a disease, clinical outcomes, and changes with therapy are needed.
Quantitative techniques and protocols for sequential use of NILDA for following fibrosis regression are needed. These could help better reflect scar regression given the ceiling effect (i.e., unique F4 stage irrespective of fibrosis thickness) imposed by standard pathology, which is not observed with collagen histomorphometry.
Cost-effectiveness analysis studies will help determine appropriateness criteria of blood tests vs. imaging tests for fibrosis and/or steatosis detection in varied clinical scenarios (e.g., general population screening vs. at-risk populations).

FUTURE RESEARCH

Substantial progress has been made in the area of imaging-based NILDA. However, further research is needed. Although imaging-based NILDA are generally precise in estimating liver fibrosis, their availability for use in general practice is currently limited. As such, there is a need for broader awareness of the utility of imaging-based NILDA while considering (a) greater dissemination of testing in various clinical settings, (b) recognition of imaging-based NILDA accuracy by payors, and (c) hardware/software cost reduction. Populations with high risk for CLD (e.g., those showing components of the metabolic syndrome or untreated viral hepatitis) should be given priority for early access to imaging-based NILDA to facilitate diagnosis at the early stages of fibrosis and timely interventions. This is particularly true for the newly defined MAFLD given the a priori consideration of cardiometabolic criteria, which further selects for a higher risk of progressive liver disease, when compared to the previous NAFLD definition.[14] Importantly, the new steatotic liver disease diagnostic pathway needs further NILDA validation. Emerging tools such as machine learning could optimize imaging-based NILDA accuracy by considering clinical features and key blood tests readily accessible to any healthcare system.[15] The writing group summarized major areas for future research in Table 15. In the era of precision medicine, high-throughput technologies applied to experimental models will continue to generate a wealth of novel disease and injury-specific NILDA biomarkers for dynamic fibrosis assessment. Selection and validation of candidate biomarkers for fibrosis assessment from these multiomics databases will be challenging. Progress in this field requires a paradigm shift from static and semiquantitative assessment of fibrosis as the reference standard toward utilization of dynamic disease-specific models that are associated with clinical outcomes.

ACKNOWLEDGMENTS

We thank Ruben Hernaez, Alfred Sidney Barritt IV, and the AASLD Practice Guidelines Committee, PGC, for their expertise, patience, and editorial guidance, Elizabeth C. Verna, Chair, Cynthia Levy, Chair-Elect, Saul Karpen, Governing Board Liaison, Scott W. Biggins, Therese Bittermann, Po-Hung (Victor) Chen, Kathleen E. Corey, Albert Do, Juan F. Gallegos-Orozco, Lindsay Y. King, Christina C. Lindenmeyer, Jessica L. Mellinger, Anthony J. Michaels, Arpan Mohanty, Andrew Moon, Nadia Ovchinsky. Archita Parikh Desai, Jennifer C. Price, Elizabeth Rand, Adrienne Simmons, Ashwani K. Singal, Christopher Shubert, and Puneeta Tandon. We thank Audrey Davis-Owino at AASLD. We thank Marie Kreck at Virginia Commonwealth University for editorial assistance. We would like to thank Audrey Davis-Owino and AASLD staff for their support in preparing this guideline. We also thank Marie Kreck for her editorial assistance and Ruben Hernaez for his guidance.

FUNDING INFORMATION

Funding for the development of this Practice Guideline was provided by AASLD.

CONFLICTS OF INTEREST

Richard K. Sterling received grants paid to his institution from Gilead, AbbVie, Abbott, Roche, and Zydus. Andres Duarte-Rojo received grants paid to his institution from Echosens, Axcella Health, and AMRA Medical. He consults for Axcella Health. Keyur Patel has no conflicts in relation to this manuscript. Outside of the present work he advises and is on the Data Safety Monitoring Board for Gilead and advises Intercept. Maria Isabel Fiel has no conflicts in relation to this manuscript. Outside of the present work she consults for Progenity, Alexion, and Q32. Daniel H. Leung received grants paid to his institution from AbbVie, Gilead, Mirum, and the CF Foundation. He advises AstraZeneca. Bachir Taouli has no conflicts in relation to this manuscript. Outside the present work he received grants paid to his institution from Bayer, Echosens, Regeneron, Siemens, Takeda and consults for Bayer, Guerbet, and Helio Health. Don C. Rockey has no conflicts in relation to this manuscript. Outside the present work he received grants paid to his institution from AstraZeneca, Axcella Therapeutics, Boehringer Ingelheim, Durect, Galectin, Gilead, Helio, Intercept, Inventiva, Novo Nordisk, Oclot Biological, Pfizer, Salix, Sequana Medical, and Viking. The remaining authors have no conflicts to report.

ORCID

Richard K. Sterling https://orcid.org/0000–0002–8637–2475
Andres Duarte-Rojo https://orcid.org/0000–0002–5377–9295
Sumeet K. Asrani https://orcid.org/0000–0001–9174–5670
Mouaz Alsawas https://orcid.org/0000–0002–0814–4098
Jonathan A. Dranoff https://orcid.org/0000–0003–3130–1909
Maria Isabel Fiel https://orcid.org/0000–0002–7314–6313
M. Hassan Murad https://orcid.org/0000–0001–5502–5975
Deborah Levine https://orcid.org/0000–0001–7761–6493
Tamar H. Taddei https://orcid.org/0000–0002–6500–1739
Bachir Taouli https://orcid.org/0000–0001–6409–1333
Don C. Rockey https://orcid.org/0000–0002–3751–2961

REFERENCES

1. Moon AM, Singal AG, Tapper EB. Contemporary epidemiology of chronic liver disease and cirrhosis. Clin Gastroenterol Hepatol. 2020;18:2650–66.
2. Asrani SK, Devarbhavi H, Eaton J, Kamath PS. Burden of liver diseases in the world. J Hepatol. 2019;70:151–71.
3. Bravo AA, Sheth SG, Chopra S. Liver biopsy. New Engl J Med. 2001;344:495–500.
4. Froehlich F, Lamy O, Fried M, Gonvers JJ. Practice and complications of liver biopsy. Results of a nationwide survey in Switzerland. Digest Dis Sci. 1993;38:1480–4.
5. Sterling RK, Asrani SK, Levine D, et al. AASLD Practice Guideline: Noninvasive Liver Disease Assessments of Portal Hypertension. Hepatology. 2024. doi:10.1097/HEP.0000000000000844.
6. Sterling RK, Patel K, Duarte-Rojo A, et al. AASLD practice guideline on blood-based noninvasive liver disease assessments (NILDA) of hepatic fibrosis and steatosis. Hepatology. 2024. doi:10.1097/HEP.0000000000000845.
7. Mack CL, Adams D, Assis DN, Kerkar N, Manns MP, Mayo MJ, et al. Diagnosis and management of autoimmune hepatitis in adults and children: 2019 Practice Guidance and Guidelines from the American Association for the Study of Liver Diseases. Hepatology. 2020;72:671–722.
8. Ahn JC, Connell A, Simonetto DA, C Hughes C, Shah VH. Application of artificial intelligence for the diagnosis and treatment of liver diseases. Hepatology. 2021;73:2546–63.
9. Schünemann HJ, Mustafa RA, Brozek J, Steingart KR, Leeflang M, Murad MH, et al, for the GRADE Working Group. GRADE guidelines: 21 part 1. Study design, risk of bias, and indirectness in rating the certainty across a body of evidence for test accuracy. J Clin Epidemiol. 2020;122:129–41.
10. Schünemann HJ, Mustafa RA, Brozek J, Steingart KR, Leeflang M, Murad MH, et alfor the GRADE Working Group. GRADE guidelines: 21 part 2. Test accuracy: Inconsistency, imprecision, publication bias, and other domains for rating the certainty of evidence and presenting it in evidence profiles and summary of findings tables. J Clin Epidemiol. 2020;122:142–52.
11. Fitch K, Bernstein SJ, Aguilar MD, Burnand B, LaCalle JR, Lazaro P, et al. The RAND/UCLA Appropriateness Method User's Manual. RAND. 2000.
12. Kanwal F, Tapper EB, Ho C, Asrani SK, Ovchinsky N, Poterucha J, et al. Development of quality measures in cirrhosis by the Practice Metrics Committee of the American Association for the Study of Liver Diseases. Hepatology. 2019;69:1787–97.
13. Scheuer PJ. Classification of chronic viral hepatitis: A need for reassessment. J Hepatol. 1991;13:372–4.
14. Batts KP, Ludwig J. Chronic hepatitis. An update on terminology and reporting. Am J Surg Pathol. 1995;19:1409–17.
15. Knodell RG, Ishak KG, Black WC, Chen TS, Craig R, Kaplowitz N, et al. Formulation and application of a numerical scoring system for assessing histological activity in asymptomatic chronic active hepatitis. Hepatology. 1981;1:431–5.
16. Ishak K, Baptista A, Bianchi L, Callea F, De Groote J, Gudat F, et al. Histological grading and staging of chronic hepatitis. J Hepatol. 1995;22:696–9.
17. The French METAVIR Cooperative Study GroupBedossa P. Intraobserver and interobserver variations in liver biopsy interpretation in patients with chronic hepatitis C. Hepatology. 1994;20:15–20.
18. Ludwig J, Dickson ER, McDonald GSA. Staging of chronic nonsuppurative destructive cholangitis (syndrome of primary biliary cirrhosis. Virchows Arch A Pathol Anat Histol. 1978;379:103–12.
19. Altamirano J, Miquel R, Katoonizadeh A, Abraldes JG, Duarte–Rojo A, Louvet A, et al. A histologic scoring system for prognosis of patients with alcoholic hepatitis. Gastroenterology. 2014;146:1231–9.e1-6.
20. Brunt EM, Janney CG, Di Bisceglie AM, Neuschwander-Tetri BA, Bacon BR. Nonalcoholic steatohepatitis: A proposal for grading and staging the histological lesions. Am J Gastroenterol. 1999;94:2467–74.
21. Kleiner DE, Brunt EM, Van Natta M, Behling C, Contos MJ, Cummings OW, et al, the Nonalcoholic Steatohepatitis Clinical Research Network. Design and validation of a histological scoring system for nonalcoholic fatty liver disease. Hepatology. 2006;41:1313–21.
22. Cholongitas E, Senzolo M, Standish R, Marelli L, Quaglia A, Patch D, et al. A systematic review of the quality of liver biopsy specimens. Am J Clin Pathol. 2006;125:710–21.
23. Colloredo G, Guido M, Sonzogni A, Leandro G. Impact of liver biopsy size on histological evaluation of chronic viral hepatitis: The smaller the sample, the milder the disease. J Hepatol. 2003;39:239–44.
24. Guha IN, Myers RP, Patel K, Talwalkar JA. Biomarkers of liver fibrosis: What lies beneath the receiver operating characteristic curve? Hepatology. 2011;54:1454–62.
25. Duarte-Rojo A, Altamirano JT, Feld JJ. Noninvasive markers of fibrosis: Key concepts for improving accuracy in daily clinical practice. Ann Hepatol. 2012;11:426–39.
26. Buzzetti E, Hall A, Ekstedt M, Manuguerra R, Guerrero Misas M, Covelli C, et al. Collagen proportionate area is an independent predictor of long-term outcome in patients with non-alcoholic fatty liver disease. Aliment Pharmacol Ther. 2019;49:1214–22.
27. Akobeng AK. Understanding diagnostic tests 1: Sensitivity, specificity and predictive values. Acta Paediatrica. 2007;96:338–41.
28. Hosmer DW Jr, Lemeshow S, Sturdivant RX. Applied logistic regression, 3rd ed. Wiley; 2013.
29. Yen YH, Kuo FY, Chen CH, Hu TH, Lu SN, Wang JH, et al. Ultrasound is highly specific in diagnosing compensated cirrhosis in chronic hepatitis C patients in real world clinical practice. Medicine. 2019;98:e16270.
30. Boursier J, Zarski JP, de Ledinghen V, Rousselet MC, Sturm N, Lebail B, et al, the Multicentric Group from ANRS/HC/EP23 FIBROSTAR Studies. Determination of reliability criteria for liver stiffness evaluation by transient elastography. Hepatology. 2013;57:1182–91.
31. Durango E, Dietrich C, Seitz HK, Kunz CU, Pomier-Layrargues GT, Duarte-Rojo A, et al. Direct comparison of the FibroScan XL and M probes for assessment of liver fibrosis in obese and nonobese patients. Hepat Med. 2013;5:43–52.
32. Berger A, Shili S, Zuberbuhler F, Hiriart JB, Lannes A, Chermak F, et al. Liver stiffness measurement with FibroScan: Use the right probe in the right conditions. Clin Transl Gastroenterol. 2019;10:e00023.
33. Petta S, Wai-Sun Wong V, Bugianesi E, Fracanzani AL, Cammà C, Hiriart JB, et al. Impact of obesity and alanine aminotransferase levels on the diagnostic accuracy for advanced liver fibrosis of noninvasive tools in patients with nonalcoholic fatty liver disease. Am J Gastroenterol. 2019;114:916–28.
34. Wong VWS, Vergniol J, Wong GLH, Foucher J, Chan AWH, Chermak F, et al. Liver stiffness measurement using XL probe in patients with nonalcoholic fatty liver disease. Am J Gastroenterol. 2012;107:1862–71.
35. Wong VWS, Irles M, Wong GLH, Shili S, Chan AWH, Merrouche W, et al. Unified interpretation of liver stiffness measurement by M and XL probes in non-alcoholic fatty liver disease. Gut. 2019;68:2057–64.
36. Sigrist RMS, Liau J, Kaffas AE, Chammas MC, Willmann JK. Ultrasound elastography: Review of techniques and clinical applications. Theranostics. 2017;7:1303–29.
37. Cassinotto C, Boursier J, de Lédinghen V, Lebigot J, Lapuyade B, Cales P, et al. Liver stiffness in nonalcoholic fatty liver

disease: A comparison of supersonic shear imaging, FibroScan, and ARFI with liver biopsy. Hepatology. 2016;63:1817–27.
38. Conti F, Serra C, Vukotic R, Fiorini E, Felicani C, Mazzotta E, et al. Accuracy of elastography point quantification and steatosis influence on assessing liver fibrosis in patients with chronic hepatitis C. Liver Int. 2017;37:187–95.
39. Myers RP, Pomier-Layrargues G, Kirsch R, Pollett A, Duarte-Rojo A, Wong D, et al. Feasibility and diagnostic performance of the FibroScan XL probe for liver stiffness measurement in overweight and obese patients. Hepatology. 2012;55:199–208.
40. Ghoz HM, Kröner PT, Stancampiano FF, Bowman AW, Vishnu P, Heckman MG, et al. Hepatic iron overload identified by magnetic resonance imaging-based T2* is a predictor of non-diagnostic elastography. Quant Imaging Med Surg. 2019;9:921–7.
41. Petta S, Maida M, Macaluso FS, Di Marco V, Cammà C, Cabibi D, et al. The severity of steatosis influences liver stiffness measurement in patients with nonalcoholic fatty liver disease. Hepatology. 2015;62:1101–10.
42. Colombo S, Belloli L, Zaccanelli M, Badia E, Jamoletti C, Buonocore M, et al. Normal liver stiffness and its determinants in healthy blood donors. Dig Liver Dis. 2011;43:231–6.
43. Fraquelli M, Rigamonti C, Casazza G, Donato MF, Ronchi G, Conte D, et al. Etiology-related determinants of liver stiffness values in chronic viral hepatitis B or C. J Hepatol. 2011;54:621–8.
44. Nguyen-Khac E, Thiele M, Voican C, Nahon P, Moreno C, Boursier J, et al. Non-invasive diagnosis of liver fibrosis in patients with alcohol-related liver disease by transient elastography: An individual patient data meta-analysis. Lancet Gastroenterol Hepatol. 2018;3:614–25.
45. Mukund A, Pargewar SS, Desai SN, Rajesh S, Sarin SK. Changes in liver congestion in patients with Budd-Chiari syndrome following endovascular interventions: Assessment with transient elastography. J Vasc Interv Radiol. 2017;28:683–7.
46. Guo H, Liao M, Jin J, Zeng J, Li S, Schroeder DR, et al. How intrahepatic cholestasis affects liver stiffness in patients with chronic hepatitis B: A study of 1197 patients with liver biopsy. Eur Radiol. 2020;30:1096–104.
47. Janssens F, Spahr L, Rubbia-Brandt L, Giostra E, Bihl F. Hepatic amyloidosis increases liver stiffness measured by transient elastography. Acta Gastroenterol Belg. 2020;73:52–4.
48. Wong GLH, Wong VWS, Choi PCL, Chan AWH, Chim AML, Yiu KKL, et al. Increased liver stiffness measurement by transient elastography in severe acute exacerbation of chronic hepatitis B. J Gastroenterol Hepatol. 2009;24:1002–7.
49. Liu CH, Liang CC, Huang KW, Liu CJ, Chen SI, Lin JW, et al. Transient elastography to assess hepatic fibrosis in hemodialysis chronic hepatitis C patients. Clin J Am Soc Nephrol. 2011;6:1057–65.
50. Taneja S, Borkakoty A, Rathi S, Kumar V, Duseja A, Dhiman RK, et al. Assessment of liver fibrosis by transient elastography should be done after hemodialysis in end stage renal disease patients with liver disease. Dig Dis Sci. 2017;62:3186–92.
51. Schmoyer CJ, Kumar D, Gupta G, Sterling RK. Diagnostic accuracy of non-invasive tests to detect advanced hepatic fibrosis in patients with hepatitis C and end-stage renal disease. Clin Gastroenterol Hepatol. 2020;18:2332–9.e1.
52. Vuppalanchi R, Weber R, Russell S, Gawrieh S, Samala N, Slaven JE, et al. Is fasting necessary for individuals with nonalcoholic fatty liver disease to undergo vibration-controlled transient elastography. Am J Gastroenterol. 2019;114:995–7.
53. Murawaki Y. Influence of a history of gastrectomy for gastric cancer on serum hyaluronan concentration in normal individuals and patients with chronic liver disease. Hepatol Res. 1998;10:248–54.
54. Su Y, Gu H, Weng D, Zhou Y, Li Q, Zhang F, et al. Association of serum levels of laminin, type IV collagen, procollagen III N-terminal peptide, and hyaluronic acid with the progression of interstitial lung disease. Medicine. 2017;96:e6617.
55. Koh C, Turner T, Zhao X, Minniti CP, Feld JJ, Simpson J, et al. Liver stiffness increases acutely during sickle cell vaso-occlusive crisis. Am J Hematol. 2013;88:E250–4.
56. Duarte-Rojo A, Heimbach JK, Borja-Cacho D, Barone GW, Shaheen MF, Lamps LW, et al. Usefulness of controlled attenuation parameter and liver stiffness measurement for the identification of extended-criteria donors and risk-assessment in liver transplantation. Transplantation. 2022;106:318–27.
57. Karlas T, Petroff D, Sasso M, Fan JG, Mi YQ, de Lédinghen V, et al. Individual patient data meta-analysis of controlled attenuation parameter (CAP) technology for assessing steatosis. J Hepatol. 2017;66:1022–30.
58. Kennedy P, Wagner M, Castéra L, Hong CW, Johnson CL, Sirlin CB, et al. Quantitative elastography methods in liver disease: Current evidence and future directions. Radiology. 2018;286:738–63.
59. Friedrich-Rust M, Wunder K, Kriener S, Sotoudeh F, Richter S, Bojunga J, et al. Liver fibrosis in viral hepatitis: Noninvasive assessment with acoustic radiation force impulse imaging versus transient elastography. Radiology. 2009;252:595–604.
60. Herrmann E, de Lédinghen V, Cassinotto C, Chu WCW, Leung VYF, Ferraioli G, et al. Assessment of biopsy-proven liver fibrosis by two-dimensional shear wave elastography: An individual patient data-based meta-analysis. Hepatology. 2018;67:260–72.
61. Yin M, Talwalkar JA, Glaser KJ, Manduca A, Grimm RC, Rossman PJ, et al. Assessment of hepatic fibrosis with magnetic resonance elastography. Clin Gastroenterol Hepatol. 2007;5:1207–13e2.
62. Wagner M, Besa C, Bou Ayache J, Yasar TK, Bane O, Fung M, et al. Magnetic resonance elastography of the liver: Qualitative and quantitative comparison of gradient echo and spin echo echoplanar imaging sequences. Invest Radiol. 2016;51:575–81.
63. Venkatesh SK, Yin M, Ehman RL. Magnetic resonance elastography of liver: Technique, analysis, and clinical applications. J Magn Reson Imaging. 2013;37:544–55.
64. Wagner M, Corcuera-Solano I, Lo G, Esses S, Liao J, Besa C, et al. Technical failure of MR elastography examinations of the liver: Experience from a large single-center study. Radiology. 2017;284:401–12.
65. Singh S, Venkatesh SK, Wang Z, Miller FH, Motosugi U, Low RN, et al. Diagnostic performance of magnetic resonance elastography in staging liver fibrosis: A systematic review and meta-analysis of individual participant data. Clin Gastroenterol Hepatol. 2015;13:440–51e6.
66. Cassinotto C, Lapuyade B, Guiu B, Marraud des Grottes H, Piron L, Merrouche W, et al. Agreement between 2-dimensional shear wave and transient elastography values for diagnosis of advanced chronic liver disease. Clin Gastroenterol Hepatol. 2020;18:2971–79.e3.
67. Duarte-Rojo A, Taouli B, Leung DH, et al. Imaging-based noninvasive liver disease assessment (NILDA) for staging liver fibrosis in chronic liver disease: A systematic review supporting AASLD guideline. Hepatology. 2024. doi:10.1097/HEP.0000000000000852.
68. Patel K, Asrani SK, Fiel MI, et al. Accuracy of Blood-Based Biomarkers for Staging Liver Fibrosis in Chronic Liver Disease: A Systematic Review. Hepatology. 2024. doi:10.1097/HEP.0000000000000842.
69. Shi Y, Xia F, Li Q, Li J, Yu B, Li Y, et al. Magnetic resonance elastography for the evaluation of liver fibrosis in chronic hepatitis B and C by using both gradient-recalled echo and spin-echo echo planar imaging: A prospective study. Am J Gastroenterol. 2016;111:823–33.

70. Zambam de Mattos Â, Alves de Mattos A. Transient elastography vs. aspartate aminotransferase to platelet ratio index in hepatitis C: A meta-analysis. Ann Hepatol. 2017;16:349–57.
71. Ichikawa S, Motosugi U, Ichikawa T, Sano K, Morisaka H, Enomoto N, et al. Magnetic resonance elastography for staging liver fibrosis in chronic hepatitis C. Magn Reson Med Sci. 2012; 11:291–7.
72. Numao H, Shimaya K, Kakuta A, Shibutani K, Igarashi S, Hasui K, et al. The utility of two-dimensional real-time shear wave elastography for assessing liver fibrosis in patients with chronic hepatitis C virus infection. Eur J Gastroenterol Hepatol. 2021; 33:1400–7.
73. Xiao H, Shi M, Xie Y, Chi X. Comparison of diagnostic accuracy of magnetic resonance elastography and Fibroscan for detecting liver fibrosis in chronic hepatitis B patients: A systematic review and meta-analysis. PLoS One. 2017;12:e0186660.
74. European Association for Study of Liver, Asociacion Latinoamericana para el Estudio del Higado. EASL-ALEH Clinical Practice Guidelines: Non-invasive tests for evaluation of liver disease severity and prognosis. J Hepatol. 2015;63:237–64.
75. Jiang W, Huang S, Teng H, Wang P, Wu M, Zhou X, et al. Diagnostic accuracy of point shear wave elastography and transient elastography for staging hepatic fibrosis in patients with non-alcoholic fatty liver disease: A meta-analysis. BMJ Open. 2018;8:e021787.
76. Dong XQ, Wu Z, Li J, Wang GQ, Zhao H, and the China HepB-Related Fibrosis Assessment Research Group. Declining in liver stiffness cannot indicate fibrosis regression in patients with chronic hepatitis B: A 78-week prospective study. J Gastroenterol Hepatol. 2019;34:755–63.
77. Xiao G, Zhu S, Xiao X, Yan L, Yang J, Wu G. Comparison of laboratory tests, ultrasound, or magnetic resonance elastography to detect fibrosis in patients with nonalcoholic fatty liver disease: A meta-analysis. Hepatology. 2017;66:1486–501.
78. Anstee QM, Lawitz EJ, Alkhouri N, Wong VWS, Romero-Gomez M, Okanoue T, et al. Noninvasive tests accurately identify advanced fibrosis due to NASH: Baseline data from the STELLAR trials. Hepatology. 2019;70:1521–30.
79. Rinella ME, Neuschwander-Tetri BA, Siddiqui MS, Abdelmalek MF, Caldwell S, Barb D, et al. AASLD Practice Guidance on the clinical assessment and management of nonalcoholic fatty liver disease. Hepatology. 2023;77:1797–835.
80. Liang Y, Li D. Magnetic resonance elastography in staging liver fibrosis in non-alcoholic fatty liver disease: A pooled analysis of the diagnostic accuracy. BMC Gastroenterol. 2020;20:89.
81. Pavlov CS, Casazza G, Nikolova D, Tsochatzis E, Gluud C. Systematic review with meta-analysis: Diagnostic accuracy of transient elastography for staging of fibrosis in people with alcoholic liver disease. Aliment Pharmacol Ther. 2016;43: 575–85.
82. Mueller S. Increased liver stiffness in alcoholic liver disease: Differentiating fibrosis from steatohepatitis. World J Gastroenterol. 2010;16:966–72.
83. Altamirano J, Qi Q, Choudhry S, Abdallah M, Singal AK, Humar A, et al. Non-invasive diagnosis: Non-alcoholic fatty liver disease and alcoholic liver disease. Transl Gastroenterol Hepatol. 2020;5:31.
84. Cristoferi L, Calvaruso V, Overi D, Viganò M, Rigamonti C, Degasperi E, et al, and the Italian PBC Registry. Accuracy of transient elastography in assessing fibrosis at diagnosis in naïve patients with primary biliary cholangitis: A dual cut-off approach. Hepatology. 2021;74:1496–508.
85. Winters AC, Mittal R, Schiano TD. A review of the use of transient elastography in the assessment of fibrosis and steatosis in the post-liver transplant patient. Clin Transplant. 2019;33:e13700.
86. Bowlus CL, Arrivé L, Bergquist A, Deneau M, Forman L, Ilyas SI, et al. AASLD practice guidance on primary sclerosing cholangitis and cholangiocarcinoma. Hepatology. 2023;77: 659–702.
87. Siddiqui MS, Idowu MO, Stromberg K, Sima A, Lee E, Patel S, et al. Diagnostic performance of vibration-controlled transient elastography in liver transplant recipients. Clin Gastroenterol Hepatol. 2021;19:367–74.
88. Fallahzadeh MA, Asrani SK, Vahhab E, Ebrahim VS, Saracino G, Elwir S, et al. Prediction of long-term morbidity and mortality after liver transplantation using two-dimensional shear wave elastography compared with liver biopsy. Liver Transpl. 2022; 28:1618–27.
89. Bhat M, Tazari M, Sebastiani G. Performance of transient elastography and serum fibrosis biomarkers for non-invasive evaluation of recurrent fibrosis after liver transplantation: A meta-analysis. PLoS One. 2017;12:e0185192.
90. Lin Y, Li H, Jin C, Wang H, Jiang B. The diagnostic accuracy of liver fibrosis in non-viral liver diseases using acoustic radiation force impulse elastography: A systematic review and meta-analysis. PLoS One. 2020;15:e0227358.
91. Singh S, Venkates SK, Keaveny A, Adam S, Miller FH, Asbach P, et al. Diagnostic accuracy of magnetic resonance elastography in liver transplant recipients: A pooled analysis. Ann Hepatol. 2016;15:363–76.
92. Crespo G, Castro-Narro G, García-Juárez I, Benítez C, Ruiz P, Sastre L, et al. Usefulness of liver stiffness measurement during acute cellular rejection in liver transplantation. Liver Transpl. 2016;22:298–304.
93. Boeken T, Lucidarme O, Mbarki E, Scatton O, Savier E, Wagner M. Association of shear-wave elastography with clinical outcomes post-liver transplantation. Clin Res Hepatol Gastroenterol. 2021;45:101554.
94. Deurdulian C, Grant EG, Tchelepi H, Latterman PT, Paluch JT, Chopra S, et al. Assessment of fibrosis in liver transplant recipients: Diagnostic performance of shear wave elastography (SWE) and correlation of SWE findings with biopsy results. AJR Am J Roentgenol. 2016;213:W264–71.
95. Saeed N, Glass L, Sharma P, Shannon C, Sonnenday CJ, Tincopa MA. Incidence and risks for nonalcoholic fatty liver disease and steatohepatitis post-liver transplant: Systematic review and meta-analysis. Transplantation. 2019;103:e345–54.
96. Dong DR, Hao MN, Li C, PENG Z, LIU X, WANG GP, et al. Acoustic radiation force impulse elastography, FibroScan®, Forns' index and their combination in the assessment of liver fibrosis in patients with chronic hepatitis B, and the impact of inflammatory activity and steatosis on these diagnostic methods. Mol Med Rep. 2015;11:4174–82.
97. Friedrich-Rust M, Buggisch P, de Knegt RJ, Dries V, Shi Y, Matschenz K, et al. Acoustic radiation force impulse imaging for non-invasive assessment of liver fibrosis in chronic hepatitis B. J Viral Hepat. 2013;20:240–7.
98. Liu Y, Dong C, Yang G, Liu J, Yao S, Li H, et al. Optimal linear combination of ARFI, transient elastography and APRI for the assessment of fibrosis in chronic hepatitis B. Liver Int. 2015;35: 816–25.
99. Friedrich-Rust M, Lupsor M, de Knegt R, Dries V, Buggisch P, Gebel M, et al. Point shear wave elastography by acoustic radiation force impulse quantification in comparison to transient elastography for the noninvasive assessment of liver fibrosis in chronic hepatitis C: A prospective international multicenter study. Ultraschall Med. 2015;36:239–47.
100. Lupsor M, Badea R, Stefanescu H, Sparchez Z, Branda H, Serban A, et al. Performance of a new elastographic method (ARFI technology) compared to unidimensional transient elastography in the noninvasive assessment of chronic hepatitis C. Preliminary results. J Gastrointestin Liver Dis. 2009;18:303–10.
101. Sporea I, Sirli R, Bota S, Popescu A, Sendroiu M, Jurchis A. Comparative study concerning the value of acoustic radiation

force impulse elastography (ARFI) in comparison with transient elastography (TE) for the assessment of liver fibrosis in patients with chronic hepatitis B and C. Ultrasound Med Biol. 2012;38:1310–6.
102. Leung VY, Shen J, Wong VW, Abrigo J, Wong GL, Chim AM, et al. Quantitative elastography of liver fibrosis and spleen stiffness in chronic hepatitis B carriers: Comparison of shear-wave elastography and transient elastography with liver biopsy correlation. Radiology. 2013;269:910–8.
103. Ferraioli G, Tinelli C, Dal Bello B, Zicchetti M, Filice G, Filice C, on behalf of the Liver Fibrosis Study Group. Accuracy of real-time shear wave elastography for assessing liver fibrosis in chronic hepatitis C: A pilot study. Hepatology. 2012;56:2125–33.
104. Zeng J, Zheng J, Huang Z, Chen S, Liu J, Wu T, et al. Comparison of 2-D shear wave elastography and transient elastography for assessing liver fibrosis in chronic hepatitis B. Ultrasound Med Biol. 2017;43:1563–70.
105. Zhang D, Chen M, Wang R, Liu Y, Zhang D, Liu L, et al. Comparison of acoustic radiation force impulse imaging and transient elastography for non-invasive assessment of liver fibrosis in patients with chronic hepatitis B. Ultrasound Med Biol. 2015;41:7–14.
106. Furlan A, Tublin ME, Yu L, Chopra KB, Lippello A, Behari J. Comparison of 2D shear wave elastography, transient elastography, and MR elastography for the diagnosis of fibrosis in patients with nonalcoholic fatty liver disease. AJR Am J Roentgenol. 2020;214:W20–6.
107. Sporea I. Is it better to use two elastographic methods for liver fibrosis assessment. World J Gastroenterol. 2011;17:3824–9.
108. Ragazzo TG, Paranagua-Vezozzo D, Lima FR, de Campos Mazo DF, Pessoa MG, Oliveira CP, et al. Accuracy of transient elastography-FibroScan®, acoustic radiation force impulse (ARFI) imaging, the enhanced liver fibrosis (ELF) test, APRI, and the FIB-4 index compared with liver biopsy in patients with chronic hepatitis C. Clinics (São Paulo). 2017;72:516–25.
109. Imajo K, Kessoku T, Honda Y, Tomeno W, Ogawa Y, Mawatari H, et al. Magnetic resonance imaging more accurately classifies steatosis and fibrosis in patients with nonalcoholic fatty liver disease than transient elastography. Gastroenterology. 2016;150:626–37.e7.
110. Park CC, Nguyen P, Hernandez C, Bettencourt R, Ramirez K, Fortney L, et al. Magnetic resonance elastography vs transient elastography in detection of fibrosis and noninvasive measurement of steatosis in patients with biopsy-proven nonalcoholic fatty liver disease. Gastroenterology. 2017;152:598–607.e2.
111. Chen J, Yin M, Talwalkar JA, Oudry J, Glaser KJ, Smyrk TC, et al. Diagnostic performance of MR elastography and vibration-controlled transient elastography in the detection of hepatic fibrosis in patients with severe to morbid obesity. Radiology. 2017;283:418–28.
112. Hsu C, Caussy C, Imajo K, Chen J, Singh S, Kaulback K, et al. Magnetic resonance vs transient elastography analysis of patients with nonalcoholic fatty liver disease: A systematic review and pooled analysis of individual participants. Clin Gastroenterol Hepatol. 2019;17:630–7.e8.
113. Lee YS, Yoo YJ, Jung YK, Kim JH, Seo YS, Yim HJ, et al. Multiparametric MR is a valuable modality for evaluating disease severity of nonalcoholic fatty liver disease. Clin Transl Gastroenterol. 2020;11:e00157.
114. Dyvorne HA, Jajamovich GH, Bane O, Fiel MI, Chou H, Schiano TD, et al. Prospective comparison of magnetic resonance imaging to transient elastography and serum markers for liver fibrosis detection. Liver Int. 2016;36:659–66.
115. Huwart L, Sempoux C, Vicaut E, Salameh N, Annet L, Danse E, et al. Magnetic resonance elastography for the noninvasive staging of liver fibrosis. Gastroenterology. 2008;135:32–40.
116. Ichikawa S, Motosugi U, Morisaka H, Sano K, Ichikawa T, Tatsumi A, et al. Comparison of the diagnostic accuracies of magnetic resonance elastography and transient elastography for hepatic fibrosis. Magn Reson Imaging. 2015;33:26–30.
117. Bohte AE, de Niet A, Jansen L, Bipat S, Nederveen AJ, Verheij J, et al. Non-invasive evaluation of liver fibrosis: A comparison of ultrasound-based transient elastography and MR elastography in patients with viral hepatitis B and C. Eur Radiol. 2014;24:638–48.
118. Yoon JH, Lee JM, Joo I, Lee ES, Sohn JY, Jang SK, et al. Hepatic fibrosis: Prospective comparison of MR elastography and US shear-wave elastography for evaluation. Radiology. 2014;273:772–82.
119. Cui J, Heba E, Hernandez C, Haufe W, Hooker J, Andre MP, et al. Magnetic resonance elastography is superior to acoustic radiation force impulse for the diagnosis of fibrosis in patients with biopsy-proven nonalcoholic fatty liver disease: A prospective study. Hepatology. 2016;63:453–61.
120. Wai C. A simple noninvasive index can predict both significant fibrosis and cirrhosis in patients with chronic hepatitis C. Hepatology. 2003;38:518–26.
121. Sterling RK, Lissen E, Clumeck N, Sola R, Correa MC, Montaner J, et al. Development of a simple noninvasive index to predict significant fibrosis in patients with HIV/HCV coinfection. Hepatology. 2006;43:1317–25.
122. Angulo P, Hui JM, Marchesini G, Bugianesi E, George J, Farrell GC, et al. The NAFLD fibrosis score: A noninvasive system that identifies liver fibrosis in patients with NAFLD. Hepatology. 2007;45:846–54.
123. Boursier J, de Ledinghen V, Leroy V, Anty R, Francque S, Salmon D, et al. A stepwise algorithm using an at-a-glance first-line test for the non-invasive diagnosis of advanced liver fibrosis and cirrhosis. J Hepatol. 2007;66:1158–65.
124. Imbert-Bismut F, Ratziu V, Pieroni L, Charlotte F, Benhamou Y, Poynard T, and the MULTIVIRC Group. Biochemical markers of liver fibrosis in patients with hepatitis C virus infection: A prospective study. Lancet. 2001;357:1069–75.
125. Rosenberg WMC, Voelker M, Thiel R, Becka M, Burt A, Schuppan D, et al, the European Liver Fibrosis Group. Serum markers detect the presence of liver fibrosis: A cohort study. Gastroenterology. 2004;127:1704–13.
126. Patel K, Gordon SC, Jacobson I, Hézode C, Oh E, Smith KM, et al. Evaluation of a panel of non-invasive serum markers to differentiate mild from moderate-to-advanced liver fibrosis in chronic hepatitis C patients. J Hepatol. 2004;41:935–42.
127. Adams LA, Bulsara M, Rossi E, DeBoer B, Speers D, George J, et al. Hepascore: An accurate validated predictor of liver fibrosis in chronic hepatitis C infection. Clin Chem. 2005;51:1867–73.
128. Calès P, Oberti F, Michalak S, Hubert-Fouchard I, Rousselet MC, Konaté A, et al. A novel panel of blood markers to assess the degree of liver fibrosis. Hepatology. 2005;42:1373–81.
129. Gamil M, Alboraie M, El-Sayed M, Elsharkawy A, Asem N, Elbaz T, et al. Novel scores combining AFP with non-invasive markers for prediction of liver fibrosis in chronic hepatitis C patients. J Med Virol. 2018;90:1080–6.
130. Sirli R, Sporea I, Bota S, Popescu A, Cornianu M. A comparative study of non-invasive methods for fibrosis assessment in chronic HCV infection. Hepat Mon. 2010;10:88–94.
131. Ferraioli G, Tinelli C, Malfitano A, Bello BD, Filice G, Filice C, et al, the Liver Fibrosis Study Group. Performance of real-time strain elastography, transient elastography, and aspartate-to-platelet ratio index in the assessment of fibrosis in chronic hepatitis C. AJR Am J Roentgenol. 2012;199:19–25.
132. Fernandes FF, Perazzo H, Andrade LE, Dellavance A, Terra C, Pereira G, et al. Latent class analysis of noninvasive methods and liver biopsy in chronic hepatitis C: An approach without a gold standard. BioMed Res Int. 2017;2017:8252980.
133. Paranaguá-Vezozzo DC, Andrade A, Mazo DFC, Nunes V, Guedes AL, Ragazzo TG, et al. Concordance of non-invasive

mechanical and serum tests for liver fibrosis evaluation in chronic hepatitis C. World J Hepatol. 2017;9:436–42.
134. Ichino N. A new index for non-invasive assessment of liver fibrosis. World J Gastroenterol. 2010;16:4809–16.
135. Abdelsameea E, Alsebaey A, Abdel-Razek W, Ehsan N, Morad W, Salama M, et al. Elastography and serum markers of fibrosis versus liver biopsy in 1270 Egyptian patients with hepatitis C. Eur J Gastroenterol Hepatol. 2020;32:1553–8.
136. Conti F, Serra C, Vukotic R, Felicani C, Mazzotta E, Gitto S, et al. Assessment of liver fibrosis with elastography point quantification vs other noninvasive methods. Clin Gastroenterol Hepatol. 2019;17:510–7.e3.
137. Liu CH, Liu CJ, Hong CM, Su TH, Yang HC, Chen KM, et al. A noninvasive diagnosis of hepatic fibrosis by BioFibroScore® in chronic hepatitis C patients. J Gastroenterol Hepatol. 2018;33: 291–7.
138. Silva Junior RG, Schmillevitch J, Nascimento MFA, Miranda MLQ, Brant PEAC, Schulz PO, et al. Acoustic radiation force impulse elastography and serum fibrosis markers in chronic hepatitis C. Scand J Gastroenterol. 2014;49:986–92.
139. Joo SK, Kim JH, Oh S, Kim BG, Lee KL, Kim HY, et al. Prospective comparison of noninvasive fibrosis assessment to predict advanced fibrosis or cirrhosis in Asian patients with hepatitis C. J Clin Gastroenterol. 2015;49:697–704.
140. Li SM, Li GX, Fu DM, Wang Y, Dang LQ. Liver fibrosis evaluation by ARFI and APRI in chronic hepatitis C. World J Gastroenterol. 2014;20:9528–33.
141. Zarski JP, Sturm N, Guechot J, Paris A, Zafrani ES, Asselah T, et al, the ANRS HCEP 23 Fibrostar Group. Comparison of nine blood tests and transient elastography for liver fibrosis in chronic hepatitis C: The ANRS HCEP-23 study. J Hepatol. 2012;56:55–62.
142. Castéra L, Bail BL, Roudot-Thoraval F, Bernard PH, Foucher J, Merrouche W, et al. Early detection in routine clinical practice of cirrhosis and oesophageal varices in chronic hepatitis C: Comparison of transient elastography (FibroScan) with standard laboratory tests and non-invasive scores. J Hepatol. 2009; 50:59–68.
143. Castera L, Winnock M, Pambrun E, Paradis V, Perez P, Loko MA, et al. Comparison of transient elastography (FibroScan), FibroTest, APRI and two algorithms combining these non-invasive tests for liver fibrosis staging in HIV/HCV coinfected patients: ANRS CO13 HEPAVIH and FIBROSTIC collaboration. HIV Med. 2014;15:30–9.
144. Schmid P, Bregenzer A, Huber M, Rauch A, Jochum W, Müllhaupt B, et al, the Swiss HIV Cohort Study. Progression of liver fibrosis in HIV/HCV co-infection: A comparison between non-invasive assessment methods and liver biopsy. PLoS One. 2015;10:e0138838.
145. Tseng CH, Chang CY, Mo LR, Lin JT, Tai CM, Perng DS, et al. Acoustic radiation force impulse elastography with APRI and FIB-4 to identify significant liver fibrosis in chronic hepatitis B patients. Ann Hepatol. 2018;17:789–94.
146. Zeng X, Xu C, Li M, Xia J, Liu M, Zhu P, et al. The diagnostic value of FibroScan in assessing significant liver fibrosis in patients with chronic hepatitis B. West Indian Med J. 2015;65: 106–10.
147. Yan LB, Zhang QB, Zhu X, He M, Tang H. Serum S100 calcium binding protein A4 improves the diagnostic accuracy of transient elastography for assessing liver fibrosis in hepatitis B. Clin Res Hepatol Gastroenterol. 2018;42:64–71.
148. Lemoine M, Shimakawa Y, Nayagam S, Khalil M, Suso P, Lloyd J, et al. The gamma-glutamyl transpeptidase to platelet ratio (GPR) predicts significant liver fibrosis and cirrhosis in patients with chronic HBV infection in West Africa. Gut. 2016;65: 1369–76.
149. Liu J, Zhao J, Zhang Y, Ji Y, Lin S, Dun G, et al. Noninvasive assessment of liver fibrosis stage using ultrasound-based shear wave velocity measurements and serum algorithms in patients with viral hepatitis B: A retrospective cohort study. J Ultrasound Med. 2017;36:285–93.
150. Lu XJ, Yang XJ, Sun JY, Zhang X, Yuan ZX, Li XH. FibroBox: A novel noninvasive tool for predicting significant liver fibrosis and cirrhosis in HBV infected patients. Biomark Res. 2020;8:48.
151. Lee HW, Kang W, Kim BK, Kim SU, Park JY, Kim DY, et al. Red cell volume distribution width-to-platelet ratio in assessment of liver fibrosis in patients with chronic hepatitis B. Liver Int. 2016; 36:24–30.
152. Bosselut N, Taibi L, Guéchot J, Zarski JP, Sturm N, Gelineau MC, et al, the ANRS HCEP 23 Fibrostar Group. Including osteoprotegerin and collagen IV in a score-based blood test for liver fibrosis increases diagnostic accuracy. Clin Chim Acta. 2013;415:63–8.
153. Mahadeva S, Mahfudz AS, Vijayanathan A, Goh KL, Kulenthran A, Cheah PL. Performance of transient elastography (TE) and factors associated with discordance in non-alcoholic fatty liver disease. J Dig Dis. 2013;14:604–10.
154. Joo SK, Kim W, Kim D, Kim JH, Oh S, Lee KL, et al. Steatosis severity affects the diagnostic performances of noninvasive fibrosis tests in nonalcoholic fatty liver disease. Liver Int. 2018; 38:331–41.
155. Wong VWS, Vergniol J, Wong GLH, Foucher J, Chan HLY, Le Bail B, et al. Diagnosis of fibrosis and cirrhosis using liver stiffness measurement in nonalcoholic fatty liver disease. Hepatology. 2010;51:454–62.
156. Okajima A, Sumida Y, Taketani H, Hara T, Seko Y, Ishiba H, et al. Liver stiffness measurement to platelet ratio index predicts the stage of liver fibrosis in non-alcoholic fatty liver disease. Hepatol Res. 2017;47:721–30.
157. Tovo CV, Villela-Nogueira CA, Leite NC, Panke CL, Port GZ, Fernandes S, et al. Transient hepatic elastography has the best performance to evaluate liver fibrosis in non-alcoholic fatty liver disease (NAFLD). Ann Hepatol. 2019;18:445–9.
158. Petta S, Wong VWS, Cammà C, Hiriart JB, Wong GLH, Vergniol J, et al. Serial combination of non-invasive tools improves the diagnostic accuracy of severe liver fibrosis in patients with NAFLD. Aliment Pharmacol Ther. 2017;46: 617–27.
159. Banini BA, Patel S, Yu JW, Kang L, Bailey C, Strife BJ, et al. Derivation and validation of a model to predict clinically significant portal hypertension using transient elastography and FIB-4. J Clin Gastroenterol. 2023;57:189–97.
160. Cui J, Ang B, Haufe W, Hernandez C, Verna EC, Sirlin CB, et al. Comparative diagnostic accuracy of magnetic resonance elastography vs. eight clinical prediction rules for non-invasive diagnosis of advanced fibrosis in biopsy-proven non-alcoholic fatty liver disease: A prospective study. Aliment Pharmacol Ther. 2015;41:1271–80.
161. Thiele M, Madsen BS, Hansen JF, Detlefsen S, Antonsen S, Krag A. Accuracy of the enhanced liver fibrosis test vs fibrotest, elastography, and indirect markers in detection of advanced fibrosis in patients with alcoholic liver disease. Gastroenterology. 2018;154:1369–79.
162. Voican CS, Louvet A, Trabut JB, Njiké-Nakseu M, Dharancy S, Sanchez A, et al. Transient elastography alone and in combination with FibroTest® for the diagnosis of hepatic fibrosis in alcoholic liver disease. Liver Int. 2017;37:1697–705.
163. Kim BK, Kim HS, Park JY, Kim DY, Ahn SH, Chon CY, et al. Prospective validation of ELF test in comparison with Fibroscan and FibroTest to predict liver fibrosis in Asian subjects with chronic hepatitis B. PLoS One. 2012;7:e41964.
164. Trembling PM, Lampertico P, Parkes J, Tanwar S, Viganò M, Facchetti F, et al. Performance of enhanced liver fibrosis test and comparison with transient elastography in the identification of liver fibrosis in patients with chronic hepatitis B infection. J Viral Hepat. 2014;21:430–8.

165. Sterling RK, King WC, Wahed AS, Kleiner DE, Khalili M, Sulkowski M, et al, the HIV-HBV Cohort Study of the Hepatitis B Research Network. Evaluating noninvasive markers to identify advanced fibrosis by liver biopsy in HBV/HIV co-infected adults. Hepatology. 2020;71:411–21.
166. Petta S, Wong VWS, Cammà C, Hiriart JB, Wong GLH, Marra F, et al. Improved noninvasive prediction of liver fibrosis by liver stiffness measurement in patients with nonalcoholic fatty liver disease accounting for controlled attenuation parameter values. Hepatology. 2017;65:1145–55.
167. Staufer K, Halilbasic E, Spindelboeck W, Eilenberg M, Prager G, Stadlbauer V, et al. Evaluation and comparison of six noninvasive tests for prediction of significant or advanced fibrosis in nonalcoholic fatty liver disease. United European Gastroenterol J. 2019;7:1113–23.
168. Wu S, Yang Z, Zhou J, Zeng N, He Z, Zhan S, et al. Systematic review: Diagnostic accuracy of non-invasive tests for staging liver fibrosis in autoimmune hepatitis. Hepatol Int. 2019;13: 91–101.
169. Corpechot C, Gaouar F, El Naggar A, Kemgang A, Wendum D, Poupon R, et al. Baseline values and changes in liver stiffness measured by transient elastography are associated with severity of fibrosis and outcomes of patients with primary sclerosing cholangitis. Gastroenterology. 2014;146:970–9.e6.
170. Corpechot C, Carrat F, Poujol-Robert A, Gaouar F, Wendum D, Chazouillères O, et al. Noninvasive elastography-based assessment of liver fibrosis progression and prognosis in primary biliary cirrhosis. Hepatology. 2012;56:198–208.
171. Friedrich-Rust M, Rosenberg W, Parkes J, Herrmann E, Zeuzem S, Sarrazin C. Comparison of ELF, FibroTest and FibroScan for the non-invasive assessment of liver fibrosis. BMC Gastroenterol. 2010;10:103.
172. Castéra L, Vergniol J, Foucher J, Le Bail B, Chanteloup E, Haaser M, et al. Prospective comparison of transient elastography, Fibrotest, APRI, and liver biopsy for the assessment of fibrosis in chronic hepatitis C. Gastroenterology. 2005;128: 343–50.
173. Boursier J, de Ledinghen V, Zarski JP, Rousselet MC, Sturm N, Foucher J, et al. A new combination of blood test and fibroscan for accurate non-invasive diagnosis of liver fibrosis stages in chronic hepatitis C. Am J Gastroenterol. 2011;106: 1255–63.
174. Heo JY, Kim BK, Park JY, Kim DY, Ahn SH, Kim HS, et al. Combination of transient elastography and an enhanced liver fibrosis test to assess the degree of liver fibrosis in patients with chronic hepatitis B. Gut Liver. 2018;12:190–200.
175. Miailhes P, Pradat P, Chevallier M, Lacombe K, Bailly F, Cotte L, et al. Proficiency of transient elastography compared to liver biopsy for the assessment of fibrosis in HIV/HBV-coinfected patients. J Viral Hepat. 2011;18:61–9.
176. Loong TCW, Wei JL, Leung JCF, Wong GLH, Shu SST, Chim AML, et al. Application of the combined FibroMeter vibration-controlled transient elastography algorithm in Chinese patients with non-alcoholic fatty liver disease. J Gastroenterol Hepatol. 2017;32:1363–9.
177. Floreani A, Cazzagon N, Martines D, Cavalletto L, Baldo V, Chemello L. Performance and utility of transient elastography and noninvasive markers of liver fibrosis in primary biliary cirrhosis. Dig Liver Dis. 2011;43:887–92.
178. Boursier J, Vergniol J, Sawadogo A, Dakka T, Michalak S, Gallois Y, et al. The combination of a blood test and Fibroscan improves the non-invasive diagnosis of liver fibrosis. Liver Int. 2009;29:1507–15.
179. Ducancelle A, Leroy V, Vergniol J, Sturm N, Le Bail B, Zarski JP, et al. A single test combining blood markers and elastography is more accurate than other fibrosis tests in the main causes of chronic liver diseases. J Clin Gastroenterol. 2017;51:639–49.
180. Wong GLH, Wong VWS, Choi PCL, Chan AWH, Chan HLY. Development of a non-invasive algorithm with transient elastography (Fibroscan) and serum test formula for advanced liver fibrosis in chronic hepatitis B. Aliment Pharmacol Ther. 2010;31:1095–103.
181. Wong GLH, Chan HLY, Choi PCL, Chan AWH, Yu Z, Lai JWY, et al. Non-invasive algorithm of enhanced liver fibrosis and liver stiffness measurement with transient elastography for advanced liver fibrosis in chronic hepatitis B. Aliment Pharmacol Ther. 2014;39:197–208.
182. Petta S, Vanni E, Bugianesi E, Di Marco V, Cammà C, Cabibi D, et al. The combination of liver stiffness measurement and NAFLD fibrosis score improves the noninvasive diagnostic accuracy for severe liver fibrosis in patients with nonalcoholic fatty liver disease. Liver Int. 2015;35:1566–73.
183. Boursier J, Guillaume M, Leroy V, Irlès M, Roux M, Lannes A, et al. New sequential combinations of non-invasive fibrosis tests provide an accurate diagnosis of advanced fibrosis in NAFLD. J Hepatol. 2019;71:389–96.
184. Shima T, Sakai K, Oya H, Katayama T, Mitsumoto Y, Mizuno M, et al. Diagnostic accuracy of combined biomarker measurements and vibration-controlled transient elastography (VCTE) for predicting fibrosis stage of non-alcoholic fatty liver disease. J Gastroenterol. 2020;55:100–12.
185. Inadomi C, Takahashi H, Ogawa Y, Oeda S, Imajo K, Kubotsu Y, et al. Accuracy of the Enhanced Liver Fibrosis test, and combination of the Enhanced Liver Fibrosis and non-invasive tests for the diagnosis of advanced liver fibrosis in patients with non-alcoholic fatty liver disease. Hepatol Res. 2020;50:682–92.
186. Srivastava A, Gailer R, Tanwar S, Trembling P, Parkes J, Rodger A, et al. Prospective evaluation of a primary care referral pathway for patients with non-alcoholic fatty liver disease. J Hepatol. 2019;71:371–8.
187. Davyduke T, Tandon P, Al-Karaghouli M, Abraldes JG, Ma MM. Impact of implementing a "FIB-4 first" strategy on a pathway for patients with NAFLD referred from primary care. Hepatol Commun. 2019;3:1322–33.
188. Castéra L, Sebastiani G, Le Bail B, de Lédinghen V, Couzigou P, Alberti A. Prospective comparison of two algorithms combining non-invasive methods for staging liver fibrosis in chronic hepatitis C. J Hepatol. 2010;52:191–8.
189. Boursier J, de Ledinghen V, Zarski JP, Fouchard-Hubert I, Gallois Y, Oberti F, Calès P, the multicentric groups from SNIFF 32, VINDIAG 7, and ANRS/HC/EP23 FIBROSTAR studies. Comparison of eight diagnostic algorithms for liver fibrosis in hepatitis C: New algorithms are more precise and entirely noninvasive. Hepatology. 2012;55:58–67.
190. Dong H, Xu C, Zhou W, Liao Y, Cao J, Li Z, et al. The combination of 5 serum markers compared to FibroScan to predict significant liver fibrosis in patients with chronic hepatitis B virus. Clin Chim Acta. 2018;483:145–50.
191. Newsome PN, Sasso M, Deeks JJ, Paredes A, Boursier J, Chan WK, et al. FibroScan-AST (FAST) score for the non-invasive identification of patients with non-alcoholic steatohepatitis with significant activity and fibrosis: A prospective derivation and global validation study. Lancet Gastroenterol Hepatol. 2020;5:362–73.
192. Cassinotto C, Boursier J, Paisant A, Guiu B, Irles-Depe M, Canivet C, et al. Transient versus two-dimensional shear-wave elastography in a multistep strategy to detect advanced fibrosis in NAFLD. Hepatology. 2021;73:2196–205.
193. Vilar-Gomez E, Lou Z, Kong N, Vuppalanchi R, Imperiale TF, Chalasani N. Cost effectiveness of different strategies for detecting cirrhosis in patients with nonalcoholic fatty liver disease based on United States health care system. Clin Gastroenterol Hepatol. 2020;18:2305–14.e12.
194. Shiratori Y, Imazeki F, Moriyama M, Yano M, Arakawa Y, Yokosuka O, et al. Histologic improvement of fibrosis in patients

with hepatitis C who have sustained response to interferon therapy. Ann Intern Med. 2000;132:517–24.
195. Marcellin P, Gane E, Buti M, Afdhal N, Sievert W, Jacobson IM, et al. Regression of cirrhosis during treatment with tenofovir disoproxil fumarate for chronic hepatitis B: A 5-year open-label follow-up study. Lancet. 2012;381:468–75.
196. Mallet V, Gilgenkrantz H, Serpaggi J, Verkarre V, Vallet-Pichard A, Fontaine H, et al. Brief communication: The relationship of regression of cirrhosis to outcome in chronic hepatitis C. Ann Intern Med. 2008;149:399–403.
197. Mathurin P, Moussalli J, Cadranel J, Thibault V, Charlotte F, Dumouchel P, et al. Slow progression rate of fibrosis in hepatitis C virus patients with persistently normal alanine transaminase activity. Hepatology. 1998;27:868–72.
198. Vilar-Gomez E, Martinez-Perez Y, Calzadilla-Bertot L, Torres-Gonzalez A, Gra-Oramas B, Gonzalez-Fabian L, et al. Weight loss through lifestyle modification significantly reduces features of nonalcoholic steatohepatitis. Gastroenterology. 2015;149: 367–78.e5.
199. Singh S, Allen AM, Wang Z, Prokop LJ, Murad MH, Loomba R. Fibrosis progression in nonalcoholic fatty liver vs nonalcoholic steatohepatitis: A systematic review and meta-analysis of paired-biopsy studies. Clin Gastroenterol Hepatol. 2015;13: 643–654e9.
200. Kumagi T, Guindi M, Fischer SE, Arenovich T, Abdalian R, Coltescu C, et al. Baseline ductopenia and treatment response predict long-term histological progression in primary biliary cirrhosis. Am J Gastroenterol. 2010;105:2186–94.
201. Erman A, Sathya A, Nam A, Bielecki JM, Feld JJ, Thein HH, et al. Estimating chronic hepatitis C prognosis using transient elastography-based liver stiffness: A systematic review and meta-analysis. J Viral Hepat. 2018;25:502–13.
202. Lampertico P, Invernizzi F, Viganò M, Loglio A, Mangia G, Facchetti F, et al. The long-term benefits of nucleos(t)ide analogs in compensated HBV cirrhotic patients with no or small esophageal varices: A 12-year prospective cohort study. J Hepatol. 2015;63:1118–25.
203. van der Meer A, Veldt B, Feld JJ, et al. Improved platelet count and smaller spleen size long after sustained virological response in chronic hepatitis C patients with advanced fibrosis. Hepatology (Baltimore. Md). 2011;54:820A.
204. Pan JJ, Bao F, Du E, Skillin C, Frenette CT, Waalen J, et al. Morphometry confirms fibrosis regression from sustained virologic response to direct-acting antivirals for hepatitis C. Hepatol Commun. 2018;2:1320–30.
205. Wong GLH, Wong VWS, Choi PCL, Chan AWH, Chim AML, Yiu KKL, et al. On-treatment monitoring of liver fibrosis with transient elastography in chronic hepatitis B patients. Antivir Ther. 2011;16:165–72.
206. Liang X, Xie Q, Tan D, Ning Q, Niu J, Bai X, et al. Interpretation of liver stiffness measurement-based approach for the monitoring of hepatitis B patients with antiviral therapy: A 2-year prospective study. J Viral Hepat. 2018;25:296–305.
207. Kong Y, Sun Y, Zhou J, Wu X, Chen Y, Piao H, et al. Early steep decline of liver stiffness predicts histological reversal of fibrosis in chronic hepatitis B patients treated with entecavir. J Viral Hepat. 2019;26:576–85.
208. Sun J, Li Y, Sun X, Yu H, Liu Y. Dynamic changes of the aspartate aminotransferase-to-platelet ratio and transient elastography in predicting a histologic response in patients with chronic hepatitis B after entecavir treatment. J Ultrasound Med. 2019;38:1441–8.
209. Wei W, Wu X, Zhou J, Sun Y, Kong Y, Yang X. Noninvasive evaluation of liver fibrosis reverse using artificial neural network model for chronic hepatitis B patients. Comput Math Methods Med. 2019;2019:7239780.
210. Kamarajah SK, Chan WK, Nik Mustapha NR, Mahadeva S. Repeated liver stiffness measurement compared with paired liver biopsy in patients with non-alcoholic fatty liver disease. Hepatol Int. 2018;12:44–55.
211. Garg H, Aggarwal S, Shalimar, Yadav R, Datta Gupta S, Agarwal L, et al. Utility of transient elastography (fibroscan) and impact of bariatric surgery on nonalcoholic fatty liver disease (NAFLD) in morbidly obese patients. Surg Obes Relat Dis. 2018;14:81–91.
212. Nogami A, Yoneda M, Kobayashi T, Kessoku T, Honda Y, Ogawa Y, et al. Assessment of 10-year changes in liver stiffness using vibration-controlled transient elastography in non-alcoholic fatty liver disease. Hepatol Res. 2019;49:872–80.
213. Jayakumar S, Middleton MS, Lawitz EJ, Mantry PS, Caldwell SH, Arnold H, et al. Longitudinal correlations between MRE, MRI-PDFF, and liver histology in patients with non-alcoholic steatohepatitis: Analysis of data from a phase II trial of selonsertib. J Hepatol. 2019;70:133–41.
214. Puente A, Fortea JI, Posadas M, Garcia Blanco A, Rasines L, Cabezas J, et al. Changes in circulating lysyl oxidase-like-2 (LOXL2) levels, HOMA, and fibrosis after sustained virological response by direct antiviral therapy. J Clin Med. 2019;8:1242.
215. Stasi C, Arena U, Zignego AL, Corti G, Monti M, Triboli E, et al. Longitudinal assessment of liver stiffness in patients undergoing antiviral treatment for hepatitis C. Dig Liver Dis. 2013;45: 840–3.
216. Enomoto M, Mori M, Ogawa T, Fujii H, Kobayashi S, Iwai S, et al. Usefulness of transient elastography for assessment of liver fibrosis in chronic hepatitis B: Regression of liver stiffness during entecavir therapy. Hepatol Res. 2010;40:853–61.
217. Rinaldi L, Ascione A, Messina V, Rosato V, Valente G, Sangiovanni V, et al. Influence of antiviral therapy on the liver stiffness in chronic HBV hepatitis. Infection. 2018;46:231–8.
218. D'Ambrosio R, Aghemo A, Fraquelli M, Rumi MG, Donato MF, Paradis V, et al. The diagnostic accuracy of Fibroscan for cirrhosis is influenced by liver morphometry in HCV patients with a sustained virological response. J Hepatol. 2013;59: 251–6.
219. Winters A, Luedtke S, Moreland A, Jangouk P, Weng G, Silveira M, et al. In hepatitis C virus-related advanced fibrosis and cirrhosis, early decline of liver stiffness following antiviral therapy with DAAs is related to decline in liver inflammation. J Hepatol. 2017;66:S280.
220. Ogawa E, Furusyo N, Toyoda K, Takeoka H, Maeda S, Hayashi J. The longitudinal quantitative assessment by transient elastography of chronic hepatitis C patients treated with pegylated interferon alpha-2b and ribavirin. Antiviral Res. 2009;83:127–34.
221. Patel K, Benhamou Y, Yoshida EM, Kaita KD, Zeuzem S, Torbenson M, et al. An independent and prospective comparison of two commercial fibrosis marker panels (HCV FibroSURE and FIBROSpect II) during albinterferon alfa-2b combination therapy for chronic hepatitis C. J Viral Hepat. 2009;16: 178–86.
222. Vergniol J, Foucher J, Castéra L, Bernard PH, Tournan R, Terrebonne E, et al. Changes of non-invasive markers and FibroScan values during HCV treatment. J Viral Hepat. 2009; 16:132–40.
223. Poynard T, Moussalli J, Munteanu M, Thabut D, Lebray P, Rudler M, et al, the FibroFrance-GHPS group. Slow regression of liver fibrosis presumed by repeated biomarkers after virological cure in patients with chronic hepatitis C. J Hepatol. 2013;59:675–83.
224. Poynard T, Ngo Y, Munteanu M, Thabut D, Massard J, Moussalli J, et al. Biomarkers of liver injury for hepatitis clinical trials: A meta-analysis of longitudinal studies. Antivir Ther. 2010;15:617–31.
225. Olveira A, Domínguez L, Troya J, Arias A, Pulido F, Ryan P, et al, the PALT-M-Study Group Investigators. Persistently

altered liver test results in hepatitis C patients after sustained virological response with direct-acting antivirals. J Viral Hepat. 2018;25:818–24.
226. Ji D, Chen Y, Shang Q, Liu H, Tan L, Wang J, et al. Unreliable estimation of fibrosis regression during treatment by liver stiffness measurement in patients with chronic hepatitis B. Am J Gastroenterol. 2021;116:1676–85.
227. Gonzalez HC, Duarte-Rojo A. Virologic cure of hepatitis C: Impact on hepatic fibrosis and patient outcomes. Curr Gastroenterol Rep. 2016;18:32.
228. Papachrysos N, Hytiroglou P, Papalavrentios L, Sinakos E, Kouvelis I, Akriviadis E. Antiviral therapy leads to histological improvement of HBeAg-negative chronic hepatitis B patients. Ann Gastroenterol. 2015;28:374–8.
229. Rockey DC. Liver fibrosis reversion after suppression of hepatitis B virus. Clin Liver Dis. 2016;20:667–79.
230. Vergniol J, Boursier J, Coutzac C, Bertrais S, Foucher J, Angel C, et al. Evolution of noninvasive tests of liver fibrosis is associated with prognosis in patients with chronic hepatitis C. Hepatology. 2014;60:65–76.
231. Higuchi M, Tamaki N, Kurosaki M, Inada K, Kirino S, Yamashita K, et al. Changes of liver stiffness measured by magnetic resonance elastography during direct-acting antivirals treatment in patients with chronic hepatitis C. J Med Virol. 2021;93:3744–51.
232. Ajmera VH, Liu A, Singh S, Yachoa G, Ramey M, Bhargava M, et al. Clinical utility of an increase in magnetic resonance elastography in predicting fibrosis progression in nonalcoholic fatty liver disease. Hepatology. 2020;71:849–60.
233. Allen AM, Shah VH, Therneau TM, Venkatesh SK, Mounajjed T, Larson JJ, et al. Multiparametric magnetic resonance elastography improves the detection of NASH regression following bariatric surgery. Hepatol Commun. 2020;4:185–92.
234. Cowin GJ, Jonsson JR, Bauer JD, Ash S, Ali A, Osland EJ, et al. Magnetic resonance imaging and spectroscopy for monitoring liver steatosis. J Magn Reson Imaging. 2008;28:937–45.
235. Szczepaniak LS, Nurenberg P, Leonard D, Browning JD, Reingold JS, Grundy S, et al. Magnetic resonance spectroscopy to measure hepatic triglyceride content: Prevalence of hepatic steatosis in the general population. Am J Physiol Endocrinol Metab. 2005;288:E462–8.
236. Yokoo T, Bydder M, Hamilton G, Middleton MS, Gamst AC, Wolfson T, et al. Nonalcoholic fatty liver disease: Diagnostic and fat-grading accuracy of low-flip-angle multiecho gradient-recalled-echo MR imaging at 1.5 T. Radiology. 2009;251:67–76.
237. Meisamy S, Hines CDG, Hamilton G, Sirlin CB, McKenzie CA, Yu H, et al. Quantification of hepatic steatosis with T1-independent, T2-corrected MR imaging with spectral modeling of fat: Blinded comparison with MR spectroscopy. Radiology. 2011;258:767–75.
238. Hu HH, Kim HW, Nayak KS, Goran MI. Comparison of fat-water MRI and single-voxel MRS in the assessment of hepatic and pancreatic fat fractions in humans. Obesity (Silver Spring, Md). 2010;18:841–7.
239. Tang A, Tan J, Sun M, Hamilton G, Bydder M, Wolfson T, et al. Nonalcoholic fatty liver disease: MR imaging of liver proton density fat fraction to assess hepatic steatosis. Radiology. 2013;267:422–31.
240. Idilman IS, Aniktar H, Idilman R, Kabacam G, Savas B, Elhan A, et al. Hepatic steatosis: Quantification by proton density fat fraction with MR imaging versus liver biopsy. Radiology. 2013;267:767–75.
241. Permutt Z, Le TA, Peterson MR, Seki E, Brenner DA, Sirlin C, et al. Correlation between liver histology and novel magnetic resonance imaging in adult patients with non-alcoholic fatty liver disease - MRI accurately quantifies hepatic steatosis in NAFLD. Aliment Pharmacol Ther. 2012;36:22–9.
242. Noureddin M, Lam J, Peterson MR, Middleton M, Hamilton G, Le TA, et al. Utility of magnetic resonance imaging versus histology for quantifying changes in liver fat in nonalcoholic fatty liver disease trials. Hepatology. 2013;58:1930–40.
243. Middleton MS, Van Natta ML, Heba ER, Alazraki A, Trout AT, Masand P, et al, the NASH Clinical Research Network. Diagnostic accuracy of magnetic resonance imaging hepatic proton density fat fraction in pediatric nonalcoholic fatty liver disease. Hepatology. 2018;67:858–72.
244. Siddiqui MS, Harrison SA, Abdelmalek MF, Anstee QM, Bedossa P, Castera L, et al, on behalf of the Liver Forum Case Definitions Working Group. Case definitions for inclusion and analysis of endpoints in clinical trials for nonalcoholic steatohepatitis through the lens of regulatory science. Hepatology. 2018;67:2001–12.
245. Harry S, Lai LL, Nik Mustapha NR, Abdul Aziz YF, Vijayananthan A, Rahmat K, et al. Volumetric liver fat fraction determines grade of steatosis more accurately than controlled attenuation parameter in patients with nonalcoholic fatty liver disease. Clin Gastroenterol Hepatol. 2020;18:945–53e2.
246. Caussy C, Alquiraish MH, Nguyen P, Hernandez C, Cepin S, Fortney LE, et al. Optimal threshold of controlled attenuation parameter with MRI-PDFF as the gold standard for the detection of hepatic steatosis. Hepatology. 2018;67:1348–59.
247. Le TA, Chen J, Changchien C, Peterson MR, Kono Y, Patton H, et al, the San Diego Integrated NAFLD Research Consortium (SINC). Effect of colesevelam on liver fat quantified by magnetic resonance in nonalcoholic steatohepatitis: A randomized controlled trial. Hepatology. 2012;56:922–32.
248. Loomba R, Sirlin CB, Ang B, Bettencourt R, Jain R, Salotti J, et al, the San Diego Integrated NAFLD Research Consortium (SINC). Ezetimibe for the treatment of nonalcoholic steatohepatitis: Assessment by novel magnetic resonance imaging and magnetic resonance elastography in a randomized trial (MOZART trial. Hepatology. 2015;61:1239–50.
249. Han MAT, Altayar O, Hamdeh S, Takyar V, Rotman Y, Etzion O, et al. Rates of and factors associated with placebo response in trials of pharmacotherapies for nonalcoholic steatohepatitis: Systematic review and meta-analysis. Clin Gastroenterol Hepatol. 2019;17:616–29.e26.
250. Lawitz EJ, Coste A, Poordad F, Alkhouri N, Loo N, McColgan BJ, et al. Acetyl-CoA carboxylase inhibitor GS-0976 for 12 weeks reduces hepatic de novo lipogenesis and steatosis in patients with nonalcoholic steatohepatitis. Clin Gastroenterol Hepatol. 2018;16:1983–91.e3.
251. Qi Q, Weinstock AK, Chupetlovska K, Borhani AA, Jorgensen DR, Furlan A, et al. Magnetic resonance imaging-derived proton density fat fraction (MRI-PDFF) is a viable alternative to liver biopsy for steatosis quantification in living liver donor transplantation. Clin Transplant. 2021;35:e14339.
252. Schwenzer NF, Springer F, Schraml C, Stefan N, Machann J, Schick F. Non-invasive assessment and quantification of liver steatosis by ultrasound, computed tomography and magnetic resonance. J Hepatol. 2009;51:433–45.
253. Dasarathy S, Dasarathy J, Khiyami A, Joseph R, Lopez R, McCullough AJ. Validity of real time ultrasound in the diagnosis of hepatic steatosis: A prospective study. J Hepatol. 2009;51:1061–7.
254. Hernaez R, Lazo M, Bonekamp S, Kamel I, Brancati FL, Guallar E, et al. Diagnostic accuracy and reliability of ultrasonography for the detection of fatty liver: A meta-analysis. Hepatology. 2011;54:1082–90.
255. Bril F, Ortiz-Lopez C, Lomonaco R, Orsak B, Freckleton M, Chintapalli K, et al. Clinical value of liver ultrasound for the

diagnosis of nonalcoholic fatty liver disease in overweight and obese patients. Liver Int. 2015;35:2139–46.
256. Paige JS, Bernstein GS, Heba E, Costa EAC, Fereirra M, Wolfson T, et al. A pilot comparative study of quantitative ultrasound, conventional ultrasound, and MRI for predicting histology-determined steatosis grade in adult nonalcoholic fatty liver disease. AJR Am J Roentgenol. 2017;208:W168–77.
257. Stern C, Castera L. Non-invasive diagnosis of hepatic steatosis. Hepatol Int. 2017;11:70–8.
258. European Association for the Study of the Liver (EASL), European Association for the Study of Diabetes (EASD), and European Association for the Study of Obesity (EASO). EASL-EASD-EASO Clinical Practice Guidelines for the management of non-alcoholic fatty liver disease. J Hepatol. 2016;64: 1388–402.
259. Fujiwara Y, Kuroda H, Abe T, Ishida K, Oguri T, Noguchi S, et al. The B-mode image-guided ultrasound attenuation parameter accurately detects hepatic steatosis in chronic liver disease. Ultrasound Med Biol. 2018;44:2223–32.
260. Tamaki N, Koizumi Y, Hirooka M, Yada N, Takada H, Nakashima O, et al. Novel quantitative assessment system of liver steatosis using a newly developed attenuation measurement method. Hepatol Res. 2018;48:821–8.
261. Lin SC, Heba E, Wolfson T, Ang B, Gamst A, Han A, et al. Noninvasive diagnosis of nonalcoholic fatty liver disease and quantification of liver fat using a new quantitative ultrasound technique. Clin Gastroenterol Hepatol. 2015;13:1337–45.e6.
262. Bae JS, Lee DH, Lee JY, Kim H, Yu SJ, Lee JH, et al. Assessment of hepatic steatosis by using attenuation imaging: A quantitative, easy-to-perform ultrasound technique. Eur Radiol. 2019;29:6499–507.
263. Ferraioli G, Maiocchi L, Savietto G, Tinelli C, Nichetti M, Rondanelli M, et al. Performance of the attenuation imaging technology in the detection of liver steatosis. J Ultrasound Med. 2021;40:1325–32.
264. Ferraioli G, Maiocchi L, Raciti MV, Tinelli C, De Silvestri A, Nichetti M, et al. Detection of liver steatosis with a novel ultrasound-based technique: A pilot study using MRI-derived proton density fat fraction as the gold standard. Clin Transl Gastroenterol. 2019;10:e00081.
265. Davidson LE, Kuk JL, Church TS, Ross R. Protocol for measurement of liver fat by computed tomography. J Appl Physiol (Bethesda, Md). 2006;100:864–8.
266. Kodama Y, Ng CS, Wu TT, Ayers GD, Curley SA, Abdalla EK, et al. Comparison of CT methods for determining the fat content of the liver. AJR Am J Roentgenol. 2007;188:1307–12.
267. Chen X, Li K, Yip R, Perumalswami P, Branch AD, Lewis S, et al. Hepatic steatosis in participants in a program of low-dose CT screening for lung cancer. Eur J Radiol. 2017;94:174–9.
268. Castera L, Vilgrain V, Angulo P. Noninvasive evaluation of NAFLD. Nat Rev Gastroenterol Hepatol. 2013;10:666–75.
269. Sasso M, Beaugrand M, de Ledinghen V, Douvin C, Marcellin P, Poupon R, et al. Controlled attenuation parameter (CAP): a novel VCTE™ guided ultrasonic attenuation measurement for the evaluation of hepatic steatosis: Preliminary study and validation in a cohort of patients with chronic liver disease from various causes. Ultrasound Med Biol. 2010;36:1825–35.
270. Sasso M, Tengher-Barna I, Ziol M, Miette V, Fournier C, Sandrin L, et al. Novel controlled attenuation parameter for noninvasive assessment of steatosis using Fibroscan®: Validation in chronic hepatitis C. J Viral Hepat. 2012;19:244–53.
271. Sasso M, Audière S, Kemgang A, Gaouar F, Corpechot C, Chazouillères O, et al. Liver steatosis assessed by controlled attenuation parameter (CAP) measured with the XL probe of the FibroScan: A pilot study assessing diagnostic accuracy. Ultrasound Med Biol. 2016;42:92–103.
272. Ferraioli G, Tinelli C, Lissandrin R, Zicchetti M, Rondanelli M, Perani G, et al. Interobserver reproducibility of the controlled attenuation parameter (CAP) for quantifying liver steatosis. Hepatol Int. 2014;8:576–81.
273. Recio E, Cifuentes C, Macías J, Mira JA, Parra-Sánchez M, Rivero-Juárez A, et al. Interobserver concordance in controlled attenuation parameter measurement, a novel tool for the assessment of hepatic steatosis on the basis of transient elastography. Eur J Gastroenterol Hepatol. 2013;25:905–11.
274. Shen F. Controlled attenuation parameter for non-invasive assessment of hepatic steatosis in Chinese patients. World J Gastroenterol. 2014;20:4702–11.
275. Jung KS, Kim BK, Kim SU, Chon YE, Cheon KH, Kim SB, et al. Factors affecting the accuracy of controlled attenuation parameter (CAP) in assessing hepatic steatosis in patients with chronic liver disease. PLoS One. 2014;9:e98689.
276. Chon YE, Jung KS, Kim SU, Park JY, Park YN, Kim DY, et al. Controlled attenuation parameter (CAP) for detection of hepatic steatosis in patients with chronic liver diseases: A prospective study of a native Korean population. Liver Int. 2014; 34:102–9.
277. Lédinghen V, Wong GLH, Vergniol J, Chan HLY, Hiriart JB, Chan AWH, et al. Controlled attenuation parameter for the diagnosis of steatosis in non-alcoholic fatty liver disease. J Gastroenterol Hepatol. 2016;31:848–55.
278. Eddowes PJ, Sasso M, Allison M, Tsochatzis E, Anstee QM, Sheridan D, et al. Accuracy of FibroScan controlled attenuation parameter and liver stiffness measurement in assessing steatosis and fibrosis in patients with nonalcoholic fatty liver disease. Gastroenterology. 2019;156:1717–30.
279. Kjærgaard M, Thiele M, Jansen C, Stæhr Madsen B, Görtzen J, Strassburg C, et al. High risk of misinterpreting liver and spleen stiffness using 2D shear-wave and transient elastography after a moderate or high calorie meal. PLoS One. 2017;12:e0173992.
280. Ratchatasettakul K, Rattanasiri S, Promson K, Sringam P, Sobhonslidsuk A. The inverse effect of meal intake on controlled attenuation parameter and liver stiffness as assessed by transient elastography. BMC Gastroenterol. 2017;17:50.
281. Andrade P, Rodrigues S, Rodrigues-Pinto E, Gaspar R, Lopes J, Lopes S, et al. Diagnostic accuracy of controlled attenuation parameter for detecting hepatic steatosis in patients with chronic liver disease. GE Port J Gastroenterol. 2017;24:161–8.
282. Castéra L, Foucher J, Bernard PH, Carvalho F, Allaix D, Merrouche W, et al. Pitfalls of liver stiffness measurement: A 5-year prospective study of 13,369 examinations. Hepatology. 2010;51:828–35.
283. Chan WK, Nik Mustapha NR, Wong GLH, Wong VWS, Mahadeva S. Controlled attenuation parameter using the FibroScan® XL probe for quantification of hepatic steatosis for non-alcoholic fatty liver disease in an Asian population. United European Gastroenterol J. 2017;5:76–85.
284. de Lédinghen V, Vergniol J, Foucher J, Merrouche W, le Bail B. Non-invasive diagnosis of liver steatosis using controlled attenuation parameter (CAP) and transient elastography. Liver Int. 2012;32:911–8.
285. de Lédinghen V, Vergniol J, Capdepont M, Chermak F, Hiriart JB, Cassinotto C, et al. Controlled attenuation parameter (CAP) for the diagnosis of steatosis: A prospective study of 5323 examinations. J Hepatol. 2014;60:1026–31.
286. Bohte AE, van Werven JR, Bipat S, Stoker J. The diagnostic accuracy of US, CT, MRI and ^{1}H-MRS for the evaluation of hepatic steatosis compared with liver biopsy: A meta-analysis. Eur Radiol. 2011;21:87–97.
287. Myers RP, Pollett A, Kirsch R, Pomier-Layrargues G, Beaton M, Levstik M, et al. Controlled attenuation parameter (CAP): A noninvasive method for the detection of hepatic steatosis based on transient elastography. Liver Int. 2012;32:902–10.
288. Siddiqui MS, Yamada G, Vuppalanchi R, Van Natta M, Loomba R, Guy C, et al. Diagnostic accuracy of noninvasive fibrosis

models to detect change in fibrosis stage. Clin Gastroenterol Hepatol. 2019;17:1877–85.e5.
289. Galaski J, Schulz L, Krause J, Lohse A. Discordance in steatosis classification between liver biopsy and transient elastography for high controlled attenuation parameter (CAP) values. Z Gastroenterol. 2018;56:36–42.
290. Jun DW, Kim SG, Park SH, Jin SY, Lee JS, Lee JW, et al, the Korean NAFLD Study Group (KNSG). External validation of the non-alcoholic fatty liver disease fibrosis score for assessing advanced fibrosis in Korean patients. J Gastroenterol Hepatol. 2017;32:1094–9.
291. Wong VWS, Petta S, Hiriart JB, Cammà C, Wong GLH, Marra F, et al. Validity criteria for the diagnosis of fatty liver by M probe-based controlled attenuation parameter. J Hepatol. 2017; 67:577–84.
292. Mendes LC, Ferreira PA, Miotto N, Zanaga L, Lazarini MS, Gonçales ESL, et al. Controlled attenuation parameter for steatosis grading in chronic hepatitis C compared with digital morphometric analysis of liver biopsy: Impact of individual elastography measurement quality. Eur J Gastroenterol Hepatol. 2018;30:959–66.
293. Friedrich-Rust M, Romen D, Vermehren J, Kriener S, Sadet D, Herrmann E, et al. Acoustic radiation force impulse-imaging and transient elastography for non-invasive assessment of liver fibrosis and steatosis in NAFLD. Eur J Radiol. 2012;81: e325–31.
294. Kumar M, Rastogi A, Singh T, Behari C, Gupta E, Garg H, et al. Controlled attenuation parameter for non-invasive assessment of hepatic steatosis: Does etiology affect performance? J Gastroenterol Hepatol. 2013;28:1194–201.
295. Runge JH, Smits LP, Verheij J, Depla A, Kuiken SD, Baak BC, et al. MR spectroscopy-derived proton density fat fraction is superior to controlled attenuation parameter for detecting and grading hepatic steatosis. Radiology. 2018;286:547–56.
296. Naveau S, Voican CS, Lebrun A, Gaillard M, Lamouri K, Njiké-Nakseu M, et al. Controlled attenuation parameter for diagnosing steatosis in bariatric surgery candidates with suspected nonalcoholic fatty liver disease. Eur J Gastroenterol Hepatol. 2017;29:1022–30.
297. Karlas T, Petroff D, Garnov N, Böhm S, Tenckhoff H, Wittekind C, et al. Non-invasive assessment of hepatic steatosis in patients with NAFLD using controlled attenuation parameter and ^{1}H-MR spectroscopy. PLoS One. 2014;9:e91987.
298. Lupsor-Platon M, Feier D, Stefănescu H, Tamas A, Botan E, Sparchez Z, et al. Diagnostic accuracy of controlled attenuation parameter measured by transient elastography for the non-invasive assessment of liver steatosis: A prospective study. J Gastrointestin Liver Dis. 2015;24:35–42.
299. Lee HW, Park SY, Kim SU, Jang JY, Park H, Kim JK, et al. Discrimination of nonalcoholic steatohepatitis using transient elastography in patients with nonalcoholic fatty liver disease. PLoS One. 2016;11:e0157358.
300. Price JC, Dodge JL, Ma Y, Scherzer R, Korn N, Tillinghast K, et al. Controlled attenuation parameter and magnetic resonance spectroscopy-measured liver steatosis are discordant in obese HIV-infected adults. AIDS (London, England). 2017;31: 2119–25.
301. Darweesh SK, Omar H, Medhat E, Abd-Al Aziz RA, Ayman H, Saad Y, et al. The clinical usefulness of elastography in the evaluation of nonalcoholic fatty liver disease patients: A biopsy-controlled study. Eur J Gastroenterol Hepatol. 2019;31:1010–6.
302. de Lédinghen V, Hiriart JB, Vergniol J, Merrouche W, Bedossa P, Paradis V. Controlled attenuation parameter (CAP) with the XL probe of the Fibroscan®: A comparative study with the M probe and liver biopsy. Dig Dis Sci. 2017;62:2569–77.
303. Siddiqui MS, Vuppalanchi R, Van Natta ML, Hallinan E, Kowdley KV, Abdelmalek M, et al, the NASH Clinical Research Network. Vibration-controlled transient elastography to assess fibrosis and steatosis in patients with nonalcoholic fatty liver disease. Clin Gastroenterol Hepatol. 2019;17:156–63.e2.
304. Chan WK, Nik Mustapha NR, Mahadeva S, Wong VWS, Cheng JYK, Wong GLH. Can the same controlled attenuation parameter cutoffs be used for M and XL probes for diagnosing hepatic steatosis? J Gastroenterol Hepatol. 2018;33:1787–94.
305. Xu L, Lu W, Li P, Shen F, Mi YQ, Fan JG. A comparison of hepatic steatosis index, controlled attenuation parameter and ultrasound as noninvasive diagnostic tools for steatosis in chronic hepatitis B. Dig Liver Dis. 2017;49:910–7.
306. Ooi GJ, Earnest A, Kemp WW, Burton PR, Laurie C, Majeed A, et al. Evaluating feasibility and accuracy of non-invasive tests for nonalcoholic fatty liver disease in severe and morbid obesity. Int J Obes. 2018;42:1900–11.
307. Jun BG, Park WY, Park EJ, Jang JY, Jeong SW, Lee SH, et al. A prospective comparative assessment of the accuracy of the FibroScan in evaluating liver steatosis. PLoS One. 2017;12: e0182784.
308. Petroff D, Blank V, Newsome PN, Shalimar, Voican CS, Thiele M, et al. Assessment of hepatic steatosis by controlled attenuation parameter using the M and XL probes: An individual patient data meta-analysis. Lancet Gastroenterol Hepatol. 2021;6:185–98.
309. Beyer C, Hutton C, Andersson A, Imajo K, Nakajima A, Kiker D, et al. Comparison between magnetic resonance and ultrasound-derived indicators of hepatic steatosis in a pooled NAFLD cohort. PLoS One. 2021;16:e0249491.
310. Audière S, Labourdette A, Miette V, Fournier C, Ternifi R, Boussida S, et al. Improved ultrasound attenuation measurement method for the non-invasive evaluation of hepatic steatosis using FibroScan. Ultrasound Med Biol. 2021;47:3181–95.
311. Garteiser P, Castera L, Coupaye M, Doblas S, Calabrese D, Dioguardi Burgio M, et al. Prospective comparison of transient elastography, MRI and serum scores for grading steatosis and detecting non-alcoholic steatohepatitis in bariatric surgery candidates. JHEP Rep. 2021;3:100381.
312. Yen YH, Kuo FY, Lin CC, Chen CL, Chang KC, Tsai MC, et al. Predicting hepatic steatosis in living liver donors via controlled attenuation parameter. Transplant Proc. 2018;50:3533–8.
313. Zhuang RH, Weinstock AK, Ganesh S, Behari J, Malik SM, Bataller R, et al. Characterization of hepatic steatosis using controlled attenuation parameter and MRI-derived proton density fat fraction in living donor liver transplantation. Clin Transplant. 2011;36:e14786.
314. Caussy C, Brissot J, Singh S, Bassirian S, Hernandez C, Bettencourt R, et al. Prospective, same-day, direct comparison of controlled attenuation parameter with the M vs the XL probe in patients with nonalcoholic fatty liver disease, using magnetic resonance imaging-proton density fat fraction as the standard. Clin Gastroenterol Hepatol. 2020;18:1842–50.e6.
315. Siddiqui MS, Carbone S, Vincent R, Patel S, Driscoll C, Celi FS, et al. Prevalence and severity of nonalcoholic fatty liver disease among caregivers of patients with nonalcoholic fatty liver disease cirrhosis. Clin Gastroenterol Hepatol. 2019;17: 2132–3.
316. Castera L, Friedrich-Rust M, Loomba R. Noninvasive assessment of liver disease in patients with nonalcoholic fatty liver disease. Gastroenterology. 2019;156:1264–81.e4.
317. Ahn SB, Jun DW, Kang B, Kim M, Chang M, Nam E. Optimal cutoff value for assessing changes in intrahepatic fat amount by using the controlled attenuation parameter in a longitudinal setting. Medicine. 2018;97:e13636.
318. Shin NY, Kim MJ, Lee MJ, Han SJ, Koh H, Namgung R, et al. Transient elastography and sonography for prediction of liver fibrosis in infants with biliary atresia. J Ultrasound Med. 2014; 33:853–64.
319. Hukkinen M, Lohi J, Heikkilä P, Kivisaari R, Jahnukainen T, Jalanko H, et al. Noninvasive evaluation of liver fibrosis and

portal hypertension after successful portoenterostomy for biliary atresia. Hepatol Commun. 2019;3:382–91.
320. Gao F, Chen YQ, Fang J, Gu SL, Li L, Wang XY. Acoustic radiation force impulse imaging for assessing liver fibrosis preoperatively in infants with biliary atresia: Comparison with liver fibrosis biopsy pathology. J Ultrasound Med. 2017;36: 1571–8.
321. Chen S, Liao B, Zhong Z, Zheng Y, Liu B, Shan Q, et al. Supersonic shearwave elastography in the assessment of liver fibrosis for postoperative patients with biliary atresia. Sci Rep. 2016;6:31057.
322. Lewindon PJ, Puertolas-Lopez MV, Ramm LE, Noble C, Pereira TN, Wixey JA, et al. Accuracy of transient elastography data combined with APRI in detection and staging of liver disease in pediatric patients with cystic fibrosis. Clin Gastroenterol Hepatol. 2019;17:2561–9.e5.
323. Garcovich M, Veraldi S, Di Stasio E, Zocco MA, Monti L, Tomà P, et al. Liver stiffness in pediatric patients with fatty liver disease: Diagnostic accuracy and reproducibility of shear-wave elastography. Radiology. 2017;283:820–7.
324. Schwimmer JB, Behling C, Angeles JE, Paiz M, Durelle J, Africa J, et al. Magnetic resonance elastography measured shear stiffness as a biomarker of fibrosis in pediatric nonalcoholic fatty liver disease. Hepatology. 2017;66:1474–85.
325. Behairy BES, Sira MM, Zalata KR, Salama ESE, Abd-Allah MA. Transient elastography compared to liver biopsy and morphometry for predicting fibrosis in pediatric chronic liver disease: Does etiology matter. World J Gastroenterol. 2016;22:4238–49.
326. Awad M, Shiha GE, Sallam FA, Mohamed A, El Tawab A. Evaluation of liver stiffness measurement by fibroscan as compared to liver biopsy for assessment of hepatic fibrosis in children with chronic hepatitis C. J Egypt Soc Parasitol. 2013; 43:805–19.
327. Hwang JY, Yoon HM, Kim JR, Lee JS, Jung AY, Kim KM, et al. Diagnostic performance of transient elastography for liver fibrosis in children: A systematic review and meta-analysis. AJR Am J Roentgenol. 2018;211:W257–66.
328. Raizner A, Shillingford N, Mitchell PD, Harney S, Raza R, Serino J, et al. Hepatic inflammation may influence liver stiffness measurements by transient elastography in children and young adults. J Pediatr Gastroenterol Nutr. 2017;64:512–7.
329. Millonig G, Reimann FM, Friedrich S, Fonouni H, Mehrabi A, Büchler MW, et al. Extrahepatic cholestasis increases liver stiffness (FibroScan) irrespective of fibrosis. Hepatology. 2008; 48:1718–23.
330. Bader RM, Jonas MM, Mitchell PD, Wiggins S, Lee CK. Controlled attenuation parameter: A measure of hepatic steatosis in patients with cystic fibrosis. J Cyst Fibros. 2019; 18:280–5.
331. Schwimmer JB, Middleton MS, Behling C, Newton KP, Awai HI, Paiz MN, et al. Magnetic resonance imaging and liver histology as biomarkers of hepatic steatosis in children with nonalcoholic fatty liver disease. Hepatology. 2015;61:1887–95.
332. Desai NK, Harney S, Raza R, Al-Ibraheemi A, Shillingford N, Mitchell PD, et al. Comparison of controlled attenuation parameter and liver biopsy to assess hepatic steatosis in pediatric patients. J Pediatr. 2016;173:160–4.e1.
333. Hudert CA, Tzschätzsch H, Guo J, Rudolph B, Bläker H, Loddenkemper C, et al. US time-harmonic elastography: Detection of liver fibrosis in adolescents with extreme obesity with nonalcoholic fatty liver disease. Radiology. 2018;288: 99–106.
334. Nobili V, Vizzutti F, Arena U, Abraldes JG, Marra F, Pietrobattista A, et al. Accuracy and reproducibility of transient elastography for the diagnosis of fibrosis in pediatric nonalcoholic steatohepatitis. Hepatology. 2008;48:442–8.
335. Alkhouri N, Sedki E, Alisi A, Lopez R, Pinzani M, Feldstein AE, et al. Combined paediatric NAFLD fibrosis index and transient elastography to predict clinically significant fibrosis in children with fatty liver disease. Liver Int. 2013;33:79–85.
336. de Lédinghen V, Le Bail B, Rebouissoux L, Fournier C, Foucher J, Miette V, et al. Liver stiffness measurement in children using FibroScan: Feasibility study and comparison with Fibrotest, aspartate transaminase to platelets ratio index, and liver biopsy. J Pediatr Gastroenterol Nutr. 2007;45:443–50.
337. Majumdar A, Campos S, Gurusamy K, Pinzani M, Tsochatzis EA. Defining the minimum acceptable diagnostic accuracy of noninvasive fibrosis testing in cirrhosis: A decision analytic modeling study. Hepatology. 2020;71:627–42.
338. Mendoza YP, Shengir M, Bosch J, Sebastiani G, Berzigotti A. FIB-4 improves LSM-based prediction of complications in overweight or obese patients with compensated advanced chronic liver disease. Clin Gastroenterol Hepatol. 2022;20: 2396–98.e3.
339. Bazerbachi F, Haffar S, Wang Z, Cabezas J, Arias-Loste MT, Crespo J, et al. Range of normal liver stiffness and factors associated with increased stiffness measurements in apparently healthy individuals. Clin Gastroenterol Hepatol. 2019;17: 54–64.e1.
340. Serra-Burriel M, Graupera I, Torán P, Thiele M, Roulot D, Wai-Sun Wong V, et al, and the investigators of the LiverScreen Consortium. Transient elastography for screening of liver fibrosis: Cost-effectiveness analysis from six prospective cohorts in Europe and Asia. J Hepatol. 2019;71:1141–51.
341. Papatheodoridi M, Hiriart JB, Lupsor-Platon M, Bronte F, Boursier J, Elshaarawy O, et al. Refining the Baveno VI elastography criteria for the definition of compensated advanced chronic liver disease. J Hepatol. 2021;74:1109–16.
342. Rockey DC, Alsawas M, Rojo-Duarte A, et al. Non-invasive liver disease assessment (NILDA) to identify portal hypertension – systematic and narrative reviews supporting the AASLD practice guideline. Hepatology. 2024. (In press).
343. Unalp-Arida A, Ruhl CE. Transient elastography–assessed hepatic steatosis and fibrosis are associated with body composition in the United States. Clin Gastroenterol Hepatol. 2022;20:E808–30.
344. Selvaraj EA, Mózes FE, Jayaswal ANA, Zafarmand MH, Vali Y, Lee JA, et al, the LITMUS Investigators. Diagnostic accuracy of elastography and magnetic resonance imaging in patients with NAFLD: A systematic review and meta-analysis. J Hepatol. 2021;75:770–85.
345. Chow JCL, Wong GLH, Chan AWH, Shu SST, Chan CKM, Leung JKY, et al. Repeating measurements by transient elastography in non-alcoholic fatty liver disease patients with high liver stiffness. J Gastroenterol Hepatol. 2019;34:241–8.
346. Chuah KH, Lai LL, Vethakkan SR, Nik Mustapha NR, Mahadeva S, Chan WK. Liver stiffness measurement in non-alcoholic fatty liver disease: Two is better than one. J Gastroenterol Hepatol. 2020;35:1404–11.
347. Ioannou GN, Beste LA, Green PK, Singal AG, Tapper EB, Waljee AK, et al. Increased risk for hepatocellular carcinoma persists up to 10 years after HCV eradication in patients with baseline cirrhosis or high FIB-4 scores. Gastroenterology. 2019;157:1264–78.e4.
348. Vutien P, Kim NJ, Moon AM, Pearson M, Su F, Berry K, et al. Fibroscan liver stiffness after anti-viral treatment for hepatitis C is independently associated with adverse outcomes. Aliment Pharmacol Ther. 2020;52(11–12):1717–27.
349. Chen T, Wong R, Wong P, Rollet-Kurhajec KC, Alshaalan R, Deschenes M, et al. Occult cirrhosis diagnosed by transient elastography is a frequent and under-monitored clinical entity. Liver Int. 2015;35:2285–93.
350. de Franchis R, Bosch J, Garcia-Tsao G, Reiberger T, Ripoll C, Abraldes JG, et al. and the Baveno VII Faculty. Baveno VII - Renewing consensus in portal hypertension. J Hepatol. 2022; 76:959–74.

351. Pons M, Augustin S, Scheiner B, Guillaume M, Rosselli M, Rodrigues SG, et al. Noninvasive diagnosis of portal hypertension in patients with compensated advanced chronic liver disease. Am J Gastroenterol. 2021;116:723–32.
352. Singh R, Wilson MP, Katlariwala P, Murad MH, McInnes MDF, Low G. Accuracy of liver and spleen stiffness on magnetic resonance elastography for detecting portal hypertension: A systematic review and meta-analysis. Eur J Gastroenterol Hepatol. 2021;32:237–45.
353. Gidener T, Ahmed OT, Larson JJ, Mara KC, Therneau TM, Venkatesh SK, et al. Liver stiffness by magnetic resonance elastography predicts future cirrhosis, decompensation, and death in NAFLD. Clin Gastroenterol Hepatol. 2021;19:1915–24.e6.
354. Gidener T, Yin M, Dierkhising RA, Allen AM, Ehman RL, Venkatesh SK. MRE for prediction of long-term progression and outcome in chronic liver disease: A retrospective study. Hepatology. 2022;75:379–90.
355. Gu Q, Cen L, Lai J, Zhang Z, Pan J, Zhao F, et al. A meta-analysis on the diagnostic performance of magnetic resonance imaging and transient elastography in nonalcoholic fatty liver disease. Eur J Clin Invest. 2021;51:e13446.
356. Lee DH, Cho EJ, Bae JS, Lee JY, Yu SJ, Kim H, et al. Accuracy of two-dimensional shear wave elastography and attenuation imaging for evaluation of patients with nonalcoholic steatohepatitis. Clin Gastroenterol Hepatol. 2021;19:797–805.e7.
357. Mojtahed A, Kelly CJ, Herlihy AH, Kin S, Wilman HR, McKay A, et al. Reference range of liver corrected T1 values in a population at low risk for fatty liver disease—a UK Biobank substudy, with an appendix of interesting cases. Abdom Radiol. 2019;44:72–84.
358. Dennis A, Kelly MD, Fernandes C, Mouchti S, Fallowfield JA, Hirschfield G, et al. Correlations between MRI biomarkers PDFF and cT1 with histopathological features of non-alcoholic steatohepatitis. Front Endocrinol (Lausanne). 2021;11:575843.
359. Imajo K, Tetlow L, Dennis A, Shumbayawonda E, Mouchti S, Kendall TJ, et al. Quantitative multiparametric magnetic resonance imaging can aid non-alcoholic steatohepatitis diagnosis in a Japanese cohort. World J Gastroenterol. 2021;27:609–23.
360. Allen AM, Shah VH, Therneau TM, Venkatesh SK, Mounajjed T, Larson JJ, et al. The role of three-dimensional magnetic resonance elastography in the diagnosis of nonalcoholic steatohepatitis in obese patients undergoing bariatric surgery. Hepatology. 2020;71:510–21.
361. Hudert CA, Tzschätzsch H, Rudolph B, Bläker H, Loddenkemper C, Müller HP, et al. Tomoelastography for the evaluation of pediatric nonalcoholic fatty liver disease. Invest Radiol. 2019;54:198–203.

How to cite this article: Sterling RK, Duarte-Rojo A, Patel K, Asrani SK, Alsawas M, Dranoff JA, et al. AASLD Practice Guideline on imaging-based noninvasive liver disease assessment (NILDA) of hepatic fibrosis and steatosis. Hepatology. 2025;81:672–724. https://doi.org/10.1097/HEP.0000000000000843